Universidade de Aveiro
2020

Forough Nazar Pour

O papel do secretoma na patogenicidade de Botryosphaeriaceae

Understanding pathogenicity of Botryosphaeriaceae: focus on the secretome

Universidade de Aveiro
2020

Forough Nazar Pour

O papel do secretoma na patogenicidade de Botryosphaeriaceae

Understanding pathogenicity of Botryosphaeriaceae: focus on the secretome

Tese apresentada à Universidade de Aveiro para cumprimento dos requisitos necessários à obtenção do grau de Doutor em Biologia, realizada sob a orientação científica do Doutor Artur Jorge da Costa Peixoto Alves, Professor Auxiliar com Agregação do Departamento de Biologia da Universidade de Aveiro e da Doutora Ana Cristina de Fraga Esteves, Professora Auxiliar da Faculdade de Medicina Dentária da Universidade Católica Portuguesa.

Apoio financeiro da FCT e do FEDER através do programa COMPETE no âmbito do projeto de investigação PANDORA.
Bolsas com referência:
PTDC/AGR-FOR/3807/2012
FCOMP-01-0124-FEDER-027979

Apoio financeiro da FCT e do FSE no âmbito do III Quadro Comunitário de Apoio.

Bolsa de Doutoramento:
SFRH/BD/98971/2013

o júri

presidente

Doutor Artur da Rosa Pires
Professor Catedrático, Universidade de Aveiro

Doutor João António de Almeida Serôdio
Professor Auxiliar com Agregação, Universidade de Aveiro

Doutor António Manuel Santos Carriço Portugal
Professor Auxiliar, Universidade de Coimbra

Doutora Rebeca Cobos Román
Investigadora, Universidade de León

Doutora Raquel Monteiro Marques da Silva
Investigadora Auxiliar, Universidade Católica Portuguesa

Doutora Ana Cristina de Fraga Esteves
Professora Auxiliar, Universidade Católica Portuguesa

agradecimentos

At the end of this step of my graduate period has allowed for a bit of reflection, and the many people who have contributed to both my work, and my life during of this period.

First, I would like to express my full thanks and sincere gratitude to my supervisors; Prof. Artur Alves and Prof. Ana Cristina Esteves for supporting me during these past years. Prof. Artur Alves who gave me the opportunity to work in his group. Thank you for all of guidance, unlimited assistance consultations and support. To Prof. Ana Cristina Esteves, for her endless support and guidance, for her patience, motivation, and immense knowledge. I could not have imagined having a better supervisor for my Ph.D. studies.

I would like to thank Dr. Ana Sofia Duarte for her invaluable suggestions, beneficial advices, patience and her endless helps. She also taught me how to look at the life and science. I owe her in whole of my life.

My sincere thanks also go to Dr. Rebeca Cobos, who received me in her working group, wherein I learned a lot. Without her precious support it would not be possible to conduct this research. I also would like to thank Jose, Sandra, Cristina and all the team of Vine and Wine Research Institute, always kind.

I thank Prof. João Serôdio and his group, for helping with the FluorCam system, analysing the data and their endless helps.

I am also grateful to Prof. Bart Devreese for the lab facilities on proteomics technologies and analysing the data. To Gonzalez Van Driessche a very special thanks for your support in laboratory methodologies.

I would like to thank Bruna, Vanessa and Micaela; without your help I could not have completed my lab work.

I would like to acknowledge all the people from the MicroLab during all these years for the amazing environment and the good moments.

I am also grateful to my lab mates from MicroLab: Carina, Cátia, Marta Alves, Susana, Carla, Liliana, Anabela. I am grateful for all support and unconditional help.

To Carina a very special thanks for your friendship and for the sharing of knowledge.

To Cátia a sincere thanks for her friendship and endless helps. Without your help I could not complete my PhD.

I would like to express my full thanks and sincere gratitude to my dear family for their encouragements, emotional supports and fortitude efforts in my lifetime.

Last but not the least, I want to thank my husband Reza for always being there for me, and for his endless love, support, encouragement and understanding through all these years.

palavras-chave

Botryosphaeriaceae, *Neofusicoccum parvum*, fitotoxicidade, citotoxicidade, secretoma, LC-MS, proteinas indutoras de necrose e produção de etileno (NLPs)

resumo

Várias espécies da família Botryosphaeriaceae são agentes patogénicos importantes, causando doenças em plantas lenhosas que originam, por vezes, a sua morte. Alguns destes fungos são também oportunistas de humanos. No entanto, e apesar da relevância destes organismos como agentes patogénicos, os mecanismos de interação com os seus hospedeiros são ainda pouco conhecidos. Tendo em conta que as moléculas extracelulares são os efectores principais da interação fungo-planta, esta investigação centra-se essencialmente no secretoma dos fungos da família Botryosphaeriaceae. Espera-se que o aumento previsto da temperatura ambiental tenha efeitos, ainda desconhecidos, no comportamento destes agentes patogénicos. De modo a elucidar os mecanismos moleculares de toxicidade/patogenicidade dos fungos desta família, quando sujeitos a temperaturas crescentes, estudou-se a fito e citotoxicidades destes organismos. Foram analisados os meios extracelulares de cinco espécies, recorrendo-se a ensaios em folhas de tomateiros e em linhas celulares de mamíferos. Os dados mostram que a temperatura modula a cito- e fitotoxicidade das espécies de Botryosphaeriaceae estudadas. Globalmente, a temperatura de 25 ºC beneficia a fitotoxicidade enquanto que a temperatura de 37 ºC facilita a toxicidade para células animais. O secretoma de uma espécie – *Neofusiccocum parvum* – foi caracterizado mais profundamente. O perfil de proteínas extracelulares desta espécie na presença de ramos de eucalipto foi caracterizado por LC-MS e comparado com o secretoma controlo, tendo sido identificadas mais de uma centena de proteínas diferencialmente expressas. Estas proteínas estão envolvidas na adesão e penetração do fungo nos tecidos do hospedeiro, na degradação das paredes celulares vegetais e das do próprio fungo, em mecanismos de patogénese, na produção de radicais livres de oxigénio e em proteólise. Foram também identificados fitotoxinas e efetores fúngicos. A maioria das proteínas identificada foi expressa na presença do hospedeiro, nomeadamente enzimas que degradam componentes da parede vegetal (CWDE) como a pectina e hemicelulose e que estão envolvidas no processo de invasão do hospedeiro. A conhecida patogenicidade de *N. parvum* poderá ser explicada por uma ação concertada da atividade de CWDEs, particularmente de glicosil hidrolases e de liases de polissacarídeos. O perfil de proteínas extracelulares de *N. parvum* sugere que este fungo ajusta a expressão do secretoma às propriedades químicas das paredes vegetais, em concordância com o fato deste ser um importante fitopatogénio. Do mesmo modo, a ausência de enzimas de degradação da lenhina e a presença de várias enzimas que degradam celulose e hemicelulose coadunam-se com um estilo de vida endofítico. Adicionalmente, a presença no secretoma *de N. parvum* de enzimas capazes de degradar pectina, mesmo na ausência de material vegetal, indica que este fungo estará mais adaptado a degradar tecido vegetal vivo do que biomassa em decomposição de acordo com ser um patógeno latente. Estes resultados, sugerem que *N. parvum* possui um estilo de vida hemibiotrófico: secreta enzimas putativamente envolvidas na degradação das paredes vegetais simultaneamente modificando as suas próprias paredes, o que lhe permite colonizar o hospedeiro (biotrófico) enquanto ativamente secreta enzimas hidrolíticas e toxinas (necrotrófico). Adicionalmente foram clonados e caraterizados quatro genes que codificam “necrosis and ethylene inducing proteins” (NLPs). Os genes foram clonados com sucesso e expressos em *E. coli*. As proteínas NprvNep recombinantes mostraram ser tóxicas para plantas (folhas de tomateiro destacadas) e para células de mamífero (células Vero) de um modo dependente da dose. Os genes NLP genes em *N. parvum* são genes funcionais que codificam proteínas tóxicas tanto para tecidos vegetais como para células animais, estando potencialmente envolvidas na virulência e/ou na morte celular do hospedeiro durante a infeção. Este estudo revelou dados moleculares sobre a patogenicidade de *N. parvum* e consequentemente elucida a atuação de alguns membros da família Botryosphaeriaceae.

keywords

Botryosphaeriaceae, *Neofusicoccum parvum*, phytotoxicity, cytotoxicity, secretome, LC-MS, necrosis and ethylene-inducing proteins (NLPs)

abstract

Species of the family Botryosphaeriaceae are important fungal pathogens causing numerous diseases on many woody plants, which ultimately may result in death of the host. Some fungi in this family are also human opportunist pathogens. Despite the relevance of these pathogens the mechanism of interaction between them and their hosts is still poorly known. Since the extracellular molecules secreted by fungi are the main effectors of fungus-plant interactions, this investigation was mainly centred on Botryosphaeriaceae secretome.

The forecasted environmental temperature increase will lead to unknown effects on these pathogens. In order to shed light into the molecular mechanisms of toxicity/pathogenicity of Botryosphaeriaceae fungi under increasing temperatures, phytotoxicity and cytotoxicity of the culture filtrates of five Botryosphaeriaceae species were evaluated on detached tomato leaves and on mammalian cell lines (Vero cells and 3T3 cells). Data shows that temperature modulates the cyto- and phytotoxicity of Botryosphaeriaceae fungi. In general, 25 ºC benefits phytotoxicity while 37 ºC facilitates cytotoxicity to animal cells.

The first comprehensive characterization of the *in vitro* secretome of *Neofusiccocum parvum* was made. LC-MS was used to identify *N. parvum* protein profile in the absence and presence of *Eucalyptus* stem and this resulted in the consistent identification of over one hundred proteins diffrentially expressed involved in adhesion and penetration of pathogen to host tissues, plant and fungal cell wall degradation, pathogenesis, reactive oxygen species (ROS) generation, proteolytic processes. Also fungal effectors and fungal toxin. Identified proteins were induced mostly under host mimicry secretome, especially cell wall degrading enzymes (CWDEs) (targeting pectin and hemicellulose) which are involved in plant invasion. *Neofusicoccum parvum* aggressiveness could be explained by a synergistic activity of extracellular CWDE, particularly of glycoside hydrolases and polysaccharide lyases, that may be involved in plant host colonization. The extracellular protein profile of *N. parvum* suggest that the fungus has adjusted its secretome to the host cell wall chemical properties, which agrees with the fact that *N. parvum* being a phytopathogen. Likewise, absence of lignin degrading enzymes and existence of several cellulase and hemicellulase enzymes fits well with its endophytic lifestyle. In addition, the presence of pectin-degrading enzymes in the secretome of *N. parvum* even in the absence of host material, indicating that this fungus is more adapted to degrade intact or living plants than decaying biomass, which implies that the fungus is likely to be a latent pathogen. Overall, our results suggest that *N. parvum* has a hemibiotrophic lifestyle by the secretion of proteins putatively involved in plant cell wall degradation and concurrently masking or modifying its own cell wall , allowing the fungus to colonize the host plant (biotrophic), while actively releasing enzymes and toxins (necrotrophic).

Furthermore, cloning and characterization of four genes encoding putative necrosis and ethylene inducing proteins (NLPs) from *N. parvum* was carried out. Four NLP genes were successfully cloned and expressed in *E. coli*. Pure recombinant NprvNep proteins were toxic both to plant (detached tomato leaves) and mammalian cells (Vero cells) in a dose-dependent manner. NLP genes in *N. parvum* are functional genes encoding proteins toxic both to plant and mammalian cells, being most probably involved in virulence or cell death during infection by *N. parvum*.

This study provides additional insight into the pathogenicity mechanism of *N. parvum* and subsequently of members of the Botryosphaeriaceae family.

TABLE OF CONTENTS

FIGURES LIST

TABLES LIST

THESIS OUTLINE

The current research focuses on understanding pathogenicity of Botryosphaeriaceae fungi, that are important pathogens of trees around the world. To gain more insight into the infection mechanisms, host-pathogen interaction and to identify new proteins specific to Botryosphaeriaceae pathogenicity, *Neofusicoccum parvum* was selected as a model species. *Neofusicoccum parvum* is an aggressive phytopathogen widely distributed in the environment and it can infect a wide range of plants.

The thesis is organized in 5 chapters. Chapter 1 corresponds to a general introduction addressing the main topics of the work. In chapters 2 to 4, all the results are described and discussed. Chapter 2 describes the effect of different temperatures (25 and 37 °C) on the phytotoxicity and cytotoxicity of six species of the family Botryosphaeriaceae — *Botryosphaeria dothidea* CAA642; *Diplodia corticola* CAA500; *Neofusicoccum parvum* CAA366; *Neofusicoccum eucalyptorum* CAA558; *Neofusicoccum kwambonambiense* CAA755 and *Neofusicoccum parvum* CAA704 — on detached tomato leaves and on mammalian cell lines. *Diplodia corticola* and *N. kwambonambiense* are the most virulent strains followed by *N. parvum* CAA704. Nonetheless, *N. parvum* was selected for a deeper characterization since i) the infection mechanism of *D. corticola* had already been addressed earlier (Fernandes et al., 2014; Fernandes et al., 2015), ii) there is no molecular data on *N. kwambonambiense* and iii) *N. parvum* is one of the most aggressive phytopathogens of this study. In chapter 3, the *in vitro* basal and infection-induced *N. parvum* secretome was studied in order to identify the proteins involved in *N. parvum* pathogenesis. Identification of a secreted pathogen protein, the necrosis and ethylene-inducing protein (NLP), raised our special attention, leading to the study described in chapter 4. In chapter 4, the functional characteristics of the four NLPs genes from *N. parvum* were investigated in order to elucidate their involvement in virulence or cell death during infection by *N. parvum*. Finally, chapter 5 provides a general discussion of the thesis as well as challenges for future studies on fungal pathogenicity. In the end of the dissertation, all the raw data used is discriminated, allowing the reader to search detailed and complementary information.

The thesis is presented in article format. Two of the chapters has been published, and the remaining is ready for submission:

Chapter 2:

Nazar Pour, F., Ferreira, V., Félix, C., Serôdio, J., Alves, A., Duarte, A. S., and Esteves, A. C. (2020). Effect of temperature on the phytotoxicity and cytotoxicity of Botryosphaeriaceae fungi. *Fungal biology*, 124(6), 571-578. doi: 10.1016 / j.funbio.2020.02.012

Chapter 3:

Nazar Pour, F., Cobos, R., Rubio Coque, J. J., Serôdio, J., Alves, A., Félix, C., Ferreira, V., Esteves, A. C., and Duarte, A. S. (2020). Toxicity of recombinant necrosis and ethylene-inducing proteins (NLPs) from *Neofusicoccum parvum. Toxins*, 12(4), 235. doi: 10.3390 / toxins12040235.

Chapter 4:

Nazar Pour, F., Pedrosa, B., Oliveira, M., Félix, C., Duarte, A.C., Devreese, B., Alves, A., and Esteves, A. C. Unveiling the secretome of the fungal plant pathogen *Neofusicoccum parvum* induced by *in vitro* host mimicry.

CHAPTER 1

General introduction

THE FAMILY BOTRYOSPHAERIACEAE AND THE CASE OF *NEOFUSICOCCUM PARVUM*

The Botryosphaeriaceae includes a range of phylogenetically and morphologically diverse fungi, with a wide host range and global distribution (Liu et al., 2012; Punithalingam, 1980; Phillips et al., 2013; Slippers & Wingfield, 2007). There are 23 genera encompassing 187 species in the Botryosphaeriaceae based on a recent phylogenetic study (Dissanayake et al., 2016). The genera *Diplodia*, *Botryosphaeria*, *Neofusicoccum*, *Dothiorella*, and *Lasiodiplodia* contain a larger number of species (Slippers & Wingfield, 2007). These fungi occur primarily on woody plants including both economically important crops and native trees (Slippers & Wingfield, 2007). Many species of Botryosphaeriaceae are known pathogens that can cause cankers, diebacks, shoot blights and fruit rots on cultivated trees and more rarely diseases such as seed-capsule abortion, witches-broom, leaf diseases, seedling diseases and root cankers. However, some species of Botryosphaeriaceae have been described as latent pathogens or endophytes residing in the woody tissue of asymptomatic hosts (Sinclair & Lyon, 2005; Slippers & Wingfield, 2007). There is growing evidence that many species spread globally as endophytes in plants and plant products representing a threat to cultivated and native plants (Burgess & Wingfield, 2002; Slippers & Wingfield, 2007; Slippers et al., 2009).

Botryosphaeriaceae may switch from a latent stage to a pathogenic one mostly following the onset of stress factors such as temperature and drought. The disease symptoms develop rapidly and can cause extensive losses (Slippers & Wingfield, 2007). Thus, it is likely that increased temperature, droughts and extreme climate events, due to climate change, will have strong effects on the distribution and behavior of plant species and pathogens, and ultimately result in changes in disease impact (Eastburn et al., 2011; Sturrock et al., 2011). The family Botryosphaeriaceae is associated with plant diseases in a wide diversity of woody and horticultural plant hosts economically important, stimulating substantial interest of studying these fungi (Li et al., 2015; Punithalingam, 1980; Slippers & Wingfield, 2007; Slippers et al., 2014). Infection by Botryosphaeriaceae can occur through natural openings (*e.g.* buds, stomata, and lenticels), reproductive structures (*e.g.* seeds) or wounds (Slippers & Wingfield, 2007). The perennial cankers and consequent dieback in the vascular system caused by Botryosphaeriaceae are one of the most important symptoms often leading to death of the host plant (Úrbez-Torres et al., 2016).

Eucalyptus species are considered the most important commercial trees in many countries around the world due to high growth rates and valuable wood and fibre properties for the pulp and paper industry (Bennett, 2010). They are also the most abundant forest tree species in Portugal [26 % of the forest area, nearly 844,000 ha (ICNF, 2019)], mostly of *Eucalyptus globulus* Labill and have an enormous economic significance for the country.

It has been reported that *Eucalyptus* species, both in their native and introduced ranges, can be infected by various species of Botryosphaeriaceae fungi (Chen et al., 2011; Slippers et al., 2009), particularly when they are grown as non-native crops (Chen et al., 2011; Rodas et al., 2009). According to the most recent studies, over 30 species of Botryosphaeriaceae from eight genera have been confirmed to be associated with *Eucalyptus* species (Barradas et al., 2016; Liu et al., 2018; Pillay et al., 2013). Typical symptoms of these fungi on *Eucalyptus* include stem cankers, die-back of shoots and branches and even host death (Figure 1.1) (Slippers et al., 2009). However, very little is known about the strategies that these fungi use to infect their hosts, or about the molecules these pathogens express during infection.

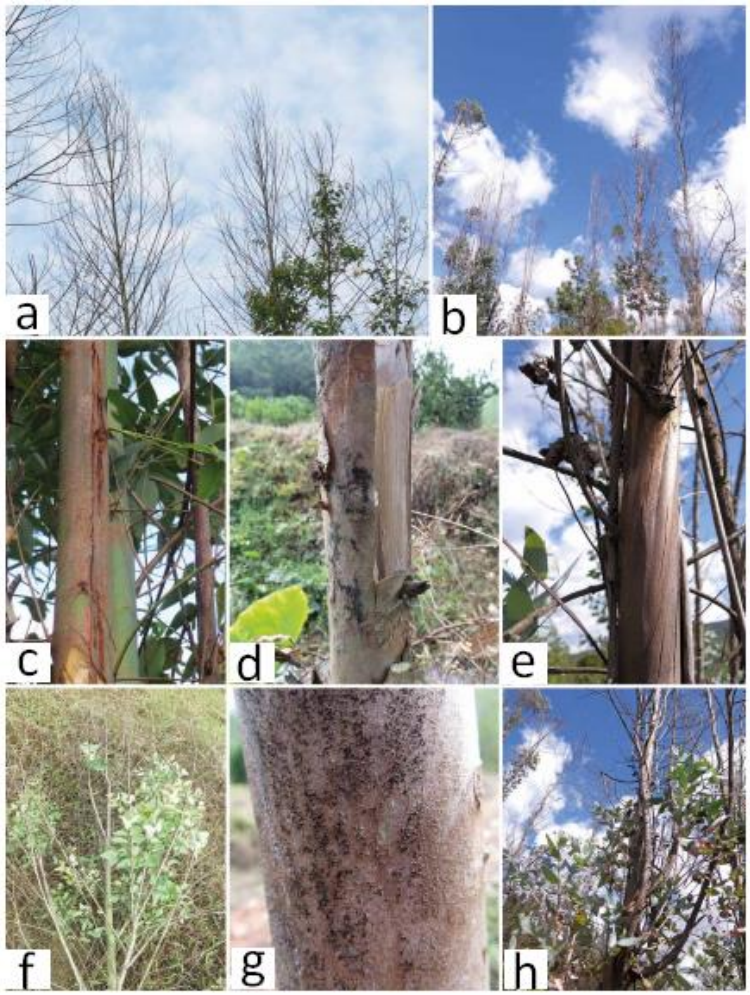

Figure 1. 1 | Disease symptoms of *Eucalyptus* plantations infected with Botryosphaeriaceae. a-b. Dieback of tree tops on *Eucalyptus grandis* clone and *Eucalyptus globulus*, respectively; c–e. Canker of the main stem of different *Eucalyptus* clones/genotypes; f. branch and twig blight of a *Eucalyptus grandis* clone; g. fruiting bodies in a *Eucalyptus* branch with abundant mature dark conidia; h. new branches germinated after main stem infection (adapted from Li et al. (2018)).

The genus *Neofusicoccum* is a member of the Botryosphaeriaceae (Botryosphaeriales, Dothideomycetes) found on a wide range of plant hosts of agricultural, forestry, ecological and economic relevance (Crous et al., 2006; Slippers &Wingfield, 2007; Slippers et al., 2013). Species belonging to this genus are considered pathogenic to numerous plants causing serious economic losses (Slippers et el., 2017). Inside the plant, *Neofusicoccum* has the ability to colonize without producing any external symptoms, remaining inside the host as an endophyte (Slippers & Wingfield, 2007). The change from an endophytic to a pathogenic phase is often related to stress such as drought, extreme temperature fluctuations, nutrient deficiencies and mechanical injuries. Infected plants can display a multiplicity of symptoms such as leaf spots, fruit rots, seedling damping-off and collar rot, cankers, blight of shoots and seedlings, blue-stain of the sapwood, gummosis, dieback and tree death (Slippers & Wingfield, 2007). In 29 species presently accepted in the genus some are known to have very broad host and geographic ranges while others exhibit some host preferences. For instance, *N. parvum* was reported from 90 hosts in 29 countries on six continents (Sakalidis et al., 2013).

Neofusicoccum parvum is a widespread and important phytopathogen of wide range of hosts around the world, including important fruit crops and forest trees. It is considered a major pathogen of *Eucalyptus* and able to cause dieback and canker disease especially under stress (Barradas et al., 2016; Burgess et al., 2005; Chen et al., 2011; Gezahgne et al., 2004; Mohali et al., 2007; Pavlic et al., 2007; Pérez et al., 2010; Rodas et al., 2009; Slippers et al., 2009). Despite the relevance of this pathogen the mechanism of interaction between this fungus and its hosts is not known. *Neofusicoccum parvum* virulence is related to the ability of this fungus to colonize woody tissue combined with the expression of extracellular proteins with phytotoxic properties and also production of several phytotoxins, including (3*R*, 4*R*) - (-) - 4-hydroxy - and (3*R*, 4*S*) - (-) – 4 – hydroxy - mellein, isosclerone, and tyrosol (Abou-Mansour et al., 2015; Evidente et al., 2010).Through pruning wounds, the pathogen colonizes the host tissues causing shoot dieback, cane bleaching, bud necrosis, and graft failure (Úrbez-Torres & Gubler, 2009). However, full understanding of the pathogenicity mechanism is still far from being accomplished.

PLANT-FUNGAL INTERACTIONS

When fungi enter the plant system, they can use different survival strategies and lifestyles such as mutualistic, symbiotic, endophytic or parasitic through which they are closely associated with their hosts (Figure 1.2). Most of these lifestyles may not lead to damages in crops. But, in some cases, endophytic fungi may change their lifestyle to pathogenic, under the influence of a trigger, leading to disease and even host mortality. So far, many reports about plant-fungal interactions lifestyles have been published (Bacon & Yates, 2006; Bonfante & Genre, 2010; Mehta et al., 2008; Rai & Agarkar, 2016; Saikkonen et al., 1998; Schulz et al., 1999).

Endophytes live within a plant for at least part of its life cycle without causing apparent disease (Schulz & Boyle, 2005). Parasites that, on the other hand, infect the plant tissue inducing disease symptoms and are considered as pathogens.

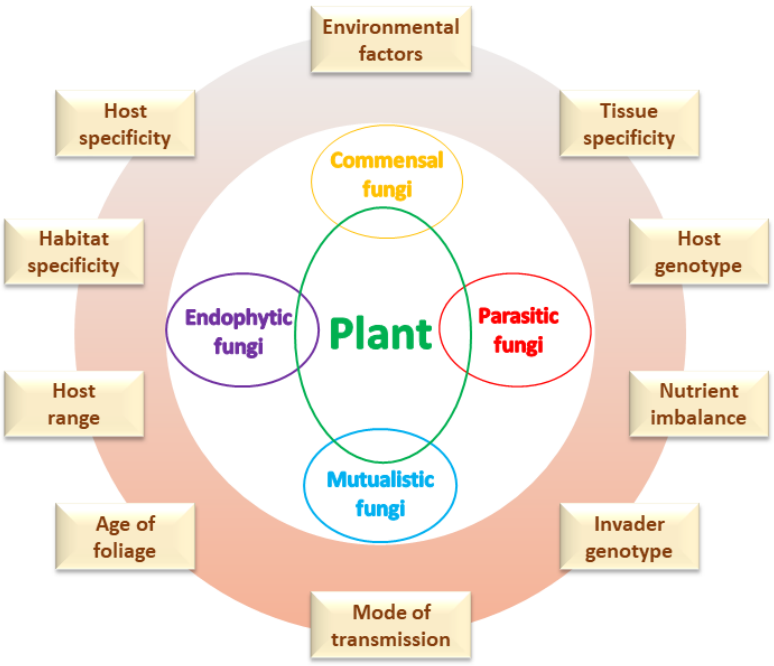

Figure 1.2 | Various plant–fungal interactions and the factors affecting these interactions (Rai & Agarkar, 2016)

Members of the family Botryosphaeriaceae have been described as endophytes and as latent pathogens causing diseases in numerous plant hosts (Sakalidis, 2011; Slippers & Wingfield, 2007; Yan et al., 2013). Biochemical and genetic responses caused by external stimuli resulting from changing environmental conditions inside hosts (changes in host behaviour or microbial equilibrium) or outside hosts (changes in climate or extreme environmental events), triggers Botryosphaeriaceae fungi to change their lifestyles from endophytic to pathogenic. Because of this transition, these fungi can be regarded as plant opportunistic pathogens since their pathogenic nature may appear when induced by environmental factors or when plants become are under stress. Due to their ability to shift between endophytic and pathogenic phases, botryosphaeriaceous taxa have been subjected to various critical studies concerning pathogenicity (Abou-Mansour et al., 2015; Amponsah et al., 2011; Baskarathevan et al., 2012; Beas-Fernandez et al., 2006; Fernandes et al., 2014; Sakalidis, 2011).

Plant pathogenic fungi are spread through all fungal groups and their interaction with plants is diverse, with few common structural characteristics. Saprotrophic fungi obtain their nutrients from dead organic materials, while other fungi establish interaction with their hosts. Biotrophic pathogens need living host tissues to exhaust while nectrotrophic pathogens first kill the host tissues through the

secretion of enzymes and toxins to be able to take the nutrients from the host. Hemibiotrophs first develop as a biotroph but complete their life cycle as necrotroph. They initially colonize plant tissues without causing any noticeable diseases. After an expanded incubation period, they gradually become necrotrophic by killing host cells, and eventually feed on dead tissue (Mendgen & Hahn, 2002). As mentioned earlier, Botryosphaeriaceae can apparently "deceive" their hosts colonizing it and later becoming necrotrophic pathogens, when the infected plants are exposed to stress factors (Marsberg et al., 2017). Necrotrophic and hemibiotrophic fungi (in their necrotrophic stage) also secrete diverse types of effectors including damage-eliciting or cell death-eliciting proteins and secondary metabolites (van Kan, 2006). Biotrophic and hemibiotrophic fungi (in their biotrophic stage) also secrete various virulence factors recognized as effectors to suppress host defense and orchestrate reprogramming of infected tissues to meet the requirements of the pathogen (Mendgen & Hahn, 2002).

The disease cycle results in the development and perpetuation of disease: fungal spread, pre-penetration/germination, host penetration, infection phase, growth/reproduction, dissemination/new infection, and dormancy (Daly, 1984) (Figure 1.3). As soon as the fungal spores land the plant surface they start to adhere to surfaces immediately upon contact by secretion of molecules, such as polysaccharides or glycoproteins (Ikeda et al., 2012; Newey et al., 2007; Tucker & Talbot, 2001; Zelinger et al., 2006). Recently, a study was conducted to examine the effect of surface wettability, hardness and surface contact on the germination and subsequent development of Botryosphaeriaceae species conidia (*B. dothidea*, *N. luteum* and *N. parvum*) (Sammonds et al., 2019). It was shown that conidia of all three species were able to adhere and germinate on a variety of surfaces being this flexibility indicative of their reported pathogenicity of different host tissues. After germination, some fungi penetrate the plants through natural openings or wounds, while several plant pathogenic fungi develop appressoria at the entry points (Herman & Williams, 2012; Łazniewska et al., 2012; Mendgen et al., 1996; Ryder & Talbot, 2015). This structure employs high turgor pressure to push the hypha across the plant cell wall, acting often with secreted cell-wall degrading enzymes (CWDE) together to enter the host plants and suppress the plant defences (Horbach et al., 2011; Kleemann et al., 2012; Pryce-Jones et al., 1999; Tucker & Talbot, 2001). Botryosphaeriaceae are known to enter the host plant through pruning wounds (Úrbez-Torres & Gubler, 2011; van Niekerk et al., 2010), natural openings such as stomata and lenticels, or even penetrate host tissue directly (Kim et al., 2001; Michailides, 1991). At the infection and invasion phases, the pathogen contacts with host cells and spreading from cell to cell leading to visible symptoms. During reproduction fungal spores are produced on the host tissue. Spores are disseminated from the site of reproduction to other susceptible host surfaces or new plants. Lastly, dormancy phase during which metabolism is reduced

by about 50 %, is an important strategy to survive long periods of time and helping the pathogen to survive under unfavourable conditions (Brown & Ogle, 1997).

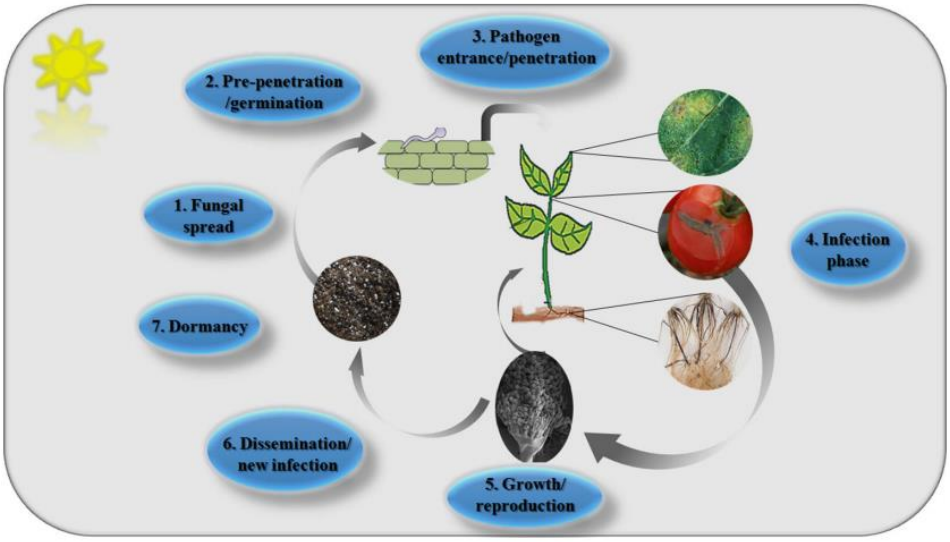

Figure 1.3 | Disease cycle. The interaction of a pathogen with a host is characterized by a series of sequential events called the disease cycle (Zeilinger et al., 2015).

Any invaders that enter the plant must still face the formidable task of overcoming the plant immune response. Plant immunity can be broken down into two components operating on different time scales (Figure 1.4). The basal defense system appears early in pathogen interaction, while the resistance (*R*) gene-mediated defense operates on the time scale of hours. In a basal defence system, plants detect Microbe, Pathogen or Damage- Associated Molecular Patterns (MAMPs, PAMPs or DAMPs), triggering what is generally called Pattern-triggered immunity (PTI) (Bigeard et al., 2015; Boller & Felix, 2009; Derevnina et al., 2016; Jones & Dangl, 2006; Muthamilarasan & Prasad, 2013; Zhang & Zhou, 2010). The recognition of PAMPs, which precedes PTI, is performed by plant proteins named pattern recognition receptors (PRRs) (Medzhitov & Janeway, 1997; Nicaise et al., 2009). PTI normally provides a fast and robust defence that restricts tissue colonization of the majority of non-adapted pathogen infections, comprising the concerted production of reactive oxygen species (ROS) and secretion of antimicrobial compounds, phytohormones, hydrolytic enzymes and inhibitors of microbial hydrolytic enzymes (Ahuja et al., 2012; Clérivet et al., 2000; El-Bebany et al., 2013; Herman & Williams, 2012; Luna et al., 2011; Pieterse et al., 2009; Torres, 2010). Pathogens evolved effectors that can work as suppressors of PTI responses leading to a susceptible state called effector triggered susceptibility (ETS). However, plants, in this evolutionary battle, evolved another family of receptors, named resistance or R proteins, that can recognise effectors and trigger an immune reaction designated as effector triggered immunity (ETI) (Jones & Dangl, 2006). ETI is typically more pathogen

specific than PTI and is often associated with the hypersensitive response (HR) which is a form of programmed cell death (PCD) (Coll et al., 2011; Heath, 2000; Jones and Dangl, 2006). HR is defined as a rapid cell death that occurs in response to pathogen attack to confine intruding (obligate) biotrophic pathogens to the site of penetration (Coll et al., 2011; Heath, 2000; Jones & Dangl, 2006). A series of biochemical perturbations such as ion flues, lipid hyperperoxidation, protein phosphorylation, nitric oxide generation, a burst of reactive oxygen species (ROS) and biosynthesis of antimicrobial compounds are stimulated in HR which keep the pathogen isolated from the rest of the plant and prevent further damage (Mehta et al., 2008; Pieterse et al., 2009). Moreover, pathogen may also express some proteins such as superoxide dismutase and catalases to overcome the plant defense or to inactivate ROS. Therefore, the interaction between host plant and pathogen is a complicated and dynamic one.

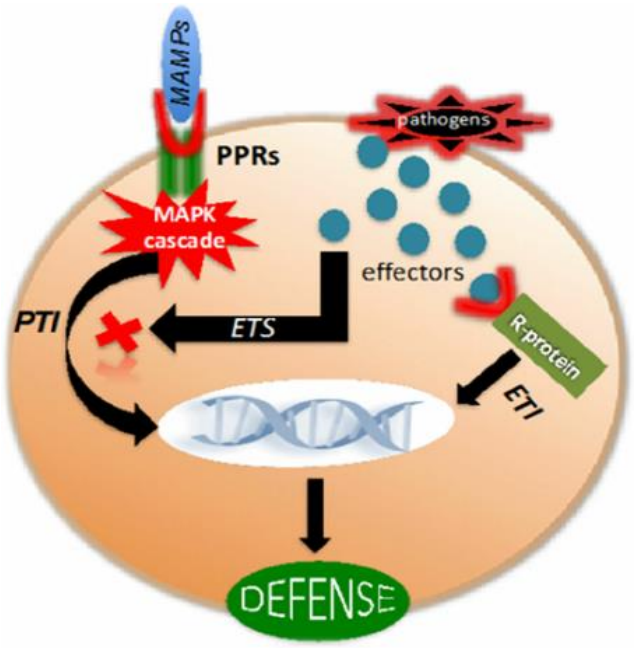

Figure 1.4 | Defence mechanisms in plants (Kazan & Lyons, 2014).

NECROSIS AND ETHYLENE-INDUCING PROTEINS (NLPS)

The Necrosis and Ethylene-inducing Proteins Nep1 are small proteins (<30 kDa) known to be related to pathogenicity initially purified from culture filtrates of *Fusarium oxysporum* f.sp. *erythroxyli* (Bailey, 1995). Since then, many other NEPs and NEP-like proteins (NLPs) were reported from a spectrum of microorganisms including bacteria, fungi and oomycetes but not from higher organisms (Pemberton & Salmond, 2004). NLPs are present in Gram-negative and Gram-positive bacteria with saprophytic or pathogenic lifestyles. In fungi and oomycetes, NLPs are especially present in species interacting with

plants, and predominantly in species that display a hemibiotrophic or necrotrophic lifestyle on plants (Qutab et al., 2006).

NLPs are secreted proteins that share a conserved heptapeptide motif (GHRHDWE) and two to six cysteine (C) residues (Fellbrich et al., 2002; Ottmann et al., 2009). Formation of at least one disulfide bridge (C-C) between conserved cysteines is a requirement for NLP activities (Gijzen & Nurnberger, 2006; Oome & Van den Ackerveken, 2014). The number of conserved C residues has been used to classify the NLPs into types 1, 2 and 3. Types 1, 2 and 3 NLPs have two, four and six C residues, respectively (Gijzen & Nurnberger, 2006; Oome & Van den Ackerveken, 2014). In addition, type 1 NLPs have a subgroup of NLPs which are noncytoxic (Oome & Van den Ackerveken, 2014).

Ottmann et al. (2009) showed that the crystal structure of an NLP from *Pythium aphanidermatum* (NLPPya) has structural similarities to the pore-forming toxins Actinoporins isolated from marine organisms (Ottmann et al., 2009). Dicot-derived membrane vesicles exposed *in vitro* to NLPs were permeabilized, suggesting that cytotoxicity is the result of membrane leakage. However, there is no evidence of pore-forming activity of NLPs in plants. In addition, inoculation of *Arabidopsis thaliana* with recombinant NLPs leads to rapid activation of plant defense and cell death (Bae et al. 2006; Qutob et al., 2006), suggesting an active role of the plant in necrosis induction.

Nowadays, NLP proteins are known to elicit a cell defense response and necrosis in large numbers of dicotyledonous plants, not monocotyledonous (Bailey, 1995; Keates et al., 2003; Staats et al., 2007; Schouten et al., 2008). A conserved 20-mer fragment (nlp20) is sufficient for immune activation by cytotoxic and non-cytotoxic NLPs in various *Brassicaceae* species including *Arabidopsis* (Böhm et al., 2014; Oome et al., 2014). Many of the 1,100 NLP-encoding sequences deposited in databases harbour this motif and are likely active triggers of plant defences (Böhm et al., 2014) Production of ethylene, H_2O_2, nitric oxide, accumulation of transcripts encoding pathogenesis-related proteins, calcium influx, release of phytoalexins, activation of MAP kinases and necrotic lesion formation (Bae et al., 2006; Fellbrich et al., 2002; Keates et al., 1998;) are active responses of plants to a perceived pathogen attack and is associated with the induction of the defense response.

Recently, glycosylinositol phosphorylceramide (GIPC) sphingolipids have been identified as target site of NLPs in tobacco (Lenarčič et al., 2017) and differences in length of the glycosyl chain in GIPC receptors between monocots and eudicots determines proper positioning of the toxin prior to membrane insertion and pore formation (Figure 1.5). Monocot GIPCs usually carry longer glycosyl chains such as compared to those found in dicot GIPCs, thus explaining why monocot plants are largely tolerant to NLP cytolysins (Figure 1.6) (Lenarčič et al., 2017). The mode of action and exact mechanism of NLPs however is unknown. Several studies suggested the contribution of NLPs to the virulence of plant pathogens (Amsellem et al., 2002; Garcia et al., 2007; Santhanam et al., 2013). In contrast, some

reports showed NLPs are dispensable for the pathogen to cause disease (Fang et al., 2017; Motteram et al., 2009; Staats et al., 2007). In general, there is a wide functional diversity of NLPs among plant pathogens that need further exploration.

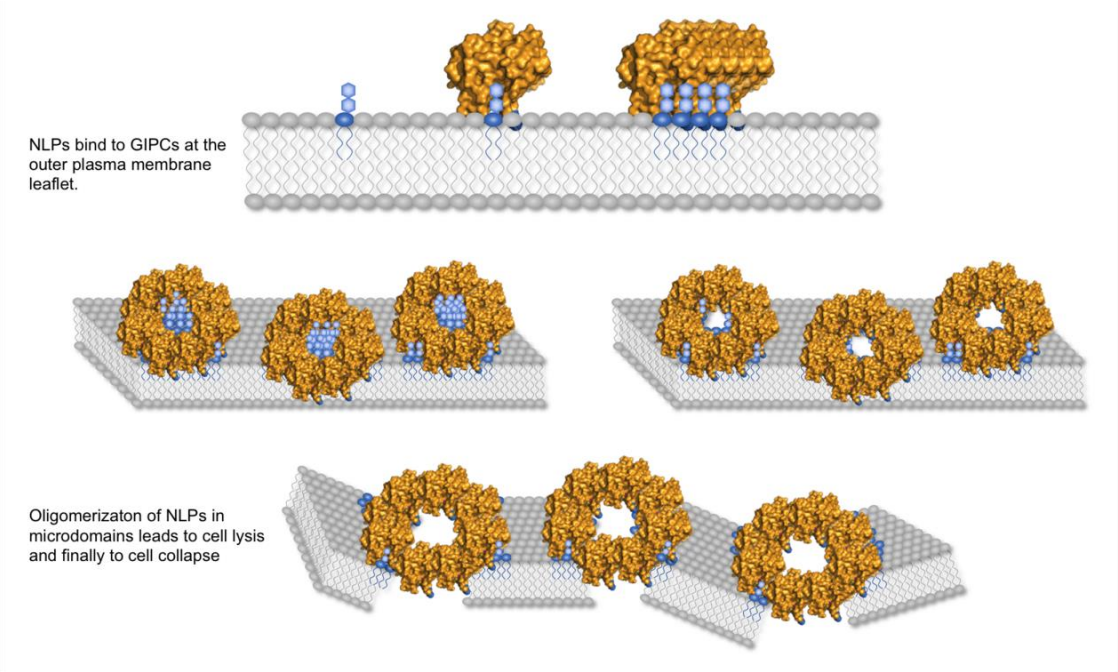

Figure 1.5 | How do NLP proteins bind to plant GIPCs and cause cell lysis? (Nürnberger, 2018)

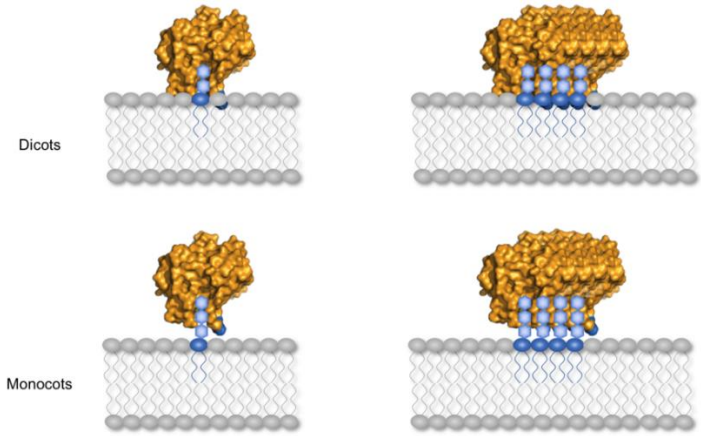

Figure 1.6 | GIPCs in dicots and monocots. (Nürnberger, 2018)

PROTEOMICS

Understanding the genome is a first step in understanding the complexity of biological function. Transcripts do not provide the complete cellular regulatory information as gene expression is post-transcriptionally regulated and proteins responsible for cell biological functions are expressed in a

highly dynamic and interactive manner (Dhingra et al., 2005). Therefore, for a picture closer to the functional panorama of a cell, protein levels need to be determined directly. Proteomics is the systematic study of the proteins expressed by a genome or by a cell or tissue, including their interactions, modification, localization and functions (Coiras et al., 2008). Proteomics has been increasingly used to exploit the potential of fungi in biotechnological and medical applications (Kniemeyer, 2011; Oda et al., 2006; Oliveira & Graaff, 2011), as well as to understand the molecular mechanisms behind plant-pathogenic interactions (Bhadauria et al., 2010; Felix et al., 2019; Fernandes et al., 2014; González-Fernández & Jorrín-Novo, 2012). More specifically, the secretome characterization of pathogenic fungi enable the identification of proteins that are potential virulence factors, providing insights into the infection mechanism and potential therapeutic targets. Fungi secrete proteins with relevant nutritional and infection roles (Faulkner & Robatzek, 2012; Jonge et al., 2011). Nonetheless, little is known regarding the proteome of the family Botryosphaeriaceae since the genome of few members of this family has been sequenced yet (Blanco-Ulate et al., 2013; Islam et al., 2012; Morales-Cruz et al., 2015; Nest et al., 2014). The first extracellular proteome study regarding organisms belonging to this family was conducted by Cobos et al. (2010), leading to identification of 16 proteins such as glucosidases, peptidases, necrosis and ethylene-inducing proteins (NLP) and PhiA proteins related to pathogenicity of *Diplodia Seriata* (Cobos et al., 2010). Fernandes et al. (2014) conducted a secretome analysis for another member of Botryosphaeriaceae, *Diplodia corticola*, to elucidate the molecular mechanisms of pathogenesis. The analysis identified several potential virulence factors (carbohydrate degrading enzymes, proteases, putative glucan-*β*-glucosidse, neuraminidase and ferulic acid esterase) involved in Cork oak (*Quercus suber*) decline. Lack of available sequenced genome data and laborious and technically difficult techniques (1D and 2D SDS-PAGE followed by mass spectrometry) used in those study limited protein identification. Another study (Uranga et al., 2017) analyzed the proteins expressed by *Lasiodiplodia. theobromae* in the presence of triglycerides and glucose using an adapted method of Folch protein extraction. This proteomic exploration has led to the identification of several proteins with biotechnological potential (*e.g.* allergenic enolases, proteases and lipases) and also pathogenesis-related proteins. Novel peptide sequences were found, contributing to genomic annotation and thus to improve fungal bioinformatics databases (Uranga et al., 2017).

AIMS

The work presented in this thesis has focused on understanding host-pathogen interactions and unravel mechanisms of pathogenicity/virulence of Botryosphaeriaceae fungi, with a special attention on *N. parvum*, one of the most aggressive species in the family. The aim has been three-sided:

- To determine the impact of temperature on phytotoxic and cytotoxic effects of six strains from five species of Botryosphaeriaceae culture filtrates with different levels of aggressiveness on detached tomato leaves and two different mammalian cell lines (3T3 cells and Vero cells).
- To characterize the secretome of *N. parvum* and evaluate its response to the *in vitro* host mimicry.
- To investigate the functional properties of necrosis and ethylene inducing proteins (NLPs) in order to infer their role in *N. parvum* pathogenicity.

REFERENCES

Abou-Mansour, E., Débieux, J.-L., Ramírez-Suero, M., Bénard-Gellon, M., Magnin-Robert, M., Spagnolo, A., & L'Haridon, F. (2015). Phytotoxic metabolites from *Neofusicoccum parvum*, a pathogen of Botryosphaeria dieback of grapevine. *Phytochemistry*, 115, 207–215.

Ahuja, I., Kissen, R., & Bones, A. M. (2012). Phytoalexins in defense against pathogens. *Trends in Plant Science*, 17(2), 73–90.

Amponsah, N. T., Jones, E. E., Ridgway, H. J., & Jaspers, M. V. (2011). Identification, potential inoculum sources and pathogenicity of botryosphaeriaceous species associated with grapevine dieback disease in New Zealand. *European Journal of Plant Pathology*, 131(3), 467.

Amsellem, Z., Cohen, B. A., & Gressel, J. (2002). Engineering hypervirulence in a mycoherbicidal fungus for efficient weed control. *Nature Biotechnology*, 20(10), 1035–1039.

Bacon, C. W., & Yates, I. E. (2006). Endophytic root colonization by *Fusarium* species: histology, plant interactions, and toxicity. In Microbial root endophytes (pp. 133–152). Springer.

Bae, H., Kim, M. S., Sicher, R. C., Bae, H.-J., & Bailey, B. A. (2006). Necrosis- and ethylene-inducing peptide from *Fusarium oxysporum* induces a complex cascade of transcripts associated with signal transduction and cell death in *Arabidopsis*. *Plant Physiology*, 141(3), 1056–1067.

Bailey, B. A. (1995). Purification of a protein from culture filtrates of *Fusarium oxysporum* that induces ethylene and necrosis in leaves of *Erythroxylum coca*. *Phytopathology*, 85(10), 1250–1255.

Barradas, C., Alan J. L., P., Correia, A., Eugénio, D., Bragança, H., & Alves, A. (2016). Diversity and potential impact of Botryosphaeriaceae species associated with *Eucalyptus globulus* plantations in Portugal. *European Journal of Plant Pathology*, 146(2), 245–257.

Baskarathevan, J., Jaspers, M. V, Jones, E. E., Cruickshank, R. H., & Ridgway, H. J. (2012). Genetic and pathogenic diversity of *Neofusicoccum parvum* in New Zealand vineyards. *Fungal Biology*, 116(2), 276–288.

Beas-Fernandez, R., De Santiago-De Santiago, A., Hernandez-Delgado, S., & Mayek-Perez, N. (2006). Characterization of Mexican and non-Mexican isolates of *Macrophomina phaseolina* based on morphological characteristics, pathogenicity on bean seeds and endoglucanase genes. *Journal of Plant Pathology*, 53–60.

Bennett, B. M. (2010). The El Dorado of forestry: The *Eucalyptus* in India, South Africa, and Thailand, 1850–2000. *International Review of Social History*, 55(S18), 27–50.

Bhadauria, V., Banniza, S., & Wang, L. (2010). Proteomic studies of phytopathogenic fungi, oomycetes and their interactions with hosts. *European Journal of Plant Pathology*, 126(1), 81–95.

Bigeard, J., Colcombet, J., & Hirt, H. (2015). Signaling mechanisms in pattern-triggered immunity (PTI). *Molecular Plant*, 8(4), 521–539.

Blanco-Ulate, B., Rolshausen, P., & Cantu, D. (2013). Draft genome sequence of *Neofusicoccum parvum* isolate UCR-NP2, a fungal vascular pathogen associated with grapevine cankers. *Genome Announcements*, 1(3), e00339-13.

Böhm, H., Albert, I., Oome, S., Raaymakers, T. M., Van den Ackerveken, G., & Nürnberger, T. (2014). A conserved peptide pattern from a widespread microbial virulence factor triggers pattern-induced immunity in *Arabidopsis*. *PLOS Pathogens*, 10(11), e1004491.

Boller, T., & Felix, G. (2009). A renaissance of elicitors: perception of microbe-associated molecular patterns and danger signals by pattern-recognition receptors. *Annual Review of Plant Biology*, 60, 379–406.

Bonfante, P., & Genre, A. (2010). Mechanisms underlying beneficial plant–fungus interactions in mycorrhizal symbiosis. *Nature Communications*, 1, 48.

Brown, J. F., & Ogle, H. J. (1997). Plant pathogens and plant diseases. Armidale, N.S.W: Rockvale Publications for the Division of Botany, School of Rural Science and Natural Resources, University of New England.

Burgess, T. I., Barber, P. A., & Hardy, G. E. S. J. (2005). Botryosphaeria spp. associated with eucalypts in Western Australia, including the description of *Fusicoccum macroclavatum* sp. nov. *Australasian Plant Pathology*, 34(4), 557–567.

Burgess, T., & Wingfield, M. J. (2002). Impact of fungal pathogens in natural forest ecosystems: a focus on eucalypts. In Microorganisms in plant conservation and biodiversity (pp. 285–306). Springer.

Felix, C., Meneses, R., Gonçalves, M. F. M., Tilleman, L., Duarte, A. S., Jorrín-Novo, J. V., Van de Peer, Y., Deforce, D., Van Nieuwerburgh, F., Esteves, A.C., & Alves, A. (2019). A multi-omics analysis of the grapevine pathogen *Lasiodiplodia theobromae* reveals that temperature affects the expression of virulence- and pathogenicity-related genes. *Scientific Reports*, 9(1), 13144.

Chen, S., Pavlic, D., Roux, J., Slippers, B., Xie, Y., Wingfield, M. J., & Zhou, X. D. (2011). Characterization of Botryosphaeriaceae from plantation-grown *Eucalyptus* species in South China. *Plant Pathology*, 60(4), 739–751.

Clérivet, A., Deon, V., Alami, I., Lopez, F., Geiger, J. P., & Nicole, M. (2000). Tyloses and gels associated with cellulose accumulation in vessels are responses of plane tree seedlings (*Platanus* x *acerifolia*) to the vascular fungus *Ceratocystis fimbriata* f. sp *platani*. *Trees*, 15(1), 25—31.

Cobos, R., Barreiro, C., Mateos, R. M., & Coque, J.-J. R. (2010). Cytoplasmic- and extracellular-proteome analysis of *Diplodia seriata*: a phytopathogenic fungus involved in grapevine decline. *Proteome Science*, 8, 46.

Coiras, M., Camafeita, E., Lopez-Huertas, M. R., Calvo, E., Lopez, J. A., & Alcami, J. (2008). Application of proteomics technology for analyzing the interactions between host cells and intracellular infectious agents. *Proteomics*, 8(4), 852–873.

Coll, N. S., Epple, P., & Dangl, J. L. (2011). Programmed cell death in the plant immune system. *Cell Death and Differentiation*, 18(8), 1247–1256.

Crous, P. W., Slippers, B., Wingfield, M. J., Rheeder, J., Marasas, W. F. O., Philips, A. J. L., & Groenewald, J. Z. (2006). Phylogenetic lineages in the Botryosphaeriaceae. *Studies in Mycology*, 55, 235–253.

Daly, J. M. (1984). The role of recognition in plant disease. *Annual Review of Phytopathology*, 22(1), 273–307.

de Jonge, R., Bolton, M. D., & Thomma, B. P. H. J. (2011). How filamentous pathogens co-opt plants: the ins and outs of fungal effectors. *Current Opinion in Plant Biology*, 14(4), 400–406.

de Oliveira, J. M. P. F., & de Graaff, L. H. (2011). Proteomics of industrial fungi: trends and insights for biotechnology. *Applied Microbiology and Biotechnology*, 89(2), 225–237.

Derevnina, L., Dagdas, Y. F., de la Concepcion, J. C., Bialas, A., Kellner, R., Petre, B., & Kamoun, S. (2016). Nine things to know about elicitins. *The New Phytologist*, 212(4), 888–895.

Dhingra, V., Gupta, M., Andacht, & T., & Fu, Z. F. (2005). New frontiers in proteomics research: a perspective. *International Journal of Pharmaceutics*, 299(1), 1–18.

Dissanayake, A. J., Phillips, A. J. L., Li, X. H., & Hyde, K. D. (2016). Botryosphaeriaceae: current status of genera and species. *Mycosphere*, 7(7), 1001–1073.

Eastburn, D. M., McElrone, A. J., & Bilgin, D. D. (2011). Influence of atmospheric and climatic change on plant–pathogen interactions. *Plant Pathology*, 60(1), 54–69.

El-Bebany, A. F., Adam, L. R., & Daayf, F. (2013). Differential accumulation of phenolic compounds in potato in response to weakly and highly aggressive isolates of *Verticillium dahliae*. *Canadian Journal of Plant Pathology*, 35(2), 232–240.

Evidente, A., Punzo, B., Andolfi, A., Cimmino, A., Melck, D., & Luque, J. (2010). Lipophilic phytotoxins produced by *Neofusicoccum parvum*, a grapevine canker agent. *Mediterranean Phytopathology,* 49, 74–79.

Fang, Y.-L., Peng, Y.-L., & Fan, J. (2017). The Nep1-like protein family of *Magnaporthe oryzae* is dispensable for the infection of rice plants. *Scientific Reports*, 7(1), 4372.

Faulkner, C., & Robatzek, S. (2012). Plants and pathogens: putting infection strategies and defence mechanisms on the map. *Current Opinion in Plant Biology*, 15(6), 699–707.

Fellbrich, G., Romanski, A., Varet, A., Blume, B., Brunner, F., Engelhardt, S., & Nurnberger, T. (2002). NPP1, a Phytophthora-associated trigger of plant defense in parsley and Arabidopsis. *The Plant Journal: For Cell and Molecular Biology*, 32(3), 375–390.

Fernandes, I., Alves, A., Correia, A., Devreese, B., & Esteves, A. C. (2014). Secretome analysis identifies potential virulence factors of *Diplodia corticola*, a fungal pathogen involved in cork oak (*Quercus suber*) decline. *Fungal Biology*, 118(5–6), 516–523.

Garcia, O., Macedo, J. A. N., Tiburcio, R., Zaparoli, G., Rincones, J., Bittencourt, L. M. C., & Cascardo, J. C. M. (2007). Characterization of necrosis and ethylene-inducing proteins (NEP) in the basidiomycete *Moniliophthora perniciosa*, the causal agent of witches' broom in *Theobroma cacao*. *Mycological Research*, 111(Pt 4), 443–455.

Gezahgne, A., Roux, J., Slippers, B., Wingfield, M. J., & Hare, P. D. (2004). Identification of the causal agent of Botryosphaeria stem canker in Ethiopian *Eucalyptus* plantations. *South African Journal of Botany*, 70(2), 241–248.

Gijzen, M., & Nurnberger, T. (2006). Nep1-like proteins from plant pathogens: recruitment and diversification of the NPP1 domain across taxa. *Phytochemistry*, 67(16), 1800–1807.

González-Fernández, R., & Jorrín-Novo, J. V. (2012). Contribution of proteomics to the study of plant pathogenic fungi. *Journal of Proteome Research*, 11(1), 3–16.

Heath, M. C. (2000). Hypersensitive response-related death. *Plant Molecular Biology*, 44(3), 321–334.

Herman, M., & Williams, M. (2012). Fighting for their lives: plants and pathogens. *The Plant Cell*, 24(6), 1–15.

Horbach, R., Navarro-Quesada, A. R., Knogge, W., & Deising, H. B. (2011). When and how to kill a plant cell: infection strategies of plant pathogenic fungi. *Journal of Plant Physiology*, 168(1), 51–62.

ICNF (2019). IFN6 – Principais resultados– relatório sumário [pdf], 34 pp, Instituto da Conservação da Natureza e das Florestas. Lisboa.

Ikeda, K., Inoue, K., Kitagawa, H., Meguro, H., Shimoi, S., & Park, P. (2012). The role of the extracellular matrix (ECM) in phytopathogenic fungi: a potential target for disease control. *Plant Pathology*, 131–150.

Islam, M. S., Haque, M. S., Islam, M. M., Emdad, E. M., Halim, A., Hossen, Q. M. M., & Alam, M. (2012). Tools to kill: genome of one of the most destructive plant pathogenic fungi *Macrophomina phaseolina*. *BMC Genomics*, 13(1), 493.

Jones, J. D. G., & Dangl, J. L. (2006). The plant immune system. *Nature*, 444(7117), 323–329.

Kazan, K., & Lyons, R. (2014). Intervention of phytohormone pathways by pathogen effectors. *The Plant Cell*, 26(6), 2285 LP – 2309.

Keates, S E, Loewus, F. A., Helms, G. L., & Zink, D. L. (1998). 5-O-(alpha-D-galactopyranosyl)-D-glycero-pent-2-enono-1,4-lactone: characterization in the oxalate-producing fungus, *Sclerotinia sclerotiorum*. *Phytochemistry*, 49(8), 2397–2401.

Keates, Sarah E, Kostman, T. A., Anderson, J. D., & Bailey, B. A. (2003). Altered gene expression in three plant species in response to treatment with Nep1, a fungal protein that causes necrosis. *Plant Physiology*, 132(3), 1610–1622.

Kim, K. W., Park, E. W., Kim, Y. H., Ahn, K.-K., Kim, P. G., & Kim, K. S. (2001). Latency- and defense-related ultrastructural characteristics of apple fruit tissues infected with *Botryosphaeria dothidea*. *Phytopathology*, 91(2), 165–172.

Kleemann, J., Rincon-Rivera, L. J., Takahara, H., Neumann, U., Ver Loren van Themaat, E., van der Does, H. C., & O'Connell, R. J. (2012). Correction: Sequential delivery of host-induced virulence effectors by appressoria and intracellular hyphae of the phytopathogen *Colletotrichum higginsianum*. *PLOS Pathogens*, 8(8), e1002643.

Kniemeyer, O. (2011). Proteomics of eukaryotic microorganisms: the medically and biotechnologically important fungal genus *Aspergillus*. *Proteomics*, 11(15), 3232–3243.

Łaźniewska, J., Macioszek, V. K., & Kononowicz, A. K. (2012). Plant-fungus interface: the role of surface structures in plant resistance and susceptibility to pathogenic fungi. *Physiological and Molecular Plant Pathology*, 78, 24–30.

Lenarcic, T., Albert, I., Bohm, H., Hodnik, V., Pirc, K., Zavec, A. B., & Nurnberger, T. (2017). Eudicot plant-specific sphingolipids determine host selectivity of microbial NLP cytolysins. *Science* (*New York*, *N.Y.*), 358(6369), 1431–1434.

Li, G., Arnold, R. J., Liu, F., Li, J., & Chen, S. (2015). Identification and pathogenicity of *Lasiodiplodia* species from *Eucalyptus urophylla*× *grandis*, *Polyscias balfouriana* and *Bougainvillea spectabilis* in southern China. *Journal of Phytopathology*, 163(11–12), 956–967.

Li, G. Q., Liu, F. F., Li, J. Q., Liu, Q. L., & Chen, S. F. (2018). Botryosphaeriaceae from *Eucalyptus* plantations and adjacent plants in China. *Persoonia: Molecular Phylogeny and Evolution of Fungi*, 40, 63–95.

Liu, J.-K., Phookamsak, R., Doilom, M., Wikee, S., Li, Y.-M., Ariyawansha, H., & Bhat, J. D. (2012). Towards a natural classification of Botryosphaeriales. *Fungal Diversity*, 57(1), 149–210.

Luna, E., Pastor, V., Robert, J., Flors, V., Mauch-Mani, B., & Ton, J. (2011). Callose deposition: a multifaceted plant defense response. *Molecular Plant-Microbe Interaction: MPMI*, 24(2), 183–193.

Marsberg, A., Kemler, M., Jami, F., Nagel, J. H., Postma-Smidt, A., Naidoo, S., & Slippers, B. (2017). *Botryosphaeria dothidea*: a latent pathogen of global importance to woody plant health. *Molecular Plant Pathology*, 18(4), 477–488.

Medzhitov, R., & Janeway, C. A. J. (1997). Innate immunity: the virtues of a nonclonal system of recognition. *Cell*, 91(3), 295–298.

Mehta, A., Brasileiro, A. C. M., Souza, D. S. L., Romano, E., Campos, M. A., Grossi-de-Sá, M. F., & Bevitori, R. (2008). Plant–pathogen interactions: what is proteomics telling us? *The FEBS Journal*, 275(15), 3731–3746.

Mendgen, K, Hahn, M., & Deising, H. (1996). Morphogenesis and mechanisms of penetration by plant pathogenic fungi. *Annual Review of Phytopathology*, 34(1), 367–386.

Mendgen, Kurt, & Hahn, M. (2002). Plant infection and the establishment of fungal biotrophy. *Trends in Plant Science*, 7(8), 352–356.

Michailides, T. J. (1991). Pathogenicity, distribution, sources of inoculum, and infection courts of *Botryosphaeria dothidea* on pistachio. *Phytopathology*, 81(5), 566–573.

Mohali, S., Slippers, B., & Wingfield, M. J. (2007). Identification of Botryosphaeriaceae from *Eucalyptus*, *Acacia* and *Pinus* in Venezuela. *Fungal Diversity*, 25(25), 103–125.

Morales-Cruz, A., Amrine, K. C. H., Blanco-Ulate, B., Lawrence, D. P., Travadon, R., Rolshausen, P. E., & Cantu, D. (2015). Distinctive expansion of gene families associated with plant cell wall degradation, secondary metabolism, and nutrient uptake in the genomes of grapevine trunk pathogens. *BMC Genomics*, 16, 469.

Motteram, J., Kufner, I., Deller, S., Brunner, F., Hammond-Kosack, K. E., Nurnberger, T., & Rudd, J. J. (2009). Molecular characterization and functional analysis of MgNLP, the sole NPP1 domain-containing protein, from the fungal wheat leaf pathogen *Mycosphaerella graminicola*. *Molecular plant-microbe Interactions*: *MPMI*, 22(7), 790–799.

Muthamilarasan, M., & Prasad, M. (2013). Plant innate immunity: an updated insight into defense mechanism. *Journal of Biosciences*, 38(2), 433–449.

Nürnberger, T. (2018, March 15). Research Group Nürnberger, Universität Tübingen. *Identification of bacterial PAMPs and their cognate pattern recognition receptors, and exploitation of plant PRRs to engineer resistant crops*. Retrieved from https://uni-tuebingen.de/en/faculties/faculty-of-science/departments/interdepartmental-centres/center-for-plant-molecular-biology/plant-biochem/research-groups/nuernberger/.

Newey, L. J., Caten, C. E., & Green, J. R. (2007). Rapid adhesion of *Stagonospora nodorum* spores to a hydrophobic surface requires pre-formed cell surface glycoproteins. *Mycological Research*, 111(11), 1255–1267.

Nicaise, V., Roux, M., & Zipfel, C. (2009). Recent advances in PAMP-triggered immunity against bacteria: pattern recognition receptors watch over and raise the alarm. *Plant Physiology*, 150(4), 1638 LP – 1647.

Oda, K., Kakizono, D., Yamada, O., Iefuji, H., Akita, O., & Iwashita, K. (2006). Proteomic analysis of extracellular proteins from *Aspergillus oryzae* grown under submerged and solid-state culture conditions. *Applied and Environmental Microbiology*, 72(5), 3448–3457.

Oome, S., & Van den Ackerveken, G. (2014). Comparative and functional analysis of the widely occurring family of Nep1-like proteins. Molecular *Plant-Microbe Interactions*: *MPMI*, 27(10), 1081–1094.

Ottmann, C., Luberacki, B., Küfner, I., Koch, W., Brunner, F., Weyand, M., & Oecking, C. (2009). A common toxin fold mediates microbial attack and plant defense. *Proceedings of the National Academy of Sciences*, 106(25), 10359 LP – 10364.

Pavlic, D., Slippers, B., Coutinho, T. A., & Wingfield, M. J. (2007). Botryosphaeriaceae occurring on native *Syzygium cordatum* in South Africa and their potential threat to *Eucalyptus*. Plant Pathology, 56(4), 624–636.

Pemberton, C. L., & Salmond, G. P. C. (2004). The Nep1-like proteins-a growing family of microbial elicitors of plant necrosis. *Molecular Plant Pathology*, 5(4), 353–359.

Pérez, C. A., Wingfield, M. J., Slippers, B., Altier, N. A., & Blanchette, R. A. (2010). Endophytic and canker-associated Botryosphaeriaceae occurring on non-native *Eucalyptus* and native Myrtaceae trees in Uruguay. *Fungal Diversity*, 41(1), 53–69.

Phillips, A. J. L., Alves, A., Abdollahzadeh, J., Slippers, B., Wingfield, M. J., Groenewald, J. Z., & Crous, P. W. (2013). The Botryosphaeriaceae: genera and species known from culture. *Studies in Mycology*, 76(1), 51–167.

Pieterse, C. M. J., Leon-Reyes, A., Van der Ent, S., & Van Wees, S. C. M. (2009). Networking by small-molecule hormones in plant immunity. *Nature Chemical Biology*, 5, 308.

Pillay, K., Slippers, B., Wingfield, M. J., & Gryzenhout, M. (2013). Diversity and distribution of co-infecting Botryosphaeriaceae from *Eucalyptus grandis* and *Syzygium cordatum* in South Africa. *South African Journal of Botany*, 84, 38–43.

Pryce-Jones, E., Carver, T. I. M., & Gurr, S. J. (1999). The roles of cellulase enzymes and mechanical force in host penetration by *Erysiphe graminis* f.sp.*hordei*. *Physiological and Molecular Plant Pathology*, 55(3), 175–182.

Punithalingam, E. (1980). Plant diseases attributed to *Botryodiplodia theobromae* Pat. J. Cramer.

Qutob, D., Kemmerling, B., Brunner, F., Kufner, I., Engelhardt, S., Gust, A. A., & Nurnberger, T. (2006). Phytotoxicity and innate immune responses induced by Nep1-like proteins. *The Plant Cell*, 18(12), 3721–3744.

Rai, M., & Agarkar, G. (2016). Plant–fungal interactions: what triggers the fungi to switch among lifestyles? *Critical Reviews in Microbiology*, 42(3), 428–438.

Rodas, C. A., Slippers, B., Gryzenhout, M., & Wingfield, M. J. (2009). Botryosphaeriaceae associated with *Eucalyptus* canker diseases in Colombia. *Forest Pathology*, 39(2), 110–123.

Ryder, L. S., & Talbot, N. J. (2015). Regulation of appressorium development in pathogenic fungi. *Current Opinion in Plant Biology*, 26, 8–13.

Saikkonen, K., Faeth, S. H., Helander, M., & Sullivan, T. J. (1998). Fungal endophytes: a continuum of interactions with host plants. *Annual Review of Ecology and Systematics*, 29(1), 319–343.

Sakalidis, M. (2011). Investigation and analysis of taxonomic irregularities with the Botryosphaeriaceae. Murdoch University.

Sakalidis, M. L., Slippers, B., Wingfield, B. D., Hardy, G. E. S. J., & Burgess, T. I. (2013). The challenge of understanding the origin, pathways and extent of fungal invasions: global populations of the *Neofusicoccum parvum–N. ribis* species complex. *Diversity and Distributions*, 19(8), 873–883.

Sammonds, J., Jaspers, M. V, & Jones, E. E. (2019). Influence of surface characteristics on germination and early growth of Botryosphaeriaceae species. *European Journal of Plant Pathology*, 1–10.

Santhanam, P., van Esse, H. P., Albert, I., Faino, L., Nurnberger, T., & Thomma, B. P. H. J. (2013). Evidence for functional diversification within a fungal NEP1-like protein family. *Molecular Plant-Microbe Interactions*: *MPMI*, 26(3), 278–286.

Schouten, A., van Baarlen, P., & van Kan, J. A. L. (2008). Phytotoxic Nep1-like proteins from the necrotrophic fungus *Botrytis cinerea* associate with membranes and the nucleus of plant cells. *The New Phytologist*, 177(2), 493–505.

Schulz, B., & Boyle, C. (2005). The endophytic continuum. *Mycological Research*, 109(6), 661–686.

Schulz, B., Römmert, A.-K., Dammann, U., Aust, H.-Jür., & Strack, D. (1999). The endophyte-host interaction: a balanced antagonism? *Mycological Research*, 103(10), 1275–1283.

Sinclair, W. A., & Lyon, H. H. (2005). Diseases of trees and shrubs. Comstock Publishing Associates.

Slippers, B, Boissin, E., Phillips, A. J. L., Groenewald, J. Z., Lombard, L., Wingfield, M. J., & Crous, P. W. (2013). Phylogenetic lineages in the Botryosphaeriales: a systematic and evolutionary framework. *Studies in Mycology*, 76(1), 31–49.

Slippers, B, Burgess, T., Pavlic, D., Ahumada, R., Maleme, H., Mohali, S., & Wingfield, M. J. (2009). A diverse assemblage of Botryosphaeriaceae infect *Eucalyptus* in native and non-native environments. *Southern Forests: A Journal of Forest Science*, 71(2), 101–110.

Slippers, B., Crous, P. W., Jami, F., Groenewald, J. Z., & Wingfield, M. J. (2017). Diversity in the Botryosphaeriales: Looking back, looking forward. *Fungal Biology*, 121(4), 307–321.

Slippers, Bernard, Roux, J., Wingfield, M. J., Van der Walt, F. J. J., Jami, F., Mehl, J. W. M., & Marais, G. J. (2014). Confronting the constraints of morphological taxonomy in the Botryosphaeriales. *Persoonia: Molecular Phylogeny and Evolution of Fungi*, 33, 155.

Slippers, Bernard, & Wingfield, M. J. (2007). Botryosphaeriaceae as endophytes and latent pathogens of woody plants: diversity, ecology and impact. *Fungal Biology Reviews*, 21(2), 90–106.

Staats, M., VAN Baarlen, P., Schouten, A., & VAN Kan, J. A. L. (2007). Functional analysis of NLP genes from *Botrytis elliptica*. *Molecular Plant Pathology*, 8(2), 209–214.

Sturrock, R. N., Frankel, S. J., Brown, A. V, Hennon, P. E., Kliejunas, J. T., Lewis, K. J., & Woods, A. J. (2011). Climate change and forest diseases. *Plant Pathology*, 60(1), 133–149.

Torres, M. A. (2010). ROS in biotic interactions. *Physiologia Plantarum*, 138(4), 414–429.

Tucker, S. L., & Talbot, N. J. (2001). Surface attachment and pre-penetration stage development by plant pathogenic fungi. *Annual Review of Phytopathology*, 39(1), 385–417.

Uranga, C. C., Ghassemian, M., & Hernández-Martínez, R. (2017). Novel proteins from proteomic analysis of the trunk disease fungus *Lasiodiplodia theobromae* (Botryosphaeriaceae). *Biochimie Open*, 4, 88–98.

Úrbez-Torres, J. R., Castro-Medina, F., Mohali, S. R., & Gubler, W. D. (2016). Botryosphaeriaceae species associated with cankers and dieback symptoms of *Acacia mangium* and *Pinus caribaea* var. *hondurensis* in Venezuela. *Plant Disease*, 100(12), 2455–2464.

Urbez-Torres, J. R., & Gubler, W. D. (2009). Pathogenicity of Botryosphaeriaceae species isolated from grapevine cankers in California. *Plant Disease*, 93(6), 584–592.

Úrbez-Torres, J. R., & Gubler, W. D. (2011). Susceptibility of grapevine pruning wounds to infection by *Lasiodiplodia theobromae* and *Neofusicoccum parvum*. *Plant Pathology*, 60(2), 261–270.

van der Nest, M. A., Bihon, W., De Vos, L., Naidoo, K., Roodt, D., Rubagotti, E., & Wingfield, B. D. (2014). Draft genome sequences of *Diplodia sapinea*, *Ceratocystis manginecans*, and *Ceratocystis moniliformis*. *IMA Fungus*, 5(1), 135–140.

van Kan, J. A. L. (2006). Licensed to kill: the lifestyle of a necrotrophic plant pathogen. *Trends in Plant Science*, 11(5), 247–253.

van Niekerk, J. M., Calitz, F. J., Halleen, F., & Fourie, P. H. (2010). Temporal spore dispersal patterns of grapevine trunk pathogens in South Africa. *European Journal of Plant Pathology*, 127(3), 375–390.

Yan, J.-Y., Xie, Y., Zhang, W., Wang, Y., Liu, J.-K., Hyde, K. D., & Yao, S.-W. (2013). Species of Botryosphaeriaceae involved in grapevine dieback in China. *Fungal Diversity*, 61(1), 221–236.

Zeilinger, S., Gupta, V. K., Dahms, T. E. S., Silva, R. N., Singh, H. B., Upadhyay, R. S., & Nayak S, C. (2015). Friends or foes? Emerging insights from fungal interactions with plants. *FEMS Microbiology Reviews*, 40(2), 182–207.

Zelinger, E., Hawes, C. R., Gurr, S. J., & Dewey, F. M. (2006). Attachment and adhesion of conidia of *Stagonospora nodorum* to natural and artificial surfaces. *Physiological and Molecular Plant Pathology*, 68(4), 209–215.

Zhang, J., & Zhou, J.-M. (2010). Plant immunity triggered by microbial molecular signatures. *Molecular Plant*, 3(5), 783–793.

CHAPTER 2

Effect of temperature on the phytotoxicity and cytotoxicity of Botryosphaeriaceae fungi

ABSTRACT

Botryosphaeriaceae fungi are phytopathogens mostly of woody hosts, causing numerous diseases, which ultimately may result in death of the host plant. Also, several Botryosphaeriaceae species have been associated with human infections. The number of available reports describing the effect of the expected increase on environmental temperature on Botryosphaeriaceae fungi are still scarce. In this study, the influence of temperature on the phytotoxicity and cytotoxicity of the culture filtrates of five Botryosphaeriaceae species — *Botryosphaeria dothidea* CAA642; *Diplodia corticola* CAA500; *Neofusicoccum parvum* CAA366 and CAA704; *N. eucalyptorum* CAA558 and *N. kwambonambiense* CAA755 — were evaluated on detached tomato leaves and on mammalian cell lines (Vero cells and 3T3 cells).

All culture filtrates of fungi grown at 25 °C were toxic to tomato leaves: symptoms were evaluated based on visual inspection of necrosis areas and on the maximum quantum yield of photosystem II (PSII), F_v/F_m. *Diplodia corticola* and *N. kwambonambiense* culture filtrates were the most toxic, followed by *N. parvum* CAA704 and *B. dothidea*. On the contrary, *N. parvum* CAA366 and *N. eucalyptorum* were the least pathogenic. However, except for *B. dothidea* culture filtrate, phytotoxicity dramatically decreased when strains were grown at 37 °C. All strains, except for *N. parvum* CAA366 and *N. eucalyptorum,* grown either at 25 °C or 37 °C, were cytotoxic to both animal cell lines (3T3 and Vero cells). *Neofusicoccum parvum* CAA366 and *N. eucalyptorum* were only cytotoxic to 3T3 cells. The culture filtrate of *D. corticola* grown at 25 °C was the most cytotoxic to mammalian cells, followed by the culture filtrate of *B. dothidea*. Also, we showed that *B. dothidea* was the most cytotoxic strain to both cell lines, at 37 °C, followed by *D. corticola* and *N. parvum* CAA704. Although the toxicity of *B. dothidea* to both cell lines and of *N. kwambonambiense* to Vero cells increased with temperature, the opposite was found for *D. corticola*, *N. parvum* CAA366, and *N. eucalyptorum*.

Phytotoxicity and cytotoxicity of Botryosphaeriaceae suggest that temperature modulates the expression of toxic compounds. In a scenario of a global increase of temperature, this modulation may contribute to new infections to plants by *B. dothidea* but also to humans specially in the case of *B. dothidea*.

KEYWORDS: phytotoxicity; cytotoxicity; phytopathogenic fungi; Botryosphaeriaceae; climate change

INTRODUCTION

Earth is facing a global climate change, with a predicted continuous increase of temperature, CO_2 level and heavy precipitation (IPCC, 2014). Increasing temperature is altering microorganisms' biogeographical distribution (Bebber et al., 2013) and modifying the dynamics of microorganism-host interactions (Eastburn et al., 2011). Environmental modifications also may convert symbiotic or commensal relations into pathogenic interactions (Bliska & Casadevall, 2009). Exposure of phytopathogenic fungi to these alterations may reveal threats to human health and to several economically important crops. Nevertheless, little effort has been directed to the identification of the impact that increased temperature will have on microorganism-host interactions (Eastburn et al., 2011; Gallana et al., 2015).

The family Botryosphaeriaceae comprises phytopathogens, saprobes or endophytes, mostly on woody hosts (Barradas et al., 2016; Burgess et al., 2006; Gramaje et al., 2012; Linaldeddu et al., 2009; Mohali et al., 2007; Sakalidis et al., 2013). These fungi generally exist as hemibiotrophs in healthy plant tissues, which makes them particularly important in international trade, since they may spread undetected from one region to another, promoting potentially severe damage to hosts (Slippers & Wingfield, 2007). The interchange from an endophytic lifestyle to a pathogenic one has been suggested to be triggered by stress such as drought, extreme temperature fluctuations, nutrient deficiencies and mechanical injuries (Slippers & Wingfield, 2007). Therefore, it is foreseen that these stress-related fungal pathogens will benefit from the current scenario of climate change. Infected plants can exhibit a multiplicity of disease symptoms such as dieback, canker, fruit rot, and ultimately death (Lawrence et al., 2017; Urbez-Torres & Gubler, 2009; Zlatkovic et al., 2016). Although foliar symptoms are observable, these pathogens have never been isolated from leaves, suggesting that extracellular molecules (metabolites and proteins) are the main drive for pathogenicity. It has been demonstrated that they are able to produce cell wall-degrading enzymes and phytotoxic metabolites whose synergistic action plays a role in the development of foliar symptoms (Andolfi et al*.,* 2011; Félix et al., 2019b; Gonçalves et al., 2019). In addition, a recent study also highlighted the role of secreted proteins for the cytotoxicity of *N. parvum* culture filtrates (Bénard-Gellon et al., 2015). Since extracellular molecules of these fungi are the main effectors for fungus-plant interactions, we centred our analysis on their extracellular molecules (present on the *in vitro* culture filtrate).

Barradas et al. (2016) characterised the phytopathogenicity/aggressiveness - based on the lesion length on *Eucalyptus* stem - of *Neofusicoccum parvum* (CAA704 and CAA366), *N. kwambonambiense*, *N. eucalyptorum*, *Diplodia corticola*, and *Botryosphaeria dothidea*. All six species were pathogenic to *Eucalyptus* but with distinct in aggressiveness: *D. corticola* and *N. kwambonambiense* were the most aggressive while *B. dothidea* was the least aggressive.

Botryosphaeriaceae fungi have occasionally been associated with human infections. This is the case of *L. theobromae* (Kindo et al., 2010; Saha et al., 2012a, 2012b; Summerbell et al., 2004; Thew & Todd, 2008; Woo et al., 2008) and *Macrophomina phaseolina* (Arora et al., 2012; Tan et al., 2008). Recently, *Botryosphaeria dothidea* a common plant pathogen has been associated with a case of ungual phaeohyphomycosis (Noguchi et al., 2017). A recent study revealed that the secretome of *L. theobromae* is cytotoxic to mammalian cells, supporting its ability to infect humans (Félix et al., 2016). In humans, fungal infections are difficult to treat due to the elevated toxicity of the fungicides available (Shalchian-Tabrizi et al., 2008).

Nonetheless, despite the relevance of these phytopathogens, only a few studies have highlighted the toxicity of the culture filtrates from Botryosphaeriaceae species to leaves of different plants (Bénard-Gellon et al., 2015; Guan et al., 2016; Martos et al., 2008; Ramírez -Suero et al., 2014; Reveglia et al., 2019). Furthermore, almost no studies have been carried out on the toxicity of Botryosphaeriaceae fungi culture filtrates towards animal cells. At last, there are only some studies that investigated the effect of temperature on the toxicity of the Botryosphaeriaceae fungus culture filtrate *Lasiodiplodia theobromae* (Félix et al., 2016, 2018, 2019).

Therefore, in this study the phytotoxic and cytotoxic effects of six strains from five species of Botryosphaeriaceae culture filtrates — *Neofusicoccum parvum* CAA704 and CAA366, *N. kwambonambiense* CAA755, *N. eucalyptorum* CAA558, *Diplodia corticola* CAA500, and *Botryosphaeria dothidea* CAA642, with different levels of aggressiveness — were evaluated on detached tomato leaves and two different mammalian cell lines (3T3 cells and Vero cells). The modulation by temperature of the phytotoxic and cytotoxic potential of these species was also assessed.

MATERIALS AND METHODS

Fungal strains and plant material

Six fungal strains, from five Botryosphaeriaceae species isolated from *Eucalyptus globulus* in Portugal were used: *Botryosphaeria dothidea* CAA642, *Diplodia corticola* CAA500, *Neofusicoccum parvum* CAA366, *N. parvum* CAA704, *N. eucalyptorum* CAA558, and *N. kwambonambiense* CAA755. Cultures were maintained on half-strength Potato Dextrose Agar (PDA) (HIMEDIA, India) (Lopes et al., 2016).

Before assays, each strain was re-grown, by plating a mycelial plug on PDA and incubating at 25 °C for 5 days. Then, a plug of mycelium from the leading edge of the plate was inoculated into PDA plate and incubated at 25 °C for 7 days, except for CAA558 (10 days). Afterwards, two 5 mm plugs of mycelium were inoculated into a 250 mL Erlenmeyer flask containing 50 mL of Potato Dextrose Broth (PDB) and each strain was incubated in triplicate at 25 °C and 37 °C for 10 (CAA755 and CAA366), 12 (CAA704, CAA500 and CAA642) or 20 days (CAA558), due to their different growth patterns. The cultures were filtered with filter paper and mycelium dry weight was determined after drying (50 °C, 48h, Félix et al.,

2016). The extracellular media obtained were filtered (0.2 µm Whatman filter) and kept at -80 °C until phytotoxicity and cytotoxicity assays.

Tomato seeds (*Solanum lycopersicum* var. *cerasiforme*) were cultivated in plastic trays with vermiculite: peat [2:1 (w/w)] mixture and kept at 25-28 °C (16 h light period) in a growth chamber. All seedlings were equally well watered and fertilized weekly (5 ml/L Nutriquisa 5-8-10®) and grown for 90 days under the conditions describe

Phytotoxicity assays on detached tomato leaves

Phytotoxicity was assessed by a leaf puncture assay (Félix et al., 2019). 3-month old tomato leaves were used. Three droplets (each drop 20 µL) of the culture filtrate were applied on the leaves. The leaves were previously punctured in three places using a sterilized needle and the stem placed in sterile water in a closed Petri dish. As control, a droplet (20 µL) of PDB was applied on the leaves. Leaves were kept at room temperature (22-25 °C). Symptoms' development was monitored daily for 6 dpi. All assays were carried out in triplicate.

Chlorophyll fluorescence imaging

In vivo chlorophyll fluorescence was measured using a FluorCAM 800MF imaging fluorometer (Photon System Instruments, Brno, Czech Republic), comprising a computer operated control unit (SN-FC800-082; Photon System Instruments) and a CCD camera (CCD381; PSI) with a f1.2 (2.8-6 mm) objective (Eneo, Rödermark, Germany), as describe by Serôdio et al. (2013). Images of chlorophyll fluorescence parameters F_o and F_m (dark-level and maximum fluorescence level, respectively), before and after actinic illumination by applying modulated measuring light and saturation pulses (<0.1 and >7,500 µmol photons m^{-2} s^{-1}, respectively), provided by red LED panels (612 nm emission peak, 40-nm bandwidth). Images (512×512 pixels) were processed by defining areas of interest (AOIs) matching the whole area of each leaf, by excluding the non-fluorescent background signal using the FluorCam7 software (Photon System Instruments). Images of F_o and F_m were captured on tomato leaves dark-adapted for 20 min. The values of F_o and F_m were were calculated by averaging all pixel values in each AOI (Serôdio et al., 2017). The maximum quantum yield of photosystem II (PSII) was calculated as $F_v/F_m = (F_m-F_o)/F_m$ (Schreiber et al., 1986). For the production of the images shown in Figure 2.1, the scale of false colour of F_v/F_m values was normalized between 0.0 and 0.8 to ensure consistency between the different treatments. F_v/F_m decreased following a biphasic pattern with a fast initial decrease and a slower (with a tendency for stabilization) second phase. The differences between strains were quantified and are expressed by the rate of Fv/Fm decrease during the initial linear phase (Table 1).

Cytotoxicity assays on mammalian cell cultures

Mycelium dry weight was used to normalize the initial amount of culture filtrate. Culture filtrates were diluted [1:1, 1:4 and 1:16 (v:v)] with PBS (Phosphate Buffered Saline, Gibco). *In vitro* cytotoxicity assays were performed as described earlier (Duarte et al., 2015) with some modifications. A Vero cell line (ECACC 88020401, African Green Monkey Kidney cells, GMK clone) and a 3T3 cell line (DSMZ-ACC 173), Swiss Albino Mouse Embryonic Fibroblasts) were maintained and grown as described (Ammerman et al., 2008). 50 µl of a suspension of Vero and 3T3 cells in DMEM (Dulbecco's modified Eagle medium, Gibco) supplemented with 10 % heat-inactivated FBS (Fetal Bovine Serum, Gibco) and 1 % AA (Antibiotic Antimycotic Solution, Sigma-Aldrich) was distributed into a 96-well tissue culture plate (10^4 cells/well) and incubated at 37 °C in 5 % CO_2 for 24 h. After that, 50µl of each dilution prepared from culture filtrates [1:1, 1:4 and 1:16 (v:v)] was added to each well. The microtiter plates were incubated at 37 °C in 5 % CO_2 for 24 h. After exposure, the medium was removed by aspiration and 50 µL of DMEM with 10 % resazurin (0.1 mg/mL in PBS) was added to each well to assess cell viability. The absorbance was measured at 570 and 600 nm wavelength in a microtiter plate spectrophotometer [Synergy™ HT Multi-Detection Microplate Reader (Biotek®)]. Wells containing only DMEM but no cells were used as negative control, and wells with cells exposed to PBS or PDB were used as positive control.

Statistical analysis

Two-way analysis of variance (ANOVA) followed by a Bonferroni's multiple comparison test was used to determine the statistical significance of cytotoxicity of each strain within the same temperature against the control (**p*<0.05, ***p*<0.01, ****p*<0.001, *****p*<0.0001). Differences between F_v/F_m among the different experiences and the rate of F_v/F_m decrease of tomato leaves were tested using a two-way ANOVA, followed by the Dunnett's multiple comparison and Bonferroni's multiple comparison test, respectively, to determine the statistical significance of phytotoxicity of each strain within the same temperature against the control (**p*<0.05, ***p*<0.01, ****p*<0.001, *****p*<0.0001). All the analyses were performed with GraphPad Prism v.7 (GraphPad Software, Inc., La Jolla, CA, USA). Data are shown as the average of three independent replicates of each condition.

RESULTS

Phytotoxicity of culture filtrates

Phytotoxicity of culture filtrates of six phytopathogens including *B. dothidea* CAA642, *D. corticola* CAA500, *N. eucalyptorum* CAA558, *N. kwambonambiense* CAA755, *N. parvum* CAA704 and *N. parvum* CAA366, (grown at 25 °C and 37 °C) was assessed via tomato leaf puncture assay (Figure 2.1, S2.1 and

S2.2). No symptoms were observed when PDB was used as a control over the experiment time (Figure 2.1).

All culture filtrates from fungi grown at 25 °C were able to induce visible necrosis or chlorosis on detached tomato leaves. When the leaves of tomato plants were inoculated with the culture filtrate from *D. corticola* evident severe necrotic lesions developed within a day. At 2 days post inoculation (dpi), similar severe necrosis was also observed for leaves inoculated with *N. kwambonambiense* culture filtrate. Both culture filtrates from *D. corticola* and *N. kwambonambiense* grown at 25 °C displayed high phytotoxicity, and most of the leaves treated with these culture filtrates turned dark and necrotic at 6 dpi (Figure 2.1). The culture filtrates from *N. parvum* CAA704, *B. dothidea*, and *N. parvum* CAA366 grown at 25 °C started to cause small necrotic lesions on tomato leaves at 2 dpi. The development of symptoms was observed on leaves inoculated with *N. parvum* CAA704 culture filtrate until the end of the experiment. However, their phytotoxicity was lower compared with culture filtrates of *D. corticola* and *N. kwambonambiense* (Figure 2.1). The culture filtrate of *N. eucalyptorum* caused only a chlorotic halo around the inoculation sites in tomato leaves, without evident necrosis (Figure 2.1).

Culture filtrates of *D. corticola*, *N. kwambonambiense*, *N. parvum* CAA704 and *N. parvum* CAA366 grown at 37 °C visibly showed delayed and reduced severity symptoms in detached tomato leaves comparing to the symptoms induced by culture filtrates grown at 25 °C (Figure 2.1). *B. dothidea* and *N. eucalyptorum* culture filtrates grown at 25 °C and 37 °C caused similar effects on tomato leaves (Figure 2.1). Symptoms mostly appeared as chlorotic to pale green around inoculation sites or, in the case of *B. dothidea*, as very small dark necrotic spots until 6 dpi (Figure 2.1).

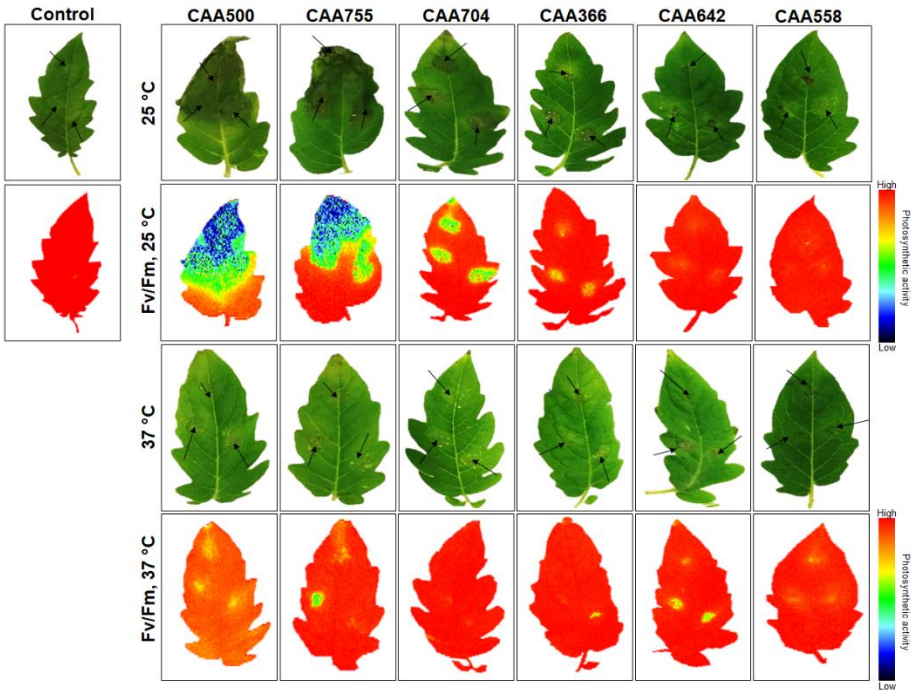

Figure 2. 1 | Effect of culture filtrate from Botryosphaeriaceae species grown at 25 °C and 37 °C on detached tomato leaves after 6 dpi. Effect of culture filtrate of *D. corticola* CAA500, *N. kwambonambiense* CAA755, *N. parvum* CAA704 and CAA366, *B. dothidea* CAA642, and *N. eucalyptorum* CAA558 on symptoms development and chlorophyll fluorescence. PDB[a)] was used as control. The colour scale bar indicates the F_v/F_m intensity in false colours from high (red) to low (black) values. All measurements were performed in biological triplicates. [[a)]PDB: Potato Dextrose Broth].

Besides visually monitoring symptom development, we evaluated the phytotoxicity of culture filtrates by measuring the maximum quantum efficiency of PSII (F_v/F_m) in control and treated leaves for 6 days (Figure 2.2). The results showed that F_v/F_m values of leaves exposed to culture filtrates grown at 25 °C significantly decreased in a time-dependent manner (Figure 2.2). Changes in F_v/F_m were correlated with symptom development. As an example, F_v/F_m values of leaves treated with the culture filtrate of *D. corticola* grown at 25 °C decreased rapidly at 1 dpi from 0.79 ± 0.007 to 0.58 ± 0.023, which is coincident with onset of the visual necrosis symptoms (Figures 2.1 and 2.2A). Similarly, F_v/F_m values of the remaining culture filtrates were reduced at 2 dpi, when visual necrosis symptoms had been observed (Figures 2.1 and 2.2).

As expected, the lowest F_v/F_m value was recorded in severely damaged leaves inoculated with *D. corticola* and *N. kwambonambiense* culture filtrates grown at 25 °C from 0.79 ± 0.007and 0.80 ± 0.009 to 0.32 ± 0.05 and 0.40 ± 0.07, respectively at 6 dpi (Figure 2.2A and B). The leaves inoculated with *N. parvum* CAA704 culture filtrate grown at 25 °C also showed a significant reduction in F_v/F_m values from 0.79 ± 0.005 at 1 dpi to 0.53 ± 0.08 at 6 dpi (Figure 2.2C). There was only a slight reduction of F_v/F_m

value in leaves inoculated with *B. dothidea*, *N. parvum* CAA366, and *N. eucalyptorum* to 0.66 ± 0.07, 0.64 ± 0.05, and 0.71 ± 0.02, respectively at 6 dpi (Figures 2.1D, E and F).

At 37 °C, culture filtrates of *B. dothidea* and *N. kwambonambiense* induced a reduction of F_v/F_m values (Figure 2.2, Table 2.1) that, at the end of the experiment, was significantly different from the control (Figure 2.2). Furthermore, the decline in F_v/F_m values was lower comparing to that grown at 25 °C (Figure2.2, Table 2.1).

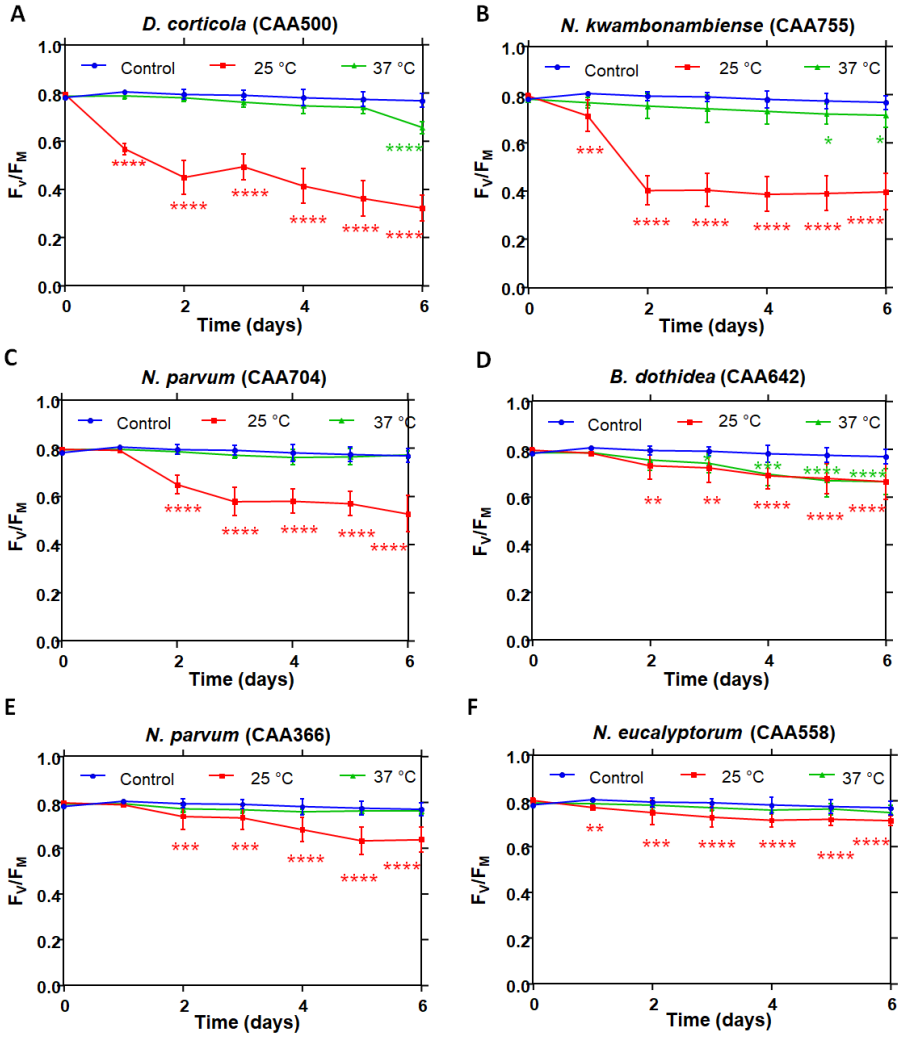

Figure 2. 2 | Evaluation of phytotoxic effect of culture filtrates of Botryosphaeriaceae species on F_v/F_m value of tomato leaves. Culture filtrates were obtained from *D. corticola* CAA500 (**A**), *N. kwambonambiense* CAA755 (**B**), *N. parvum* CAA704 (**C**), *B. dothidea* CAA642 (**D**), *N. parvum* CAA366 (**E**), and *N. eucalyptorum* CAA558 (**F**). PDB[a)] was used as control. Each curve represents the mean ± SD of three independent leaves. Two-way ANOVA, followed by a Dunnet's multiple comparison test was used to determine the statistical significance of phytotoxicity of each strain within the same temperature against the control (*p<0.05, **p<0.01, ***p<0.001, ****p<0.0001). [a)PDB: Potato Dextrose Broth]

The rate of F_v/F_m decrease (determined as the slope of the linear phase of F_v/F_m decrease) (Table 2.1) confirms the visual symptoms: at 25 °C, culture filtrates of *D. corticola*, *N. kwambonambiense* and *N. parvum* CAA704 induced a significant reduction of the F_v/F_m rate decrease of tomato leaves. Overall, fungus growing at higher temperatures leads to lower phytotoxicity.

Table 2. 1 | Rate of F_v/F_m decrease of tomato leaves, induced by culture filtrates of Botryosphaeriaceae fungi. Fungi were grown at 25 °C or at 37 °C. Two-way ANOVA, followed by a Bonferroni's multiple comparison test was used to determine the statistical significance of phytotoxicity of each strain within the same temperature against the control (**p*<0.05, ***p*<0.01, ****p*<0.001, *****p*<0.0001).

Condition/strain	**25 °C**	**37 °C**
Control	0.006 ± 0.003	0.006 ± 0.003
D. corticola CAA500	0.172 ± 0.011****	0.003 ± 0.003
N. kwambonambiense CAA755	0.196 ± 0.018****	0.014 ± 0.008
B. dothidea CAA642	0.032 ± 0.008	0.015 ± 0.006
N. parvum CAA704	0.073 ± 0.010****	0.004 ± 0.002
N. parvum CAA366	0.030 ± 0.008	0.012 ± 0.003
N. eucalyptorum CAA558	0.026 ± 0.007	0.005 ± 0.003

Cytotoxicity of culture filtrates

In addition to phytotoxicity, we investigated the cytotoxicity of the culture filtrates from the strains *D. corticola* CAA500, *N. kwambonambiense* CAA755, *N. parvum* CAA704 and CAA366, *B. dothidea* CAA642, and *N. eucalyptorum* CAA558, grown at 25 °C and 37 °C, to Vero and 3T3 mammalian cell cultures (Figure 2.3).

The culture filtrates of *D. corticola*, *N. parvum* CAA704, and *B. dothidea* grown either at 25 °C or 37 °C significantly decreased Vero cells' viability (Figures 2.3A, B, and C). The culture filtrate of *N. kwambonambiense* only caused significant reduction in Vero cells viability when the strain was grown at 37 °C (Figure 2.3D). The culture filtrates of *N. parvum* CAA366 and *N. eucalyptorum* grown either at 25 °C or 37 °C did not show any significant effect on Vero cells' viability (Figures 2.3E and F).

All strains grown either at 25 °C or 37 °C showed significant mortality of 3T3 cells comparing to control (Figures 2.4A, B, C, D, and F), except for *N. parvum* (CAA366) grown at 37 °C, dilution 1:1 (Figure 2.4E). The cytotoxic effect of *B. dothidea* culture filtrate to both Vero and 3T3 cells increased with growth temperature, 25 and 37 °C, leading to the loss of about 47 % and 94 % cell viability, respectively (Figures 2.3C and 4C). In contrast, increasing temperature had an opposite effect on *D. corticola*, as

shown by a significant reduction of cytotoxicity on both cell lines (Figures 2.3A and 4A): 3T3 cell mortality was over 90 % for dilutions 1:1 and 1:4 of *D. corticola* culture filtrate when grown at 25 °C, while at 37 °C, a lower reduction of cell survival was found (<50 %).

Neofusicoccum parvum CAA704 (grown either at 25 °C or 37 °C) induced a slight decrease on the viability of Vero cells and 3T3 cells that was not significantly affected by fungi growth temperature (Figures 2.3B and 4B).

Neofusicoccum kwambonambiense culture filtrate was not cytotoxic to Vero cells, when the fungus was grown at 25 °C, and induced a slight, but significant toxic effect when the fungus was grown at 37 °C (Figure 2.3D). 3T3 cells were susceptible to *N. kwambonambiense* regardless of growth temperature (Figure 2.4D).

The cell viability for Vero cells exposed to culture filtrates of *N. parvum* CAA366 and *N. eucalyptorum* was 100 % at both temperatures (Figures 2.3E and F). However, both culture filtrates grown either at 25 °C or 37 °C induced a reduction in cell viability of 3T3 cell line, although cytotoxic effects were more pronounced when *N. eucalyptorum* was grown at 25 °C (Figure 2.4E and F).

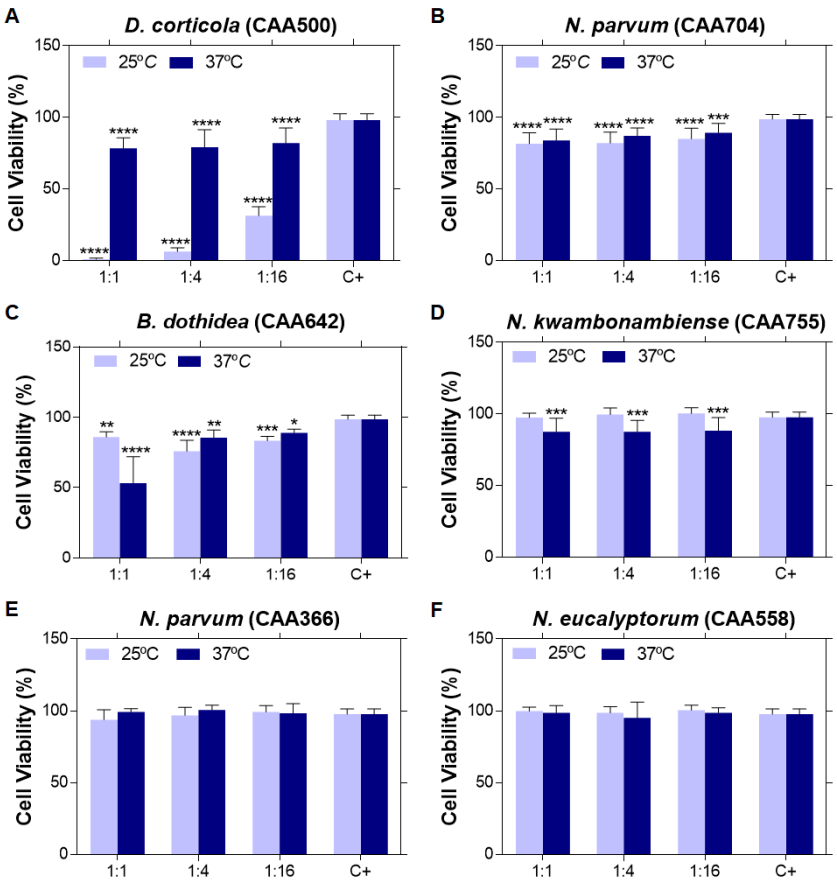

Figure 2. 3 | Evaluation of Vero cells' viability (%) after exposure to the culture filtrates [1:1, 1:4, and 1:16 (v/v)] of Botryosphaeriaceae species grown at 25 °C and 37 °C. Vero cell line was exposed to *D. corticola* CAA500 (**A**), *N. parvum* CAA704 (**B**), *B. dothidea* CAA642 (**C**), *N. kwambonambiense* CAA755 (**D**), *N. parvum* CAA366 (**E**), and

N. eucalyptorum CAA558 (**F**) culture filtrates. Wells containing only medium, but no cells were used as negative control. Cells exposed to PBS[a)] or PDB[b)] were used as positive control. Data is presented as average ± standard error. Two-way ANOVA, followed by a Bonferroni multiple comparisons test, was used to determine the statistical significance of cytotoxicity to the control (*p<0.05, **p<0.01, ***p<0.001, ****p<0.0001). [a)]PBS: Phosphate Buffered Saline; [b)]PDB: Potato Dextrose Broth]

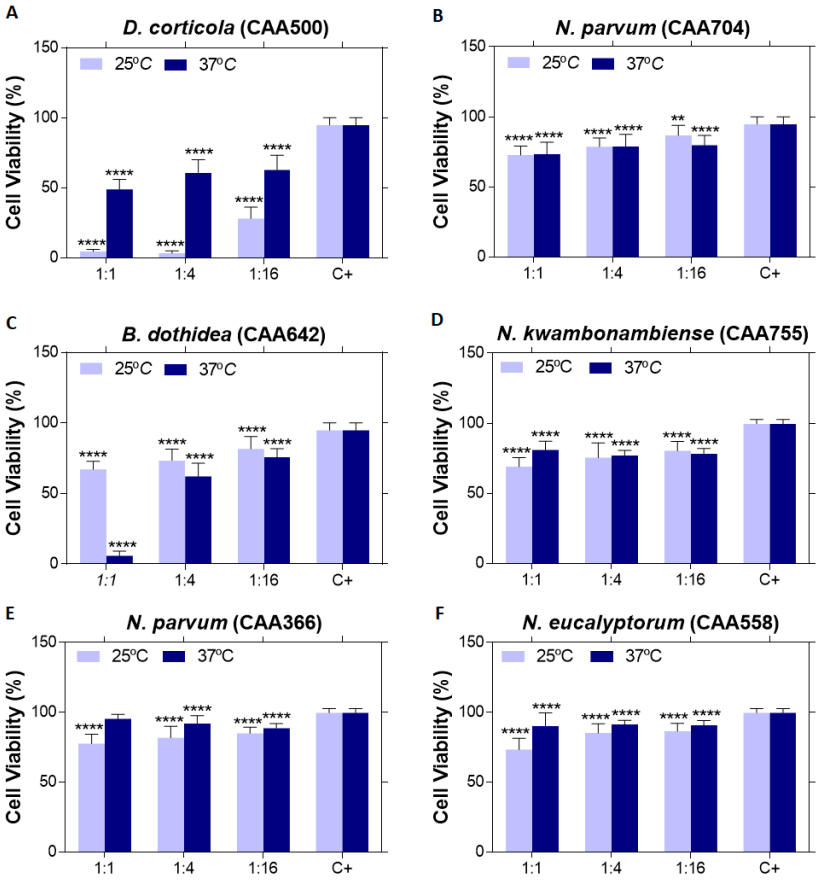

Figure 2. 4 | Evaluation of 3T3 cells' viability (%) after exposure to the culture filtrates [1:1, 1:4, and 1:16 (v/v)] of Botryosphaeriaceae species grown at 25 °C and 37 °C. 3T3 cell line was exposed to *D. corticola* CAA500 (**A**), *N. parvum* CAA704 (**B**), *B. dothidea* CAA642 (**C**), *N. kwambonambiense* CAA755 (**D**), *N. parvum* CAA366 (**E**), and *N. eucalyptorum* CAA558 (**F**) culture filtrates. Wells containing only medium, but no cells were used as negative control. Cells exposed to PBS[a)] or PDB[b)] were used as positive control. Data is presented as average ± standard error. Two-way ANOVA, followed by a Bonferroni multiple comparisons test, was used to determine the statistical significance of cytotoxicity to the control (*p<0.05, **p<0.01, ***p<0.001, ****p<0.0001). [a)]PBS: Phosphate Buffered Saline; [b)]PDB: Potato Dextrose Broth]

DISCUSSION

In this study, the culture filtrates produced by six strains from five species of Botryosphaeriaceae grown at 25 °C and 37 °C were evaluated for toxicity on tomato leaves and on mammalian cells. Healthy-unstressed leaves usually display an F_v/F_m ratio of approximately 0.8, whereas stress

conditions cause photosynthetic inactivation or damage resulting in F_v/F_m reduction (Krause Weis, 1991). F_v/F_m values of control and inoculated leaves indirectly indicate the degree of tissue damage (Murchie & Lawson, 2013) and showed to be excellent indicators of pathogenicity. In the detached leaves trial, all culture filtrates of fungi grown at 25 °C induced visual phytotoxicity symptoms accompanied by a reduction of the F_v/F_m values. F_v/F_m decreased following a biphasic pattern with a fast-initial decrease and a slower (with a tendency for stabilization) second phase. The marked differences in aggressiveness between strains were quantified and are expressed by the rate of F_v/F_m decrease during the linear phase.

Differences in virulence and pathogenicity within these strains have been previously reported in artificial inoculation trials of *Eucalyptus globulus* (Barradas et al., 2016). The least virulent isolate to *E. globulus* was *B. dothidea* while *D. corticola* and *N. kwambonambiense* were the most aggressive. The remaining strains, including *N. parvum* CAA704, *N. parvum* CAA366, (previously reported as *N. algeriense*) and *N. eucalyptorum* CAA558 were considered as intermediate pathogens of *E. globulus* (Barradas et al., 2016). Similarly, in our study, the culture filtrate of *D. corticola* and *N. kwambonambiense* were the most toxic to detached tomato leaves (higher F_v/F_m initial decrease rates). We also investigated the effect of growth temperature on the phytotoxicity of culture filtrates. The phytotoxicity of all strains decreased with the increase of temperature. Only *B. dothidea* preserved its virulence at 37 °C, producing similar sized lesions at the end of the experiment, corroborating the data by Qiu et al. (2016) which suggested that *B. dothidea* is more virulent at higher temperatures (35 °C). Michailides & Owaga (2004) had also reported that infections on pistachio caused by *B. dothidea* developed rapidly in the late spring and summer.

Interestingly, the same trend was observed for toxicity towards mammalian cells (Vero and 3T3 cells): all strains promoted lower toxicity when grown at 37 °C, except *N. parvum* CAA704 and *B. dothidea* CAA642. In fact, *B. dothidea* toxicity increased when the fungus is grown at 37 °C, resulting in higher cell mortality rates, especially of 3T3 cells.

Phytotoxicity and cytotoxicity data suggest that the expression of toxic compounds produced by Botryosphaeriaceae strains are modulated by temperature. Modulation of virulence determinants by temperature was already suggested by Félix et al. (2016) that showed that temperature modulates the expression of extracellular proteins and metabolites by *Lasiodiplodia theobromae.* On the other hand, in our study, we observed that temperature had no influence on the cytotoxic effect of the culture filtrate of *N. parvum* CAA704, suggesting that the modulation of temperature on the cytotoxic effect of the culture filtrate is strain dependent.

Optimal growth temperature for Botryosphaeriaceae species is usually between 25 °C and 30 °C (Qiu et al., 2016). Thus, we can argue that the ability to infect humans may result from an adaptation to

increasing temperatures. Our data shows that *B. dothidea* is highly cytotoxic to mammalian cells when grown at 37 °C, suggesting that it could be able to adapt to human body temperature, and potentially become able to infect human hosts. In fact, *B. dothidea* has been reported on a (single, up to now) case of phaeohyphomycosis infection in a human patient (Noguchi et al., 2017).

Our data seem to suggest that plant cells are less sensitive than mammalian cells to the culture filtrates, which could be related to a higher defense competence towards these fungi, eventually related to the capacity of plant cells to degrade fungal toxic compounds, while mammalian cells cannot (De Gara et al., 2010). Among the cell lines studied, 3T3 cells are more sensitive than Vero cells, in agreement to the literature (Das & Devi, 2015; Félix et al., 2018, 2019).

CONCLUSIONS

We showed that temperature modulates phytotoxicity and cytotoxicity of Botryosphaeriaceae fungi. In general, phyto and cytotoxicity are higher when fungi are grown at 25 °C. Nonetheless, *B. dothidea, D. corticola* and *N. parvum* CAA704 induce high cell mortality when grown at 37 °C, in agreement with their human infection potential. A deeper study of the human/animal pathogenic potential of these fungi is still necessary, but our data indicates that higher environmental temperatures may lead to higher virulence.

We also showed that the well-known chlorophyll fluorescence index F_v/F_m can be used to quantify the damages to plant cells during pathogenicity assays, being more accurate than the traditional inspection of visual symptoms.

ACKNOWLEDGMENTS

Thanks are due, for the financial support to CESAM (UID/AMB/50017/2019) to FCT/MEC through national funds. This study was partially supported by the project [ALIEN (PTDC/AGR-PRO/2183/2014 - POCI-01-0145-FEDER-016788)] funded by FEDER, through COMPETE2020 - Programa Operacional Competitividade e Internacionalização (POCI), and by national funds (OE), through FCT/MCTES. The authors also acknowledge the FCT financial support to F Nazar Pour (BD/98971/2013). Thanks are also due to FCT and UCP for the CEEC institutional financing of AC Esteves and AS Duarte.

REFERENCES

Ammerman, N.C., Beier-Sexton, M., & Azad, A.F. (2008). Growth and maintenance of Vero cell lines. *Curr. Protoc. Microbiol*, Appendix 4, Appendix 4E.

Andolfi, A., Mugnai, L., Luque, J., Surico, G., Cimmino, A., & Evidente, A. (2011). Phytotoxins produced by fungi associated with grapevine trunk diseases. *Toxins*, 3(12), 1569–1605.

Arora P., Dilbaghi N., & Chaudhury, A. (2012). Opportunistic invasive fungal pathogen *Macrophomina phaseolina* prognosis from immunocompromised humans to potential mitogenic RBL with an

exceptional and novel antitumor and cytotoxic effect. *European Journal of Clinical Microbiology & Infectious Diseases: Official Publication of the European Society of Clinical Microbiology*, 31(2), 101–107.

Barradas, C., Alan, J.L.P., Correia A., Eugénio, D., Bragança, H., & Alves, A. (2016). Diversity and potential impact of Botryosphaeriaceae species associated with *Eucalyptus globulus* plantations in Portugal. *European Journal of Plant Pathology*, 146(2), 245–257.

Bebber, D. P., Ramotowski, M. A. T., & Gurr, S. J. (2013). Crop pests and pathogens move polewards in a warming world. *Nature Climate Change*, 3, 985-988.

Bénard-Gellon, M., Farine, S., Goddard, M. L., Schmitt, M., Stempien, E., Pensec, Laloue, H., Mazet-Kieffer, F., Fontaine, F., Larignon, P., Chong, J., Tarnus, C., & Bertsch, C. (2015). Toxicity of extracellular proteins from *Diplodia seriata* and *Neofusicoccum parvum* involved in grapevine Botryosphaeria dieback. *Protoplasma*, 252(2), 679–687.

Bliska, J. B., & Casadevall, A. (2009). Intracellular pathogenic bacteria and fungi-a case of convergent evolution? *Nature Reviews. Microbiology*, 7(2), 165–171.

Burgess, T. I., Sakalidis, M. L., & Hardy, G. E. (2006). Gene flow of the canker pathogen *Botryosphaeria australis* between *Eucalyptus globulus* plantations and native eucalypt forests in Western Australia. *Austral Ecology*, 31(5), 559–566.

Das, M., & Devi, G. (2015). In vitro cytotoxicity and glucose uptake activity of fruits *Terminalia bellirica* in Vero, L-6 and 3T3 cell lines. *Journal of Applied Pharmaceutical Science*, 5(12), 092–095.

De Gara, L., Locato, V., Dipierro, S., & de Pinto, M. C. (2010). Redox homeostasis in plants. The challenge of living with endogenous oxygen production. *Respiratory Physiology & Neurobiology*, 173, 13-9.

Eastburn, D. M., McElrone, A. J., & Bilgin, D. D. (2011). Influence of atmospheric and climatic change on plant–pathogen interactions. *Plant Pathology*, 60(1), 54–69.

Félix, C., Duarte, A. S., Vitorino, R., Guerreiro, A. C. L., Domingues, P., Correia, A. C. M., & Esteves, A. C. (2016). Temperature modulates the secretome of the phytopathogenic fungus *Lasiodiplodia theobromae*. *Frontiers in Plant Science*, 7, 1096.

Félix, C., Salvatore, M. M., DellaGreca, M., Meneses, R., Duarte, A. S., Salvatore, F., & Esteves, A. C. (2018). Production of toxic metabolites by two strains of *Lasiodiplodia theobromae*, isolated from a coconut tree and a human patient. *Mycologia*, 110(4), 642–653.

Félix, C., Salvatore, M. M., DellaGreca, M., Ferreira, V., Duarte, A. S., Salvatore, F., & Andolfi, A. (2019a). Secondary metabolites produced by grapevine strains of *Lasiodiplodia theobromae* grown at two different temperatures. *Mycologia*, *111*(3), 466–476.

Félix, C., Meneses R., Gonçalves, M.F.M., Tilleman, L., Duarte, A.S., Jorrin-Novo, J.V., Van de Peer, Y., Deforce, D., Van Nieuwerburgh, F., Esteves, A.C., & Alves, A. (2019b). A multi-omics analysis of the grapevine pathogen *Lasiodiplodia theobromae* reveals that temperature affects the expression of virulence- and pathogenicity-related genes. *Scientific Reports*, 9.

Gallana, M., Ryser-Degiorgis, M. P., Wahli, T., & Segner, H. (2015). Climate change and infectious diseases of wildlife: altered interactions between pathogens, vectors and hosts. *Current Zoology*, 59(3), 427–437.

Goncalves, M.F.M., Nunes, R.B., Tilleman, L., Van de Peer, Y., Deforce, D., Van Nieuwerburgh, F., Esteves, A.C., & Alves, A. (2019) Dual RNA sequencing of *Vitis vinifera* during *Lasiodiplodia theobromae* infection unveils host-pathogen interactions. *International Journal of Molecular Science*, 20(23), 6083.

Gramaje, D., Agustí-Brisach, C., Pérez-Sierra, A., Moralejo, E., Olmo, D., Mostert, L., & Armengol, J. (2012). Fungal trunk pathogens associated with wood decay of almond trees on Mallorca (Spain). *Persoonia*, 28, 1–13.

Guan, X., Essakhi, S., Laloue, H., Nick, P., Bertsch, C., & Chong, J. (2016). Mining new resources for grape resistance against Botryosphaeriaceae: a focus on *Vitis vinifera* subsp. *sylvestris*. *Plant Pathology*, *65*(2), 273–284.

IPCC., 2014: Intergovernmental Panel on Climate Change., 2014. The Physical Science Basis: Working Group I Contribution to the Fifth Assessment Report of the Intergovernmental Panel on Climate Change.

Kindo, A. J., Pramod, C., Anita, S., & Mohanty, S. (2010). Maxillary sinusitis caused by *Lasiodiplodia theobromae*. *Indian Journal of Medical Microbiology*, 28(2), 167.

Krause, G. H., & Weis, E. (1991). Chlorophyll Fluorescence and Photosynthesis: *The Basics*. *Annual Review of Plant Physiology and Plant Molecular Biology*, 42(1), 313–349.

Lawrence, D. P., Peduto Hand, F., Gubler, W. D., & Trouillas, F. P. (2017). Botryosphaeriaceae species associated with dieback and canker disease of bay laurel in northern California with the description of *Dothiorella californica* sp. nov. *Fungal Biology*, 121(4), 347–360.

Linaldeddu, B. T., Sirca, C., Spano, D., & Franceschini, A. (2009). Physiological responses of cork oak and holm oak to infection by fungal pathogens involved in oak decline. *Forest Pathology*, 39(4), 232–238.

Lopes, A., Barradas, C., Phillips, A. J. L., & Alves, A. (2016). Diversity and phylogeny of *Neofusicoccum* species occurring in forest and urban environments in Portugal. *Mycosphere*, *7*, 906–920.

Martos, S., Andolfi, A., Luque, J., Mugnai, L., Surico, G., & Evidente, A. (2008). Production of phytotoxic metabolites by five species of Botryosphaeriaceae causing decline on grapevines, with special interest in the species *Neofusicoccum luteum* and *N. parvum*. *European Journal of Plant Pathology*, 121(4), 451–461.

Michailides, T. J., & Morgan, D. P. (2004). Panicle and shoot blight of pistachio: A major threat to the California pistachio industry. *APSnet Feature Story. Published Online*.

Mohali, S., Slippers, B., & Wingfield, M. J. (2007). Identification of Botryosphaeriaceae from *Eucalyptus*, *Acacia* and *Pinus* in Venezuela. *Fungal Diversity*, 25(25), 103–125.

Murchie, E. H., & Lawson, T. (2013). Chlorophyll fluorescence analysis: a guide to good practice and understanding some new applications. *Journal of Experimental Botany*, 64(13), 3983–3998.

Noguchi, H., Hiruma, M., Matsumoto, T., Kano, R., Tanaka, M., Yaguchi, T., Sonoda, K., & Ihn, H. (2017). Fungal melanonychia: Ungual phaeohyphomycosis caused by *Botryosphaeria dothidea*. *Acta Dermato-Venereologica*, 97, 765-766.

Qiu, Y., Steel, C. C., Ash, G. J., & Savocchia, S. (2014). Effects of temperature and water stress on the virulence of Botryosphaeriaceae spp. causing dieback of grapevines and their predicted distribution using CLIMEX in Australia. *XXIX International Horticultural Congress on Horticulture: Sustaining Lives*, *Livelihoods and Landscapes* (IHC2014): IV 1115, 171–182.

Ramírez-Suero, M., Bénard-Gellon, M., Chong, J., Laloue, H., Stempien, E., Abou-Mansour, E., & Farine, S. (2014). Extracellular compounds produced by fungi associated with Botryosphaeria dieback induce differential defence gene expression patterns and necrosis in *Vitis vinifera* cv. Chardonnay cells. *Protoplasma*, 251(6), 1417–1426.

Reveglia, P., Savocchia, S., Billones-Baaijens, R., Masi, M., Cimmino, A., & Evidente, A. (2019). Phytotoxic metabolites by nine species of Botryosphaeriaceae involved in grapevine dieback in Australia and identification of those produced by *Diplodia mutila*, *Diplodia seriata*, *Neofusicoccum australe* and *Neofusicoccum luteum*. *Natural Product Research*, 33(15), 2223–2229.

Saha, S., Sengupta, J., Banerjee, D., & Khetan, A. (2012). *Lasiodiplodia theobromae* keratitis: a case report and review of literature. *Mycopathologia*, 174(4), 335–339.

Saha, S., Sengupta, J., Banerjee, D., & Khetan, A. (2013). *Lasiodiplodia theobromae* keratitis: a rare fungus from eastern India. *Microbiology Research*, 3(2), e19–e19.

Sakalidis, M. L., Slippers, B., Wingfield, B. D., Hardy, G. E. S. J., & Burgess, T. I. (2013). The challenge of understanding the origin, pathways and extent of fungal invasions: global populations of the *Neofusicoccum parvum–N. ribis* species complex. *Diversity and Distributions*, 19(8), 873–883.

Schreiber, U., Schliwa, U., & Bilger, W. (1986). Continuous recording of photochemical and non-photochemical chlorophyll fluorescence quenching with a new type of modulation fluorometer. *Photosynthesis Research* 10 (1-2), 51–62.

Serôdio, J., Ezequiel, J., Frommlet, J., Laviale, M., & Lavaud, J. (2013). A method for the rapid generation of nonsequential light-response curves of chlorophyll fluorescence. *Plant Physiology*, 163(3), 1089–1102.

Serôdio, J., Schmidt, W., & Frankenbach, S. (2017). A chlorophyll fluorescence-based method for the integrated characterization of the photophysiological response to light stress. *Journal of Experimental Botany* 68(5), 1123–1135.

Shalchian-Tabrizi, K., Minge, M. A., Espelund, M., Orr, R., Ruden, T., Jakobsen, K. S., & Cavalier-Smith, T. (2008). Multigene phylogeny of Choanozoa and the origin of animals. *PLOS ONE*, 3(5), e2098.

Slippers, Bernard, & Wingfield, M. J. (2007). Botryosphaeriaceae as endophytes and latent pathogens of woody plants: diversity, ecology and impact. *Fungal Biology Reviews*, 21(2), 90–106.

Summerbell, R. C., Krajden, S., Levine, R., & Fuksa, M. (2004). Subcutaneous phaeohyphomycosis caused by *Lasiodiplodia theobromae* and successfully treated surgically. *Medical Mycology*, 42(6), 543–547.

Tan, D. H. S., Sigler, L., Gibas, C. F. C., & Fong, I. W. (2008). Disseminated fungal infection in a renal transplant recipient involving *Macrophomina phaseolina* and *Scytalidium dimidiatum*: case report and review of taxonomic changes among medically important members of the Botryosphaeriaceae. *Medical Mycology*, 46(3), 285–292.

Thew, M. R. J., & Todd, B. (2008). Fungal keratitis in far north Queensland, Australia. *Clinical & Experimental Ophthalmology*, 36(8), 721–724.

Urbez-Torres, J. R., & Gubler, W. D. (2009). Pathogenicity of Botryosphaeriaceae species isolated from grapevine cankers in California. *Plant Disease*, 93(6), 584–592.

Woo, P. C. Y., Lau, S. K. P., Ngan, A. H. Y., Tse, H., Tung, E. T. K., & Yuen, K.-Y. (2008). *Lasiodiplodia theobromae* pneumonia in a liver transplant recipient. *Journal of Clinical Microbiology*, 46(1), 380–384.

Zlatkovic, M., Keca, N., Wingfield, M. J., Jami, F., & Slippers, B. (2016). Botryosphaeriaceae associated with the die-back of ornamental trees in the Western Balkans. *Antonie van Leeuwenhoek*, 109(4), 543–564.

SUPPLEMENTARY MATERIAL

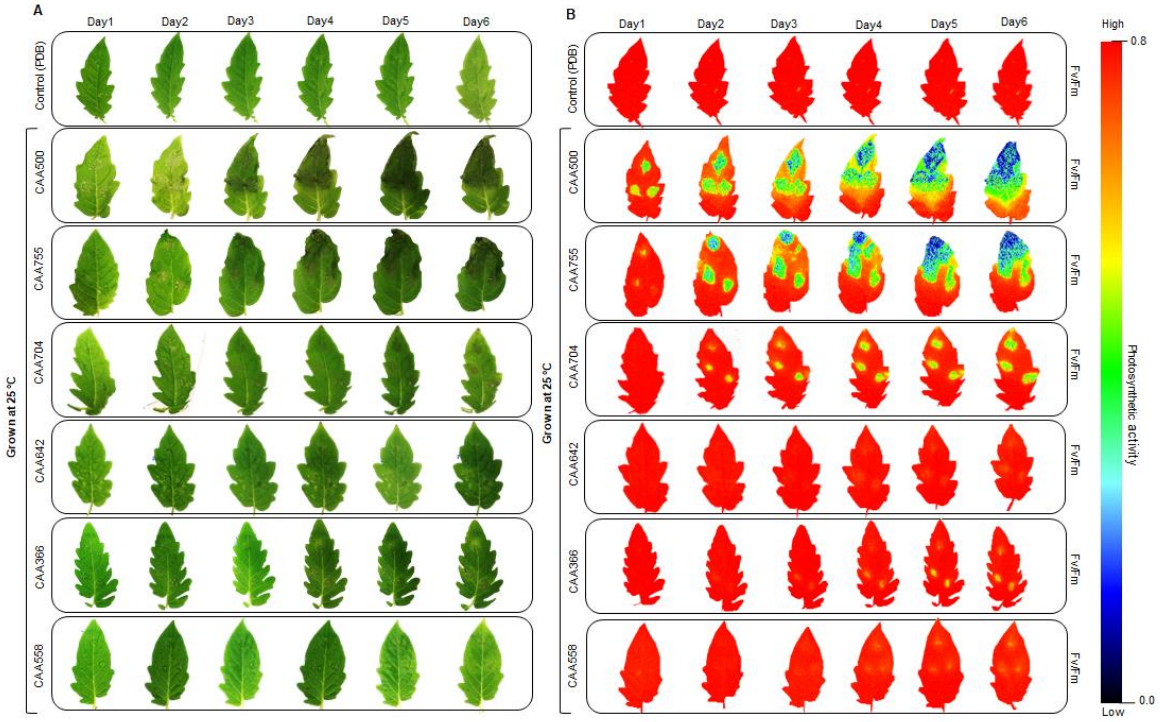

Figure S2.1 | Effect of culture filtrate of Botryosphaeriaceae fungi grown at 25 °C on detached tomato leaves after 6 days. Effect of culture filtrate of *D. corticola* CAA500, *N. kwambonambiense* CAA755, *N. parvum* CAA704, *B. dothidea* CAA642, *N. parvum* CAA366, and *N. eucalyptorum* CAA558 on symptoms development (**A**) and chlorophyll fluorescence (**B**). Leaves inoculated with PDB were used as control. The colour scale bar indicates the F_v/F_m intensity of the leaf pixels given in false colours from high (red) to low (black) values.

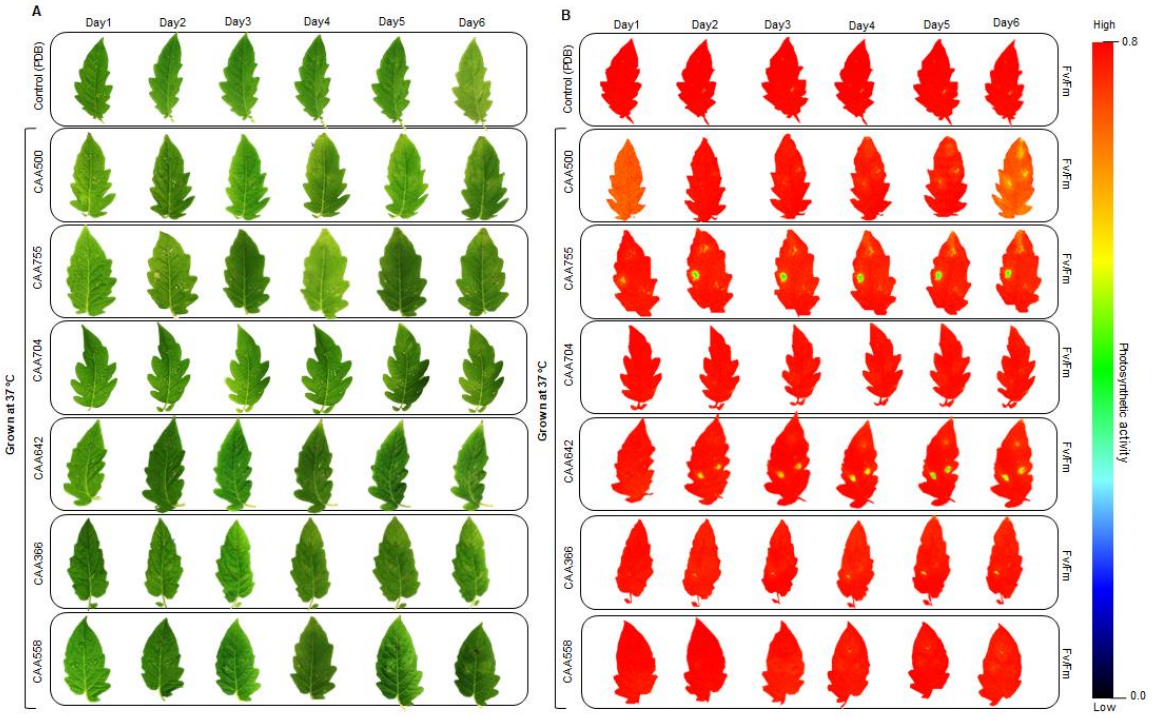

Figure S2.2 | Effect of culture filtrate of Botryosphaeriaceae fungi grown at 37 °C on detached tomato leaves after 6 days. Effect of culture filtrate of *D. corticola* CAA500, *N. kwambonambiense* CAA755, *N. parvum* CAA704, *B. dothidea* CAA642, *N. parvum* CAA366, and *N. eucalyptorum* CAA558 on symptoms development (**A**) and chlorophyll fluorescence (**B**). Leaves inoculated with PDB were used as control. The colour scale bar indicates the F_v/F_m intensity of the leaf pixels given in false colours from high (red) to low (black) values.

CHAPTER 3

Unveiling the secretome of the fungal plant pathogen *Neofusicoccum parvum* induced by *in vitro* host mimicry

ABSTRACT

Neofusicoccum parvum is a fungal plant pathogen able to infect a wide host range. Despite the considerable economic importance due to significant losses of infected plants and fruits, knowledge about virulence factors of *N. parvum* and host-pathogen interactions are rather limited. Here we present the first comprehensive characterization of the *in vitro* secretome of *N. parvum.* We used LC-MS to identify *N. parvum* protein profile in the absence and presence of *Eucalyptus* stem and this resulted in the consistent identification of over four hundred proteins. We identified 117 differentially expressed proteins, most of them induced under host mimicry specially those involved in plant cell wall degradation (targeting pectin and hemicellulose) that might facilitate growth on a plant host. Other proteins identified are involved in adhesion of pathogen to host tissues, fungal cell wall degradation, penetration, pathogenesis, reactive oxygen species (ROS) generation, proteolytic processes, fungal effector and fungal toxin. Our study revealed that the existence of many cell wall degrading enzymes, hydrolyses, oxidoreductases and proteases might be related to the aggressiveness of the fungus. The induction of chitosan synthesis required for appressorium formation and degradation proteins during interaction with *Eucalyptus* stem, reinforcing the hypothesis of an infection strategy employed by this pathogen. Host mimicry strategy have also provided important insights into the mechanisms of infection. However, further studies will be necessary to determine the exact roles of these proteins in the pathogenic mechanisms of the fungus.

KEYWORDS: *Botryosphaeriaceae, Neofusicoccum parvum*, plant fungal pathogen, secretome, LC-MS spectrometry, *Eucalyptus globulus*

INTRODUCTION

Eucalyptus species are native to Australia but due to enormous economic significance are planted in many countries around the world. They were introduced in Portugal more than 100 years ago and are nowadays the most representative forest tree species. *Eucalyptus globulus,* is the most abundant species which occupies ca. 8,500 km^2, the equivalent to ca. 9 % of the country, mostly in Central and Northwest Portugal (Deus et al., 2018). This species is well adapted to the Mediterranean-like climate and is exploited mainly due to commercial interests of the pulp and paper industries. Unfortunately, they are commonly threatened by various species of the family *Botryosphaeriaceae*.

Botryosphaeriaceae are well-known opportunistic pathogens that elicit disease symptoms in plants under stress conditions, resulting high economic losses (Li et al., 2015; Slippers et al., 2014; Slippers & Wingfield, 2007). In addition, they are known to occur in asymptomatic plant tissues as endophytes and latent pathogens on a variety of tree species including *Eucalypts* (Pérez et al., 2010; Phillips et al., 2013; Slippers & Wingfield, 2007; Smith et al., 1996). *Botryosphaeriaceae* have been associated to

Eucalyptus canker and dieback in Portugal (Barradas et al., 2016). *Botryosphaeriaceae* species are considered a significant threat to the productivity and sustainability of *Eucalyptus* spp. plantations in Portugal. In survey conducted in 2015, the predominant isolates collected from *Eucalyptus* were from the genus *Neofusicoccum* (Barradas et al., 2016). Several studies have reported a diverse assemblage of *Neofusicoccum* species occurring on *Eucalyptus* spp. both as endophytes and disease-related (Mohali et al., 2007; Pérez et al., 2010; Slippers et al., 2009).

Neofusicoccum parvum is a vascular aggressive pathogen that causes severe decline and dieback symptoms in a wide range of hosts (Blanco-Ulate et al., 2013; Phillips et al., 2013) being also common in *Eucalyptus* (Barradas et al., 2016; Chen et al., 2011; Pavlic et al., 2007; Pérez et al., 2010; Slippers et al., 2004). In general, the fungus penetrates through pruning wounds and colonizes the host tissues, causing shoot dieback, stem canker, cane bleaching, bud necrosis, and graft failure.

However, not much is known about the strategies that this fungus employs to infect its hosts, or about the molecules it expresses during infection. Several studies have suggested that *N. parvum* virulence could be related to the ability of this fungus to colonize woody tissue combined with the production of several phytotoxins (Abou-Mansour et al., 2015; Andolfi et al., 2011) and also the expression of extracellular proteins with phytotoxic properties (Bénard-Gellon et al., 2015). Recent genomic and transcriptomic analyses have shown that this pathogen has evolved special adaptive mechanisms to infect woody plants (Massonnet et al., 2017; Yan et al., 2017). These mechanisms include significant expansions of gene families associated with virulence and nutrient uptake, including cellular transporters, cell wall degrading enzymes (CWDEs), cytochrome P450s, putative effectors and biosynthesis of secondary metabolites. The interaction between grapevine and *N. parvum*, was also studied at the transcriptomic level (Massonnet et al., 2017). Host plant stems and leaves underwent extensive transcriptomic reprogramming, but woody stems reacted earlier than leaves to infection. The results suggested that leaves perceive similar signals as the infection site without interacting directly with the pathogen (Massonnet et al., 2017). The RNA-seq data were also used to investigate the virulence mechanisms used by N. parvum during the infection (Massonnet et al. 2018). Gene expression analysis showed that *N. parvum* co-expresses genes associated with secondary metabolism and plant cell wall degradation in function of the growth substrate and the stage of plant infection. Co-expressed genes were found to be physically clustered and to share common regulatory elements in their promoters, suggesting that their co-regulation might contribute to its virulence. In another study, RNA sequencing of gene expression in leaves after wood infection showed that certain genes could act as host markers of the latent period of *N. parvum* infection (Czemmel et al., 2015). Overall, these studies have thrown light on the interactions between plants and *N. parvum* dieback. However, full understanding of the pathogenicity mechanism is still far from being accomplished. In order to

investigate the mechanisms of pathogenicity of this fungus, we mainly centred our analysis on the secretome (Do Vale et al., 2015; González-Fernández et al., 2015; Jami et al., 2010; Lyu et al., 2015; Mandelc & Javornik, 2015; Shah et al., 2009), due to its relevance to the infection mechanisms and to fungus-plant interactions. However, proteomics data from the family *Botryosphaeriaceae* are limited. So far, the proteome of *Diplodia seriata* (Cobos et al., 2010), *Diplodia corticola* (Fernandes et al., 2014) and most recently *Lasiodiplodia* theobromae (Felix et al., 2019; Felix et al., 2016; Uranga et al., 2017) have been reported. Proteins identified in these studies suggest differences in the infection strategies of these fungi. The genome of *N. parvum* is sequenced and was released in 2013 (Blanco-Ulate et al., 2013). It is predicted that *N. parvum* expresses 1,097 secreted proteins. A set of enzymes that might function during the colonization of host tissues, which include 163 glycoside hydrolases, 22 polysaccharide lyases, and 8 cutinases are annotated based on homology with proteins in the CAZy database are also predicted (Blanco-Ulate et al., 2013).

The aim of this study was to characterize the secretome of *N. parvum* and evaluate its response to the *in vitro* host mimicry. Additionally, this work will also improve the knowledge on one of the aggressive phytopathogens and its interaction with plant.

MATERIALS AND METHODS

Fungal strains, plant material and culture conditions

The strain used in this study, *N. parvum* CAA704, was recovered from *E. globulus* displaying symptoms of dieback and decline in Portugal (Barradas et al., 2016). This strain also showed to be pathogenic to *E. globulus* in artificial inoculation trials (Barradas et al., 2016). Fungus was grown on PDA (Potato Dextrose Agar, Merck, Germany) plate at 25 °C for 7 days prior to the inoculations. The 3-months-old *Eucalyptus globulus* (MB43, obtained from ALTRI) seedlings were weekly watered and kept at room temperature under natural light.

Two conditions were tested: control and infection-like. For control condition, two mycelium plugs (5 mm diameter) were inoculated into a 250 mL flask containing 50 mL PDB (Potato Dextrose Broth, Merck, Germany) and incubated in triplicate at 25 °C for 12 days. For the infection-like condition a sterilized piece of *E. globulus* stem (± 2 g) was added to the PDB, as described earlier (Fernandes et al., 2014). Culture supernatant of each condition was harvested through filter paper and immediately stored at -80 °C for extracellular protein extraction. Mycelia obtained from both conditions were collected by filtration, washed with sterile water and frozen with N_2(l) for DNA and RNA extraction.

RNA extraction and cDNA synthesis

Total RNA was extracted from crushed mycelium (three biological replicates from each condition) in liquid nitrogen using the Spectrum Plant Total RNA kit (Sigma), according to the manufacturer's

instructions. Samples were treated with DNase I digestion set (RNase-Free DNase Set, Qiagen) for 15 min to remove genomic DNA. The quality and quantity of RNA were checked by gel electrophoresis and NanoDrop™ 1000 Spectrophotometer (Thermo scientific). cDNA was generated using the Nzy First-Strand cDNA Synthesis Kit (Nzytech), according to the manufacturer's instructions.

Extracellular Protein Extraction

Secreted proteins were extracted using TCA/Acetone according to the method described by Fernandes et al. (2014). To eliminate polysaccharides, the culture supernatant (35 ml) was centrifuged (48,400 g, 1 h at 4 °C). One volume of cold TCA/Acetone [20 % / 80 % (w/v)] supplemented with 0.14 % (w/v) DTT was added to the supernatant and incubated at -20 °C for 1 h. Precipitated proteins were collected by centrifugation (15000×g, 20 min, 4 °C) and the supernatant was removed. Precipitated proteins were washed with 10 mL of ice-cold acetone (2×) (15,000 g, 15 min, 4 °C) and 10 mL of ice-cold 80 % acetone (v/v) (15,000 g, 15 min, 4 °C) to discard the excess of TCA from the precipitate. Residual acetone was air-dried, and the protein pellet was resuspended in 0.1 M Tris HCl pH 8 and stored at -80 °C.

Chloroform-methanol extraction of proteins

To remove salts, detergents or phenolic compounds from extracted proteins (see Extracellular Protein Extraction), the water/chloroform/methanol protein precipitation method was used [adapted from (Wessel & Flügge, 1984)]. Briefly, a mixture of methanol, chloroform and water [4:1:3 (v/v)] were added to the sample and thoroughly vortexed. Then, the mixture was centrifuged at 14,000 g for 1 min and the top aqueous methanol layer was removed (the proteins being in the interphase). 4 volumes of methanol were added, and the mixture was vortexed and centrifuged at 14,000 ×g for 5 min. The supernatant was removed without disturbing the pellet. The air-dried pellet was finally resuspended in in 0.1 M Tris HCl pH 8 and stored at -80 °C.

Protein Quantification

Protein concentration assay was carried out with the Pierce® 660 nm Protein Assay kit (Thermo Scientific) according to the manufacturer's instructions. All samples were quantified in triplicate.

Protein separation by electrophoresis

The quality of protein samples was assessed by SDS–PAGE. Briefly, 3 µg of protein were denaturated and were separated in a 12.5 % SDS-PAGE gel electrophoresis, according to Laemmli's protocol (Laemmli, 1970), for 120 min at 120 V, in a Mini-PROTEAN 3 Cell (Bio-Rad, USA). The running buffer contained 100 mM Tris, 100 mM Bicine and 0.1 % (w/v) SDS. Gels were stained with Coomassie Brilliant Blue G-250 (CBB). After staining, gels were scanned on a GS-800 Calibrated Densitometer (Bio-Rad).

Tryptic Digestion, Mass Spectrometry Analysis, and Protein Identification

Ten µg of protein sample were diluted in NH_4HCO_3 50 mM buffer (in 30 µL). Twenty µL of BSA 0.002 µg/mL was added and the solution was incubated at 80 °C for 10 min. Reduction with 5 µL of DTT 50 mM/NH_4HCO_3 50 mM (incubation at 60 °C for 10 min) and alkylation with 5 µL of IAA 150 mM/NH_4HCO_3 50 mM (incubation in the dark for 20 min) was performed. Proteins were digested with 2 µL of trypsin 0.1 µg/µL. Afterwards samples were acidified with 1 % formic acid and incubated at 37 °C for 30 min. After a centrifugation of 16000 g for 30 min, the supernatant was transferred to new vials and a peptide purification step was performed on C18 Omix tips. The peptides were dried in a vacuum concentrator (SpeedVac, ThermoFisher Scientific) and stored at -20 °C until analysis.

Purified peptides were re-dissolved in loading solvent A (0.1 % TFA in water/ACN (98:2, v/v)) and injected an Ultimate 3000 RSLC nano system in-line connected to a Q Exactive HF mass spectrometer (Thermo). Trapping was performed at 10 µl/min for 4 min in loading solvent A on a 20 mm trapping column [made in-house, 100 µm internal diameter (I.D.), 5 µm beads, C18 Reprosil-HD, Dr. Maisch, Germany] and the sample was loaded onto a 400 mm analytical column (made in-house, 75 µm I.D., 1.9 µm beads C_{18} Reprosil-HD, Dr. Maisch). Peptides were eluted by a non-linear gradient from 2 to 56 % MS solvent B [0.1 % FA in water/acetonitrile (2:8, v/v)] over 145 minutes at a constant flow rate of 250 nL/min, followed by a 10 min wash reaching 97 % MS solvent B and re-equilibration with MS solvent A (0.1 % formic acid in water) for 20 min. The column temperature was kept constant at 50 °C in a column oven (Sonation COControl). The mass spectrometer was operated in data-dependent mode, automatically switching between MS and MS/MS acquisition for the 16 most abundant ion peaks per MS spectrum. Full-scan MS spectra (375-1500 m/z) were acquired at a resolution of 60,000 in the Orbitrap analyzer after accumulation to a target value of 3 e^6. The 16 most intense ions above a threshold value of 1.3 e^4 were isolated for fragmentation at a normalized collision energy of 28 % after filling the trap at a target value of 1E5 for maximum 80 ms. MS/MS spectra (200-2000 m/z) were acquired at a resolution of 15,000 in the Orbitrap analyzer.

The raw data generated from LC-MS was further inputted in Max-Quant (version 1.6.2.1), a quantative proteomics software developed by Cox and Mann (2008). MS1 spectra were searched with Andromeda peptide database engine against a FASTA database of proteins from UniProt and analyzed for label-free quantification of the peptides present in the samples. Peptides were generated from a tryptic digestion with up to two missed cleavages, carbamidomethylation of cysteines as fixed modifications, and oxidation of methionines and N-terminal acetylation as variable modifications. Peptide spectral matches (PSM) were validated using percolator based on q-values at a 1% false discovery rate (FDR). Identified peptides were assembled into protein groups according to the law of parsimony and filtered to 1% FDR. Perseus software (version 1.6.1.3) enabled the affiliation of the

protein groups into identified proteins. Identified proteins were filtered and only considered for analysis if present in 3 replicates and using at least 3 peptides for identification. Reverse proteins and proteins identified only by site were filtered out. A multi-scatter plot and hierarchical clustering were done to assess the quality of the experiment. To identify interactor proteins, a two sample T-test between control and infection-like samples was performed with minimal fold change (s0) of 1.8 and 1% FDR. A scatter plot, volcano plot and profile plot used to visualize the results.

Protein validation by Quantitative PCR (qPCR)

Target genes were selected according to their pattern of expression and functional annotation (Table 3.1).

Table 3.1| Reference and target genes and respective primers

Protein name	Gene	Expression condition	Primer sequence (5'-3')	Amplicon length (bp)	Reference
Elongation factor-1 α	EF1α	Reference gene	**FW:** CGGTCACTTGATCTACAAGTGC **RV:** CCTCGAACTCACCAGTACCG	302	Paolinelli et al., 2016
***Putative exo-beta protein* (PL3)**	UCRNP2_317	Up-regulated	**FW:** ATTCAGCACTCCGGTACCAC **RV:** GCCGTCCACGGACTTGAT	255	Present study
***Putative aspartic endopeptidase pep1 protein* (AP1)**	UCRNP2_6229	Up-regulated	**FW:** AGCTCCAGCTATGGTGGCTA **RV:** GACGATAGAGAAGCCGATGC	172	Present study

All reactions were performed in a CFX96 Real-Time thermocycler (BioRad) using the NzySpeedy qPCR Green Master Mix (2x) (Nzytech). For each reaction, 5 µL of the Master Mix, 0.5 µL of each primer (10 µM, forward and reverse), 4.2 µL of nuclease-free water and 0.5 µL of template cDNA was used. The PCR program used was: 95 °C - 3 min, 40 cycles of 95 °C - 15 s and 60 °C - 30 s. After this step the fluorescence intensity was measured and, at the end of the program, the temperature was increased from 65 °C to 95 °C at a rate ramp of 0.1 °C/s, allowing the melting curves elaboration. Cq values were calculated with BIO-RAD CFX Manager software and used to compare the expression between reference and target genes.

Bioinformatic analysis

The secreted proteins were classified according to the GO [biological process, UniprotKB, (http://www.uniprot.org/). Whenever necessary, protein's family and domain were determined by identification of conserved domains in the InterPro database (http://www.ebi.ac.uk/interpro). Cell wall-degrading enzymes classified according to the carbohydrate-active enzymes database CAZy (http://www.cazy.org).

All proteins were analysed for subcellular localization using the BaCelLo fungi-specific predictor (Pierleoni et al., 2006), SignalP v4.1 (Petersen et al., 2011), and SecretomeP predictor (Bendtsen et al., 2004).

Scanning Electron Microscopy (SEM) of inoculated *eucalyptus* stem

Scanning electron microscopy (SEM) was performed in a SEM, SU-70, Hitachi microscope to investigate the changes in micromorphological characteristics of *E. globulus* stem inoculated with of *N. parvum* (infection-like condition) after 12 days. Also, a piece of *E. globulus* stem supplemented in PDB with no fungus was analysed as a control. All samples first grinded and then typed on a metal plate and finally were sputtered with carbon before microscopic observation (Zabel & Morrell, 1992).

RESULTS

Scanning Electron Microscopy (SEM)

SEM images of untreated stem present non-decayed cell wall with an intact surface structure (Figure 3.1A), while the surface of treated wood is rugged and fully covered by the abundant white fungal mycelia (Figures 3.1B and 1C). SEM images also show that in inoculated wood, branched hyphae penetrate the stem (Figures 3.1B and 1C).

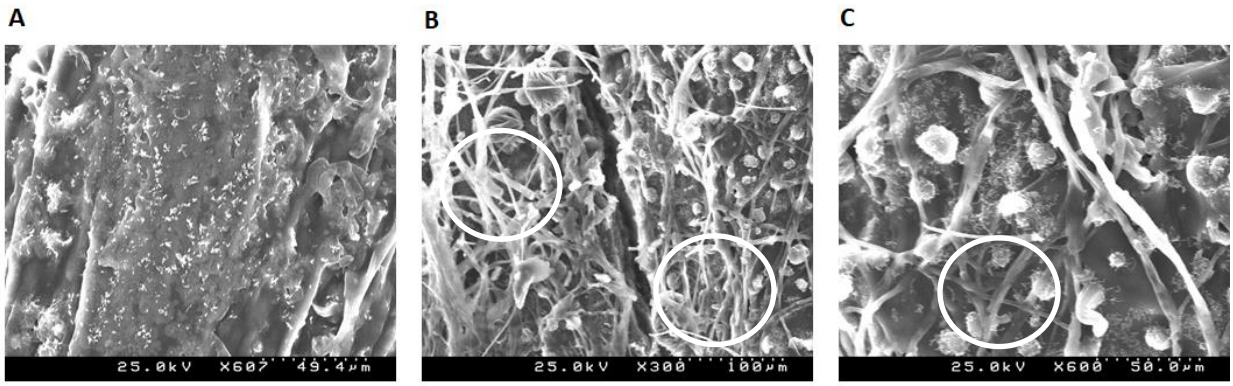

Figure 3.1 | SEM images of *Eucalyptus globulus* (MB43) stem colonized by *Neofusicoccum parvum*. control (**A**) and colonized stem (**B** and **C**) after 12 days. Magnifications of photographs are 607× (**A**), and 300x (**B**) and 600× (**C**). Circles refer to the distribution of *N. parvum* hyphae.

Secretome analysis

Prior to LC-MS, protein extracts were analysed for quality control by SDS-PAGE (Figure S3.1) The secretome of *N. parvum* grown in the absence (control) and presence of *Eucalyptus* stem (infection-like) were analyzed. The infection-like protein profiles of *N. parvum* have a myriad of proteins common to the control. In total, 471 proteins were identified in both control and infection-like secretomes, of which 131 proteins were significantly differently expressed between the two conditions (t-test, difference cutoff of 1.8). Most of these proteins are extracellular (Table 3.2 and Table S3.1), except for

14 proteins predicted as intracellular proteins (10.7 %, Table S3.1). Most of the proteins (86.3 %) were predicted to contain a Signal P motif and can traverse the classical Golgi and endoplasmic reticulum pathway. The non-classical pathway for the proteins lacking signal peptide (13.7 %) was confirmed using SecretomeP predictor (Bendtsen et al., 2004) (Table 3.2). Such proteins are known as leaderless secreted proteins (LCPs) and have been identified in most of the secretome studies (Cobos et al., 2010; Jung et al., 2012; Sibbald et al., 2006). Of these LCPs proteins, putative ethanolamine utilization protein (R1G1U2) and chitin binding protein (R1EW80) showed low SecretomeP scores (NN score = 0.223 and 0.417, respectively) (Table 3.2). However, the NN score of chitin binding protein is relatively close to the 0.5 threshold, whereby the protein might still be secreted.

Proteins were classified according to the GO (biological process) of each gene product, into 10 protein families: CAZymes, hydrolases, proteases, oxidoreductases, lyases, protein-protein interaction, carbohydrate binding proteins, RNA binding proteins and proteins with other function and unknown function (Figure 3.2).

Among differentially secreted proteins (117), 88 proteins were more abundant in infection-like conditions, while 29 proteins were more abundant in control conditions (Table 3.2, Figure 3.2). Among induced proteins in the presence of eucalyptus, we identified mainly CAZy proteins (50 proteins), esterases (9 proteins), proteases (4 proteins), oxidoreductase (5 proteins) (Figure 3.2, Table 3.2), and proteins with lyase activity (4 proteins).

Among the CAZy proteins whose abundance is affected by the interaction with *Eucalyptus* stem, glycosyl hydrolases (GH) are the most abundant group (34 out of 50 proteins), followed by proteins with auxiliary activities (AAs, 4 proteins), polysaccharide lyases (PLs, 8 proteins), carbohydrate esterases (CEs, 3 proteins) and unknown CAZy proteins (1 protein) (Table 3.2 and Table S3.1). Esterases (EC 3.1.1.x), were more abundant in the infection like conditions (Figure 3.2B).

A variety of proteases (endo and exoproteases) were also identified. Aspartic endopeptidase pep1 (R1GM42) were detected in the infection like conditions along with a variety of other metallopeptidases (M28, M35 and M43, Figure 3.2B and Table 3.2) and serine peptidases [S8(R1EAW3) and S10 (R1FV38)] down-regulated in the infection-like conditions (Figure 3.2A and Table 3.2).

A putative berberine-like protein (R1GD68) was the most abundant protein in the infection-like conditions (Table 3.2). The berberine-like protein is an oxidoredutase with a FAD binding domain.

Other functional categories - proteins involved in carbohydrate binding (R1EYI5 and R1GAK8), RNA biding (R1ERG2, R1FZX2, and R1H1L9), protein-protein interactions (R1ENG6, R1E9S0, and R1GCJ5) and proteins with other functions (R1EGT1, R1GV87, R1EAF3, R1G1U2, R1FV21, R1FVG4, R1GBA7, R1EWZ5, R1GDV3, R1GKT0, R1E681) - were also identified (Figure 3.2 and Table3.2).

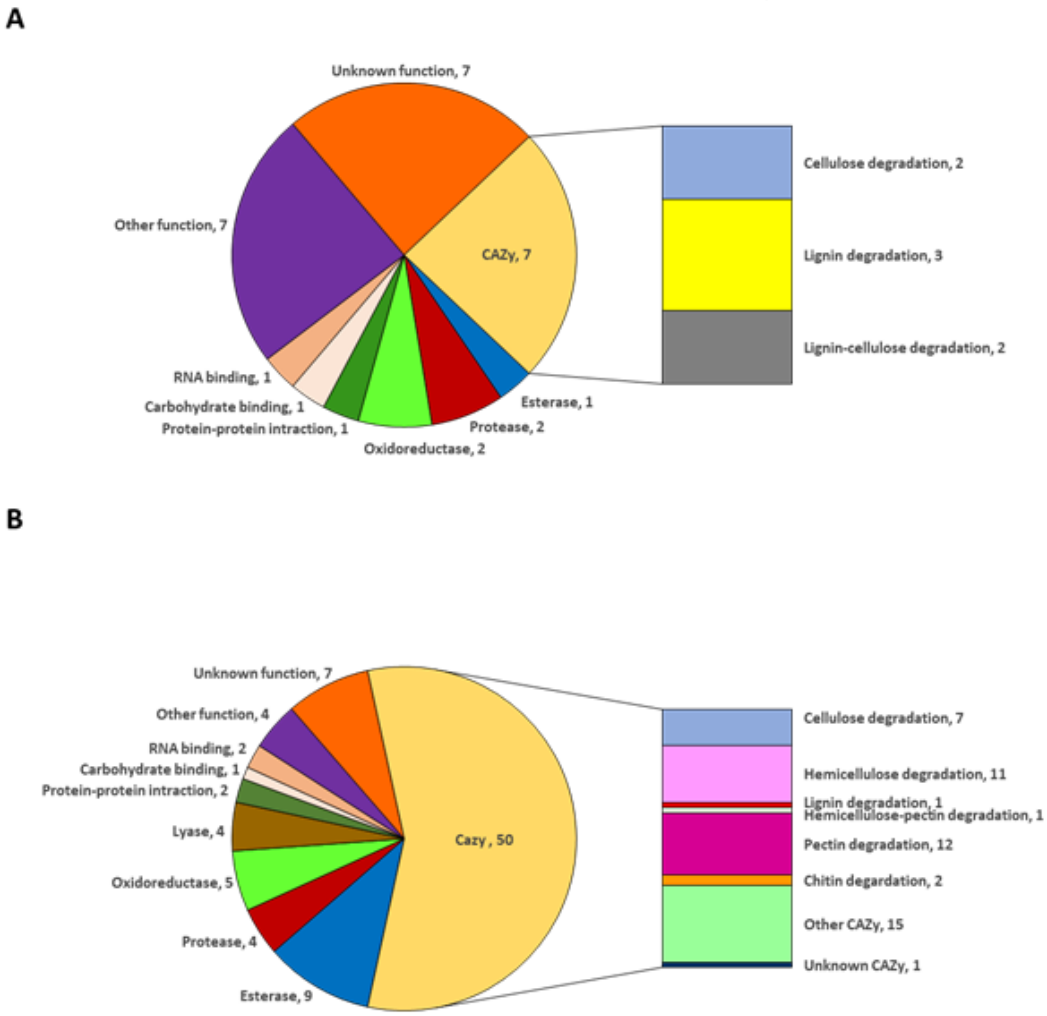

Figure 3.2 | Functional classification of the extracellular proteins secreted by *N. parvum* whose abundance was significantly different (p<0.05) between the two conditions. (**A**) Proteins less abundant in the presence of *Eucalyptus* stem, (**B**) Proteins more abundant in the infection-like condition. For each category, the number of proteins is given. The classification was obtained from the GO (biological process) of each protein according to the Uniprot database (http://www.uniprot.org/). When lacking exact functional annotations in this database, the family and domain databases (InterPro and Pfman) were used to reveal annotations of their conserved domains.

Real-time PCR analysis

To validate the reliability of the proteomics data, the relative expression level of 2 genes was confirmed using RT-qPCR with specific primers (Table 3.1). Putative exo-beta protein (PL3, R1H382) and putative aspartic endopeptidase pep1 protein (AP1, R1GM42) were selected due to their relevance to pathogenesis and up-regulation in the infection-like conditions. For both genes, gene expression was measured both in control and infection-like conditions (Figure 3.3). PL3's gene expression was significantly higher in the presence of host corroborating proteomics data; regarding AP1's gene, the expression in infection-like conditions was not significantly different from the control (Figure 3.3).

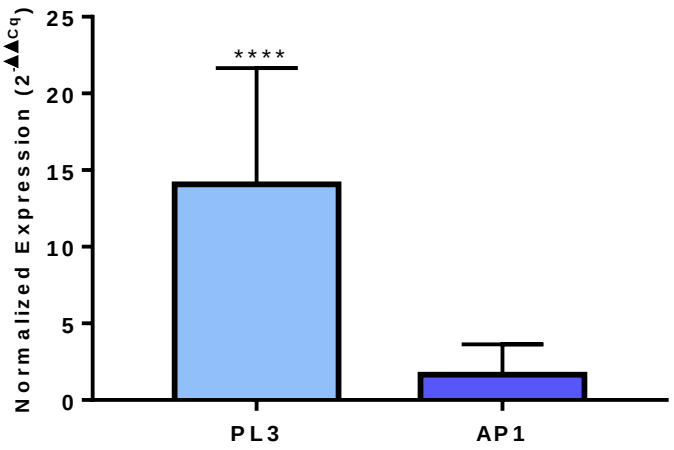

Figure 3.3 | Relative quantification by RT-qPCR of mRNA of the target genes encoding for PL3 (putative exo-beta protein (R1H382)) and AP1 (putative aspartic endopeptidase pep1 protein (R1GM42)). A t-test was conducted using the ΔCq value of each gene at two conditions tested, presence and absence of the host, using the absence of the host as control (**p*<0.05, ***p*<0.01, ****p*<0.001*****p*<0.0001).

DISCUSSION

We compared the protein profiles of the control and infection-like conditions, identified and quantified proteins whose abundance change in response to *Eucalyptus* stem, in order to highlight the proteins that may behave as virulence factors during fungal infection.

The secreted proteins were visualized in the volcano plot (Figure S3.4) in order to quick visual identification of proteins that display large magnitude fold change and high statistical significance. The presence of intracellular proteins in secretome is common and could be resulting from cell death during culture, cell lysis during protein extraction or secretion through an unknown mechanism. The number of identified proteins in this study is higher than those identified in the secretome of *D. seriata* (16 proteins) (Cobos et al., 2010), *D. corticola* (12 proteins) (Fernandes et al., 2014) and *L. theobromae* (16 proteins) (Félix et al., 2016) the closest *Botryosphaeriaceae* fungi whose secretomes were studied. Plant infection by phytopathogens, such as *N. parvum*, is a complex process that starts with the attachment of the infective propagule to the plant surface followed by penetration and infection. SEM confirmed the extensive colonization of eucalyptus stem by fungal hyphae.

Fasciclin family proteins have been identified as cell adhesion molecules in various organisms (Carr et al., 2003; Elkins et al., 1990; Gaspar et al., 2001; Kawamoto et al., 1998). In this study, the up-regulation of the putative fasciclin domain family protein (R1EWZ5) in the infection-like conditions could be responsible for the perfect attachment of fungal hyphae to the host material. In rice blast fungus, *Magnaporthe oryzae*, MoFLP1 null mutants generated by targeted fasciclin gene disruption

showed significant reduction of conidiation, conidial adhesion, and appressorium turgor, resulting in overall decreased fungal pathogenicity (Liu et al., 2009).

Plant cell wall-degrading enzymes (PCWDEs) play significant roles in plant colonization. Many plant pathogens are known to secrete a variety of PCWDEs to perceive weak regions of plant epidermal cells and penetrate the plant primary cell wall. Our results indicate that *N. parvum* is equipped with an army of extracellular PCWDE expressed even in the absence of plant tissue. As expected PCWDE were induced by the presence of *Eucalyptus* stem. It is interesting to note that in the infection-like condition there is an enrichment of glicosyl hidrolases and polysaccharide lyases able to digest plant cell wall molecules such as cellulose, hemicellulose, and pectin, that may play a role in the penetration of the *N. parvum* into the stems (Table 3.2).

Plant pathogenic fungi are known to produce many pectinases, considered as key virulence factors, due to their cell wall degrading activity (Creze et al., 2008; Herron & Benen, 2000). Pectic enzymes (in multiple forms) are the first cell wall degrading enzyme induced by pathogens when cultured on isolated plant cell walls and the first produced in infected tissue (Martínez et al., 1991; Niture et al., 2006). Pectin, even in very small quantity, helps to hold polysaccharides together and influences cell wall plasticity. Pectic enzymes induce the modification of cell wall structure, exposing cell wall components for degradation to other enzymes, cell lysis and plant tissue maceration (Panda et al., 2004). Pectin is also present in *Eucalyptus* cell walls (15.2 and 25.8 mg g^{-1} pectin, Coetzee et al., 2011) and the secretion of pectin-degrading enzymes upon interaction with *Eucalyptus* stem surely promote the close interaction between the fungus and plant. This analysis highlighted the presence of CAZymes targeting pectin (from GH53 and CE12) and several different pectate lyases (PL1, P3, PL4) to assist in breaking down the pectin (Table 3.2 and S3.1). All identified pectin-degrading enzymes in this study (Table 3.2 and S3.1) are more abundant in the presence of host material, suggesting that this fungus is more adapted to degrade intact or living plants than decaying biomass (where pectin is not existing and is already decayed), which is in consonance with the fungus being a latent pathogen.

Pectinases and polysaccharide lyases were more abundant in the presence of host material. PL4 Rhamnogalacturonate lyase (R1GGA5) was not only the most abundant enzyme among pectinases (Table 3.2 and S3.1), but also among all identified proteins (7.6 fold increase in infection-like conditions). In addition, GH28 putative extracellular exo-protein with polygalacturonase activity (R1GW72) and pectate lyase proteins (R1EWA7, RAGN84, R1GII6, R1GSQ1), all having very important roles in cell wall degradation and in fungal invasion, are more prevalent in the presence of host material (Kars & van Kan, 2007; Zhang & van Kan, 2013). In accordance, Kang and Buchenauer et al. (2000) and Tomassini et al. (2009) demonstrated that wheat infection with *Fusarium culmorum* and *Fusarium graminearum*, respectively depends on the production of CWDE enzymes such as pectinases

at the early stages of infection resulting in facilitating rapid colonization of wheat spikes. Moreover, the upregulation of these enzymes in lethal isolates of *Verticilium albo-atrum* compared to mild isolates was equally corroborated by Mandelc & Javornik (2015), having been implied its hypothetical contribution for the plant vascular system colonization.

We also identified cellulose-degrading enzymes mainly in the presence of *Eucalyptus* stem. Previous studies showed that cellulases of phytopathogenic fungi are involved in pathogenicity (Eshel et al., 2002; Sexton et al., 2000). To hydrolyse cellulose chains into monomers, the main chain must be cleaved internally, and this event is performed by endoglucanases (GH5, GH12). Likewise, the release cellobiose occurs via the action of exoglucanases (GH7), and it is subsequently converted into glucose by β-glucosidases (GH3). Putative GH 12 protein (R1GQP5) raises especial attention, due to a high increase in response to *Eucalyptus* stem (3.9-fold up, Table 3.2). Recently, the XEG1 (xyloglucanspecific endo-β-1,4-glucanase, GH12 family) isolated from *P. sojae* culture filtrates induced cell death in dicot plants but not in monocot (Ma et al., 2015). Gui et al. (2017) demonstrated that two of the six GH12 proteins in the fungus *Verticillium dahliae* Vd991 (VdEG1 and VdEG3) acted as virulence factors and as PAMPs, inducing cell death and triggering PAMP-triggered immunity (PTI) in *Nicotiana benthamiana*. The downy mildew *Hyaloperonospora arabidopsidis* also has three GH12 genes, however, none of them encodes a protein able to elicit cell death (Ma et al., 2015). Therefore, the GH12 protein upregulation in response to host suggests that this protein may be directly involved, as a virulence factor, during *N. parvum* infection, a role that should be validated, in the future, in *in planta* experiments.

A glucanase (R1GZN3, GH7) was more abundant in the presence of *Eucalyptus* stem. Cellulases belonging to GH6 and GH7 families have been described as related to fungal virulence in the phytopathogenic fungus *Magnaporthe oryzae*, where they seem to be involved in the penetration of the host epidermis and further invasion (Van vu et al., 2012). Van vu et al. (2012) showed that the transcript's levels of several cellulases from GH6 and GH7 families were upregulated more than 1000-fold upon infection compared with the levels of cellulase transcripts in vegetative mycelia on rich medium (Van vu et al., 2012). Also, Fernandes et al. (2014) suggested that several cellulases could be potentially involved in pathogenesis of *Diplodia corticola*, including endoglucanases (Fernandes et al., 2014).

Besides cell wall degrading enzymes, hemicellulases are generally involved in the degradation of hemicellulose from plant cell walls helping to colonization and providing nutrients during infection. We identified hemicellulases involved in the cleavage of the main chain of xylan (endoxylanases, GH10, GH11) and the side chain of hemicelluloses, including ß-xylosidase (GH43), arabinofuranosidase (GH43, GH51), galactosidase (GH27, GH35, GH43), acetylxylan esterase (CE5) and others (Table 3.2

and S3.1). The up-regulation of two endoxylanase enzymes [Beta-xylanase GH10 (R1FWZ0) and Endo-1,4-beta-xylanase GH11 (R1GCT8)] was observed in the *N. parvum* secretome in response to *Eucalyptus* stem. GH10 and GH11 endoxylanases play significant roles in both vertical penetration of cell walls and horizontal expansion of the rice pathogen *M. oryzae* in infected leaves (Nguyen et al., 2011). A recent study showed that two genes encoding GH10 xylanases are crucial for the virulence of the oomycete plant pathogen *Phytophthora parasitica* (Lai & Liou, 2018). In *B. cinerea*, *Xyn11A* encodes an endo-β-1,4-xylanase Xyn11A, while disruption of this gene resulted in reduced virulence (Brito et al., 2006). However, several reports failed to show an essential role of endoxylanase in fungal pathogenicity (Apel-Birkhold & Walton, 1996; Calero-Nieto et al., 2007; Gómez-Gómez et al., 2002). Therefore, the role of xylanase in the pathogenesis of pathogens may vary depending on characteristics of the pathosystems which await further investigation.

Most abundant of the CAZy proteins in the control secretome of *N. parvum* are predicted to be involved in lignin degradation (AA1, AA5, AA7) (Table 3.2 and S3.1). The most relevant were laccase-1 protein (R1G4L9), glyoxal oxidase protein (R1EDI4) and cellobiose dehydrogenase (R1H3M7) (Table 3.2 and S3.1). These enzymes belong to oxidoreductase family which can produce the H_2O_2 required for the action of extracellular peroxidases. Usually, *N. parvum* is not considered a major lignin-depolymerizing fungus, like white rot fungi (Stempien et al., 2017), but in our study, several extracellular lignin degrading enzymes were identified. However, most of those enzymes (five out of six) were less abundant in the presence of the *Eucalyptus* stem, indicating that may they have another role in *N. parvum* rather than a direct role in lignocellulose deconstruction. A similar observation was described for the white-rot fungus *Lentinula edodes* when exposed to microcrystalline cellulose, cellulose with lignosulfonate and glucose (Cai et al., 2017): CAZy proteins involved in lignin degradation were repressed by cellulose. Cai et al. (2017) suggested laccases may have a role for increasing fungal resistance to oxidative stress rather than being involved in lignocellulosic degradation.

Oxidoreductases, such as the putative berberine-like protein (R1GD68), are over-represented in the secretome of the *N. parvum* supplemented with *Eucalyptus* stem (5 fold), where they may contribute to the alkaloid biosynthesis and production of hydrogen peroxide through the oxidation of metabolites (Leferink et al., 2008). Oxidoreductases are thought to be important virulence factors induced during plant infection (Raffaele et al., 2010; Seidl et al., 2011).

Fungal cell wall degradation plays a fundamental role in fungal development during infection facilitating fungal branching and elongation (Do Vale et al., 2012). The putative chitin binding protein (R1EW80) contains a chitin deacetylase domain which catalyzes the conversion of chitin into chitosan required for appressorium formation (Kuroki et al., 2017). Interestingly, the up-regulation of this

protein in response to the host mimicry reinforces the hypothesis that this protein might play a role in appressorium formation in order to colonize the host. Some pathogens produce chitin-binding proteins that mask chitin, avoiding host recognition by shielding, or by modifying it (Rovenich et al., 2016; Sharp, 2013). Similarly, we identified a putative chitin deacetylase (CE4, R1E7G7) which is significantly up-regulated (5.6 fold) in the presence of *Eucalyptus* stem. This enzyme is also involved in chitosan generation from partly deacetylated chitin (Zhao et al., 2010). Chitin deacetylases also are involved in the protection of fungi from host plant chitinases by converting the fungal cell wall chitin into chitosan (Kouzai et al., 2012; Ride & Barber, 1990). An endo-chitosanase (GH75, R1GTL6) is also up-regulated (4.1 fold) during the interaction with *Eucalyptus* stem suggesting that chitosan generation by chitin deacetylase enhanced chitosanolytic activity of the fungus. We may hypothesize that the induction of chitosan synthesis and degradation proteins during interaction with *Eucalyptus* stem could be an infection strategy employed by this pathogen.

Proteases identified reflect their functional diversity (exo- and endo-proteases) and their synergistic interplay (Girard et al., 2013). Although some proteases were more abundant in the control [peptidase S10 (R1FV38) and peptidase S8 (R1EAW3)] most extracellular proteases identified were up-regulated upon induction with *Eucalyptus*. Several of these enzymes were previously described as virulence factors for fungal phytopathogens (Hislop et al., 1982; Movahedi & Heale, 1990; Poussereau et al., 2001; Poussereau et al., 2001; Urbanek & Yirdaw,1984). Specifically, metalloproteases such as deuterolysin have been suggested to target proteins in the plant cell wall (Lakshman et al., 2016). Also, deuterolysin is induced in a virulent strain of *Diplodia corticola* upon challenge by the host (*Quercus suber*) (Fernandes et al., 2015).

A putative ricin B lectin protein (R1GAK8), involved in carbohydrate binding, was induced in response to the host mimicry (4.3 fold). This protein contains a pectin_lyase_fold/virulence domain (IPR011050) considered a virulence factor in several species (González-Fernandez et al., 2014; Ismail & Able, 2016; Kubicek et al., 2014). Ricin B lectins inhibit protein synthesis (Endo & Tsurugi, 1987) and are highly expressed during infection (Andersson et al., 2014; Meerupati et al., 2013).

Interestingly, proteins containing ribonuclease/ribotoxin domains are more abundant in the secretome of *N. parvum* supplemented with *Eucalyptus* stem. Ribonucleases perform a variety of functions, serving as extra- or intracellular cytotoxins, and modulating host immune responses (Luhtala & Parker, 2010). Ribotoxins are fungal extracellular ribonucleases highly toxic due to their ability to enter host cells and their effective ribonucleolytic activity against the ribosome (Olombrada et al., 2014). We find that only one putative ribonuclease t2 was more abundant in the of control secretome which can be in response to phosphate starvation for phosphate scavenging from RNA

(MacIntosh, 2011). Secretion of low-molecular-weight guanyl-preferring ribonucleases (RNases) has been reported in the secretome of phytopathogen *D. corticola* (Fernandes et al., 2015).

Further, *N. pavum* secretome also contains necrotic elicitors like necrosis inducing protein (R1FXG6) and putative epl1 protein (R1G1Q3) containing cerato-platanin domain, but no significant differences between the control and infection-like profiles (Table S3.2) were identified, suggesting that this phytotoxin is constitutively expressed by *N. parvum*.

CONCLUSIONS

We described for the first time the composition of the secretome of the fungal pathogen *N. parvum*. To date, information on the pathogenicity/virulence factors induced in this pathogen by one of its hosts, *Eucalyptus,* is unavailable.

We identified several fungal glycoside hydrolases, proteases, oxidoreductase and virulence factors that can be involved in *N. parvum* pathogenesis towards *Eucalyptus* and other hosts. In our study, identified proteins mostly were induced under host mimicry secretome mostly cell wall degrading enzymes (CWDEs) specially those involved in plant cell wall degradation (targeting pectin and hemicellulose) which allow it to invade host tissues through the degradation of cell wall components of plants and extract nutrients for its own growth. Additionally, degradation of xylan (hemicellulose) and pectin is required for fungal pathogens to invasively penetrate and proliferate inside host cells. In general, the extracellular proteins of *N. parvum* suggest that the fungus has adjusted its secretome to the plant host cell wall, which agrees with the fact that *N. parvum* is a phytopathogen. Likewise, absence of lignin degrading enzymes and existence of a several cellulases and hemicellulases fits well with its endophytic/latent pathogen lifestyle. Endophytes appear to be able to degrade relatively simpler substrates, such as cellulose and hemicelluloses, rather than very complex substrates like lignin. In addition to, the presence of pectin-degrading enzymes even in the absence of host material, is in accordance with this endophytic fungus being more adapted to degrade intact or living plants than decaying biomass, which implies that the fungus is likely to be a latent pathogen. We also found the up regulation of chitosan synthesis and degradation proteins during interaction with *Eucalyptus* stem. Therefore, it is reasonable to hypothesize that it could be an infection strategy employed by this pathogen during infection. Further experiments need to be performed to corroborate this hypothesis.

ACKNOWLEDGEMENTS

Thanks are due to FCT/MCTES for the financial support to CESAM (UID/AMB/50017/2019) and F. Nazar Pour (BD/98971/2013), through national funds. This study was partially supported by FEDER funding through COMPETE program (POCI-01-0145-FEDER-016788) and Programa Operacional Regional de

Lisboa - POR Lisboa (LISBOA-01-0145-FEDER-016788) and by national funding through FCT within the research project PANDORA (PTDC/ AGR-FOR /3807/2012—FCOMP-01-0124-FEDER-027979).

Table 3.2 | Summary of the proteins differentially secreted by *Neofusicoccum parvum* (CAA704)

Protein name	Accession number[a]	Fold change[b]	p - value[c]	Unique peptides[d]	PEP[e]	Intensity[f]	SignalP[g]	Localization[i]
Cellulose degradation								
GH5 - Putative glycoside hydrolase family 5 protein	R1GZQ9	2.1	1.833	6	1.87E+09	169.3	Yes	Extracelluar
GH5 - Putative endoglucanase ii protein	R1GLD6	1.9	1.554	6	8.42E+08	97.74	Yes	Extracelluar
GH5 - Putative cellulase family protein	R1G7G3	-2.7	3.403	12	2.36E+10	323.3	Yes	Extracelluar
GH5 - Putative endo-beta--protein	R1GDK9	-3.9	2.961	18	9.7E+09	323.3	Yes	Extracelluar
GH3 - Putative beta-d-glucoside glucohydrolase protein	R1EK26	-3.5	3.584	8	1.06E+09	98.06	Yes	Extracelluar
GH3 - Putative beta-glucosidase 1 protein	R1G324	-2	2.565	11	3.43E+08	84.3	Yes	Extracelluar
GH7 - Glucanase	R1GZN3	-2.5	2.374	10	1.49E+10	323.3	Yes	Extracelluar
AA9/GH61/CBM1 - Putative fungal cellulose binding domain protein	R1GHV2	-2.1	3.779	7	2.05E+09	204.1	Yes	Extracelluar
GH12 - Putative glycoside hydrolase family 12 protein	R1GQP5	-3.9	3.605	8	1.05E+10	120.04	Yes	Extracelluar
Hemicelluose degradation								
GH35 - Putative beta-galactosidase b protein	R1E7W9	-2.5	3.430	21	4.23E+09	255.29	Yes	Extracelluar
GH43 - Putative glycosyl family protein	R1EP04	-2.9	2.330	6	5.29E+08	73.74	Yes	Extracelluar
GH10 - Beta-xylanase	R1FWZ0	-3.1	3.513	14	2.31E+10	323.31	Yes	Extracelluar
GH43 - Putative xylosidase: arabinofuranosidase protein	R1G299	-2.1	3.289	6	3.79E+08	140.27	Yes	Extracelluar

Table 3.2 | continued

Protein name	Accession number[a]	Fold change[b]	p - value[c]	Unique peptides[d]	PEP[e]	Intensity[f]	SignalP[g]	Localization[i]
GH43 - Putative xylosidase glycosyl hydrolase protein	R1G5Y4	-1.9	3.227	13	3.51E+10	323.31	Yes	Extracellular
GH27 - Alpha-galactosidase	R1G8C1	-2.6	4.883	12	1.8E+10	286.19	NN[h] (0.861)	Extracellular
GH43 - Putative galactan-beta-galactosidase protein	R1GG59	-5.5	3.216	14	3.67E+09	323.31	Yes	Extracellular
GH43 - Arabinan endo-1,5-alpha-L-arabinosidase	R1GAB3	-6.4	5.780	10	4.97E+09	117.45	Yes	Extracellular
GH51 - Putative alpha-l-arabinofuranosidase a protein	R1EVS4	-3.1	3.133	10	7.22E+08	190.73	Yes	Extracellular
CE5 - Putative acetylxylan esterase protein	R1EWW2	-2.3	1.059	2	1.54E+09	323.31	NN (0.898)	Extracellular
GH11 - Endo-1,4-beta-xylanase	R1GCT8	-2.4	1.534	7	3.41E+08	144.76	Yes	Extracellular
GH43/CBM6 - Putative glycosyl hydrolase family 43 protein	R1GE80	-2.2	3.527	16	8.42E+09	307.72	Yes	Extracellular
Lignin degradation								
AA5 - Putative glyoxal oxidase protein	R1EDI4	2.1	2.596	10	1.32E+09	86.505	Yes	Extracellular
AA1 - Putative laccase-1 protein	R1G4L9	1.9	3.262	11	1.03E+10	227.45	Yes	Extracellular
AA7 - Putative fad dependent oxidoreductase protein	R1FVT8	2.2	1.428	14	9.82E+08	123.3	Yes	Extracellular
AA3 - Putative alcohol dehydrogenase protein	R1EH41	-2.7	2.253	3	2.58E+08	35.849	NN (0.648)	Extracellular
Lignin/celulose degradation								
AA3/CBM1 - Putative cellobiose dehydrogenase protein	R1H3M7	2	1.856	16	1.72E+09	157.89	Yes	Extracellular
AA3 - Putative gmc oxidoreductase protein	R1FVG2	1.8	3.233	23	5.79E+10	323.31	NN (0.655)	Extracellular

Table 3.2 | continued

Protein name	Accession number[a]	Fold change[b]	p - value[c]	Unique peptides[d]	PEP[e]	Intensity[f]	SignalP[g]	Localization[i]
Pectin degradation								
GH53 - Arabinogalactan endo-beta-1,4-galactanase	R1G7Y3	-7	3.424	9	6.29E+09	161.62	Yes	Extracellular
CE12 - Putative rhamnogalacturonan acetylesterase protein	R1GFP8	-6.4	4.594	9	9.04E+09	155.37	Yes	Extracellular
GH53 - Arabinogalactan endo-beta-1,4-galactanase	R1GVP5	-2.3	2.391	5	5.89E+08	56.599	Yes	Extracellular
PL3 - Putative pectate lyase protein	R1EWA7	-6.6	3.224	9	6.54E+09	297.03	Yes	Extracellular
PL3 - Putative pectate lyase protein	R1GN84	-6.2	4.605	6	4.57E+09	103.84	Yes	Extracellular
PL1 - Putative pectate lyase a protein	R1GII6	-4.4	4.962	13	1.75E+10	323.31	Yes	Extracellular
PL4 - Putative rhamnogalacturonan lyase protein	R1GJ02	-5.5	4.999	18	3.48E+09	227.89	Yes	Extracellular
PL1 - Putative pectate protein	R1GSQ1	-4.8	3.712	5	1.4E+09	91.554	NN (0.592)	Extracellular
PL3 - Putative exo-beta--protein	R1H382	-2.2	2.235	24	1.8E+11	323.31	NN (0.798)	Extracellular
GH28 - Putative extracellular exo-protein	R1GW72	-3.2	3.359	5	8.03E+08	57.212	Yes	Extracellular
PL4 - Rhamnogalacturonate lyase	R1EPI5	-2	2.077	6	4.03E+08	107.86	Yes	Extracelluar
PL4 - Rhamnogalacturonate lyase	R1GGA5	-7.6	4.898	23	1.38E+10	323.31	Yes	Extracelluar
Chitin degradation								
CE4 - Putative chitin deacetylase protein	R1E7G7	-5.6	2.993	6	3.73E+09	53.089	Yes	Extracelluar
GH75 - Endo-chitosanase	R1GTL6	-4.1	1.099	4	4.37E+09	59.996	Yes	Extracelluar
Other CAZY								
GH16 - Putative glycoside hydrolase family 16 protein	R1EVI7	-2.7	2.462	3	2.12E+09	34.095	Yes	Extracelluar

Table 3.2 | continued

Protein name	Accession number[a]	Fold change[b]	p - value[c]	Unique peptides[d]	PEP[e]	Intensity[f]	SignalP[g]	Localization[i]
GH31 - Putative glycoside hydrolase family 31 protein	R1EDQ8	-3.2	2.191	6	5.04E+08	51.332	Yes	Extracelluar
GH35 - Putative beta-protein	R1EEC1	-2.4	4.893	24	3.67E+09	323.31	Yes	Extracelluar
GH3 - Putative glycoside hydrolase family 3 protein	R1GGK2	-4.6	2.928	18	3.45E+09	318.69	NN (0.804)	Extracelluar
GH88 - Putative cell wall glycosyl hydrolase protein	R1EUF4	-5.7	3.612	11	7.36E+09	157.66	Yes	Extracelluar
AA9/GH61 - Putative glycoside hydrolase family 61 protein	R1EYD0	-2.2	1.588	5	9.48E+08	105.3	Yes	Extracelluar
GH127 - Putative secreted protein	R1G8Q6	-3.6	2.818	19	6.8E+09	269.45	Yes	Extracelluar
GH43 - Putative glycoside hydrolase family 43 protein	R1GCR8	-1.9	4.089	30	1.67E+10	323.31	Yes	Extracelluar
GH88 - Putative cell wall glycosyl hydrolase protein	R1GLS8	-3.7	4.805	9	6.74E+08	88.16	Yes	Extracellular
GH115 - Putative glycoside hydrolase family 115 protein	R1GRC0	-2.5	3.092	19	8.4E+08	165.33	Yes	Extracellular
GH75 - Putative glycoside hydrolase family 79 protein	R1GVI3	-2.2	2.838	8	1.44E+10	200.77	NN (0.729)	Extracellular
GH43 - Putative glycoside hydrolase family 43 protein	R1H3P0	-2.6	3.321	11	3.52E+09	322.83	Yes	Extracellular
GH78 - Putative alpha-l-rhamnosidase protein	R1GPV4	-1.9	1.444	4	2.51E+08	32.11	Yes	Extracellular
GH43 - Putative glycoside hydrolase family 43 protein	R1EDI8	-2.1	3.481	13	2.34E+10	323.31	Yes	Extracellular
AA3 - Putative choline dehydrogenase protein	R1EPR9	-2.3	0.844	15	8.18E+08	128.24	Yes	Extracellular
Unknown CAZy								
Putative chitin binding protein	R1EW80	-2.2	2.159	8	2.53E+10	323.31	NN (0.417)	Extracellular

Table 3.2 | continued

Protein name	Accession number[a]	Fold change[b]	p - value[c]	Unique peptides[d]	PEP[e]	Intensity[f]	SignalP[g]	Localization[i]
Esterase								
Carboxylic ester hydrolase	R1GKX8	2.7	4.271	7	5.44E+08	70.895	Yes	Extracellular
Putative gdsl-like lipase acylhydrolase protein	R1E852	-4.1	2.117	6	3.13E+09	323.31	Yes	Extracellular
Carboxylic ester hydrolase	R1E8C5	-2.8	2.209	9	7.04E+08	79.717	Yes	Extracellular
Putative gdsl-like lipase acylhydrolase protein	R1GK66	-2.6	3.165	6	4.2E+08	40.614	Yes	Extracellular
Carboxylic ester hydrolase	R1GSL8	-2.1	2.550	6	1.91E+08	83.343	Yes	Extracellular
Putative carboxylesterase protein	R1EIK3	-3.7	1.530	4	7.19E+08	37.138	NN (0.768)	Extracellular
Carboxylic ester hydrolase	R1G8E3	-5.8	3.503	9	2.21E+09	171.03	Yes	Extracellular
Putative carboxylesterase family protein	R1G9C5	-2.1	3.136	5	1.71E+08	39.971	Yes	Extracellular
Putative gdsl lipase acylhydrolase family protein	R1EIF4	-1.8	2.818	6	3.13E+09	134.94	NN (0.756)	Extracellular
Carboxylic ester hydrolase/ tannase family	R1GJW0	-1.9	3.095	20	4.01E+09	323.31	Yes	Extracellular
Protease								
Peptidase S1 family - putative carboxypeptidase s1 protein	R1FV38	1.9	2.351	7	4.06E+09	175.54	Yes	Extracellular

Table 3.2 | continued

Protein name	Accession number[a]	Fold change[b]	p - value[c]	Unique peptides[d]	PEP[e]	Intensity[f]	SignalP[g]	Localization[i]
Peptidase S8 family - putative peptidase s8 s53 subtilisin kexin sedolisin protein	R1EAW3	2.2	1.289	5	1.54E+09	157.52	Yes	Extracellular
Peptidase A1 family - Putative aspartic endopeptidase pep1 protein	R1GM42	-3.2	4.661	4	4.3E+09	98.628	Yes	Extracellular
Peptidase M43 - Putative metalloprotease protein	R1FXE7	-5.1	3.311	5	3.6E+09	134.74	Yes	Extracellular
Peptidase M28 family - peptide hydrolase	R1GBR8	-2.7	2.039	6	1.35E+09	209.59	Yes	Extracellular
Peptidase M35 family - Neutral protease 2	R1EL46	-2.3	0.943	5	1.62E+09	102.51	Yes	Extracellular
Oxidoreductase								
Putative fmn-dependent dehydrogenase protein	R1E6X7	2.9	1.290	16	6.56E+08	127.23	Yes	Extracellular
Putative fad binding domain-containing protein	R1E8E1	3.6	3.973	11	4.38E+09	264.43	Yes	Extracellular
Putative cyclohexanone monooxygenase protein	R1EF40	-3.7	1.628	2	9.32E+09	20.921	Yes	Extracellular
Putative tyrosinase central domain protein	R1ERX8	-2.4	2.164	9	8.84E+08	90.821	NN (0.817)	Extracellular

Table 3.2 | continued

Protein name	Accession number[a]	Fold change[b]	p - value[c]	Unique peptides[d]	PEP[e]	Intensity[f]	SignalP[g]	Localization[i]
Putative fad fmn-containing dehydrogenase protein	R1GB06	-3.4	3.369	16	9.58E+08	192.5	Yes	Extracellular
Putative berberine-like protein	R1GD68	-5	2.241	13	2.88E+09	323.31	Yes	Extracellular
Putative gmc protein	R1ELQ0	-2.1	0.517	6	5.13E+09	40.919	Yes	Extracellular
Lyase								
Putative pectate lyase protein	R1H2U7	-2.3	3.013	4	2.56E+08	28.73	Yes	Extracellular
Putative secreted protein	R1GFS9	-3	3.218	20	2.59E+11	323.31	Yes	Extracellular
Putative pectate lyase protein	R1G436	-5.7	4.498	17	3.09E+09	217.8	Yes	Extracellular
Uncharacterized protein	R1GU06	-1.9	2.289	7	2.48E+10	323.31	Yes	Extracellular
Protein-protein intraction								
Putative six-bladed beta-propeller-like protein	R1ENG6	2.3	2.942	3	4.52E+08	36.528	Yes	Extracellular
Putative six-bladed beta-propeller-like protein	R1E9S0	-2.3	1.704	2	4.15E+08	21.736	Yes	Extracellular
Putative smp-30 gluconolaconase lre-like region protein	R1GCJ5	-2.1	0.903	5	1.13E+09	92.83	NN (0.754)	Extracellular
Carbohydrate binding								
Putative alpha-mannosidase family protein	R1EYI5	1.8	1.196	2	6.81E+08	23.805	Yes	Extracellular
Putative ricin b lectin protein	R1GAK8	-4.3	2.336	6	1.66E+09	97.147	Yes	Extracellular
RNA binding								
Putative ribonuclease t2 protein	R1ERG2	2.8	2.404	2	5.88E+08	62.528	Yes	Extracellular
Uncharacterized protein	R1FZX2	-4.1	1.575	6	1.9E+09	43.942	Yes	Extracellular
Putative extracellular guanyl-specific ribonuclease protein	R1H1L9	-2.1	0.586	3	4.24E+09	48.559	Yes	Extracellular

Table 3.2 | continued

Protein name	Accession number[a]	Fold change[b]	p - value[c]	Unique peptides[d]	PEP[e]	Intensity[f]	SignalP[g]	Localization[i]
Other function								
Putative allergen v5 tpx-1-related protein	R1EAF3	2.2	3.639	5	5.58E+09	181.15	Yes	Extracellular
Putative ethanolamine utilization protein	R1G1U2	2	2.760	5	4.1E+08	54.96	NN (0.223)	Extracellular
Putative abc-type Fe3+ transport system protein	R1FV21	2.9	1.484	6	4.15E+08	58.409	Yes	Extracellular
Putative major royal jelly protein	R1FVG4	2.7	1.896	15	5.75E+10	323.31	Yes	Extracellular
Putative abc-type Fe3+ transport system protein	R1GBA7	2.8	1.611	15	7.33E+10	323.31	Yes	Extracellular
Putative alpha beta hydrolase protein	R1EGT1	2.7	3.692	11	3.31E+09	118.1	Yes	Extracellular
Putative glutaminase protein	R1GV87	2.7	3.603	10	1.15E+09	215.65	Yes	Extracellular
Putative fasciclin domain family protein	R1EWZ5	-2	2.878	12	2.37E+09	129.86	Yes	Extracellular
Uncharacterized protein	R1GDV3	-4.1	2.108	5	3.67E+10	323.31	Yes	Extracellular
Putative bnr asp-box repeat domain protein	R1GKT0	-2.2	2.950	11	2.45E+10	323.31	Yes	Extracellular
Putative extracellular aldonolactonase protein	R1E681	-1.8	0.892	5	2.15E+09	183.99	Yes	Extracellular
Unknown								
Putative extracellular serine-threonine rich protein	R1E9T1	2.9	3.242	3	8.48E+08	78.551	Yes	Extracellular

Table 3.2 | continued

Protein name	Accession number[a]	Fold change[b]	p - value[c]	Unique peptides[d]	PEP[e]	Intensity[f]	SignalP[g]	Localization[i]
Putative membrane-spanning 4-domains subfamily a member 14 protein	R1EE60	2.9	3.242	3	8.48E+08	78.551	Yes	Extracellular
Uncharacterized protein	R1EBL8	2.1	3.282	11	1.26E+10	323.31	Yes	Extracellular
Putative GPI anchored cell wall protein	R1G7D5	2.2	1.914	4	1.35E+09	24.812	Yes	Extracellular
Uncharacterized protein	R1GMX5	2.3	3.894	6	2.11E+10	185.31	Yes	Extracellular
Uncharacterized protein	R1GRM4	2.4	1.314	4	7.62E+08	37.391	Yes	Extracellular
Uncharacterized protein	R1G5W7	2.1	0.681	2	8.78E+08	20.89	Yes	Extracellular
Uncharacterized protein	R1ESR7	-4	1.737	3	1.4E+10	48.44	Yes	Extracellular
Putative secreted protein	R1G8U3	-3.4	3.421	6	4.85E+08	49.633	Yes	Extracellular
Uncharacterized protein	R1GYB0	-5.3	1.742	7	6.21E+09	132.23	Yes	Extracellular
Putative gpi anchored cell wall protein	R1ENT4	-2.4	0.948	4	1.24E+09	40.251	Yes	Extracellular
Putative 34-dihydroxy-2-butanone 4-phosphate synthase protein	R1EY60	-2.1	1.093	2	3.23E+08	44.267	Yes	Extracellular
Uncharacterized protein	R1GLY2	-2.1	1.562	6	3.69E+08	67.175	Yes	Extracellular

Table 3.2 | continued

Protein name	Accession number[a]	Fold change[b]	p - value[c]	Unique peptides[d]	PEP[e]	Intensity[f]	SignalP[g]	Localization[i]
Putative exo-beta--glucanase protein	R1G5R2	-2.6	1.282	7	1.19E+11	323.31	Yes	Extracellular

[a]Protein accession provided by the UniprotKB database

[b]Fold change: The difference between the average intensities of two groups (log ratio control vs infection-like); Negetive fold change values indicate proteins are more abundant in the infection-like secretome and positive fold change values indicate proteins are more abundant in the control secretome.

[c]p-value: displaying significance which are expressed as -log values

[d]Unique peptides: The total number of unique peptides associated with the protein group (i.e. these peptides are not shared with another protein group)

[e]PEP: Posterior Error Probability of the identification. This value essentially operates as a pvalue, where smaller is more significant

[f]Intensity: Summed up extracted ion current (XIC) of all isotopic clusters associated with the peptide sequence, and protein intensities summed the intensities of all peptides assigned to the protein group

[g]Signal prediction calculated by using the SignalP (http://www.cbs.dtu.dk/services/SignalP/). [h]NN: Non-classically secreted proteins analysed with SecretomeP 2.0 (Bendtsen et al., 2004). Proteins with NN score ≥ 0.5 were considered unconventionally secreted.

[i]Protein localization predicted by BaCeILO predictor (Pierleoni et al., 2006).

REFERENCES

Abou-Mansour, E., Débieux, J.-L., Ramírez-Suero, M., Bénard-Gellon, M., Magnin-Robert, M., Spagnolo, A., L'Haridon, F. (2015). Phytotoxic metabolites from *Neofusicoccum parvum*, a pathogen of Botryosphaeria dieback of grapevine. *Phytochemistry*, 115, 207–215.

Andersson, K.-M., Kumar, D., Bentzer, J., Friman, E., Ahrén, D., & Tunlid, A. (2014). Interspecific and host-related gene expression patterns in nematode-trapping fungi. *BMC Genomics*, 15(1), 968.

Andolfi, A., Mugnai, L., Luque, J., Surico, G., Cimmino, A., & Evidente, A. (2011). Phytotoxins produced by fungi associated with grapevine trunk diseases. *Toxins*, 3(12), 1569–1605.

Apel-Birkhold, P. C., & Walton, J. D. (1996). Cloning, disruption, and expression of two endo-beta 1, 4-xylanase genes, XYL2 and XYL3, from *Cochliobolus carbonum*. *Applied and environmental microbiology*, 62(11), 4129–4135.

Barradas, C., Alan J. L., P., Correia, A., Eugénio, D., Bragança, H., & Alves, A. (2016). Diversity and potential impact of Botryosphaeriaceae species associated with *Eucalyptus globulus* plantations in Portugal. *European Journal of Plant Pathology*, 146(2), 245–257.

Bénard-Gellon, M., Farine, S., Goddard, M. L., Schmitt, M., Stempien, E., Pensec, F., Larignon, P. (2015). Toxicity of extracellular proteins from *Diplodia seriata* and *Neofusicoccum parvum* involved in grapevine Botryosphaeria dieback. *Protoplasma*, 252(2), 679–687.

Bendtsen, J. D., Jensen, L. J., Blom, N., Von Heijne, G., & Brunak, S. (2004). Feature-based prediction of non-classical and leaderless protein secretion. *Protein Engineering Design and Selection*, 17(4), 349–356.

Blanco-Ulate, B., Rolshausen, P., & Cantu, D. (2013). Draft genome sequence of *Neofusicoccum parvum* isolate UCR-NP2, a fungal vascular pathogen associated with grapevine cankers. *Genome Announcements*, 1(3), e00339-13.

Brito, N., Espino, J. J., & González, C. (2006). The endo-β-1, 4-xylanase Xyn11A is required for virulence in *Botrytis cinerea*. *Molecular Plant-Microbe Interactions*, 19(1), 25–32.

Cai, Y., Gong, Y., Liu, W., Hu, Y., Chen, L., Yan, L., Bian, Y. (2017). Comparative secretomic analysis of lignocellulose degradation by *Lentinula edodes* grown on microcrystalline cellulose, lignosulfonate and glucose. *Journal of Proteomics*, 163, 92–101.

Calero-Nieto, F., Di Pietro, A., Roncero, M. I. G., & Hera, C. (2007). Role of the transcriptional activator xlnR of *Fusarium oxysporum* in regulation of xylanase genes and virulence. *Molecular Plant-Microbe Interactions*, 20(8), 977–985.

Carr, M. D., Bloemink, M. J., Dentten, E., Whelan, A. O., Gordon, S. V, Kelly, G., Williamson, R. A. (2003). Solution Structure of the *Mycobacterium tuberculosis* complex protein MPB70 from tuberculosis pathogenesis to inherited human corneal disease. *Journal of Biological Chemistry*, 278(44), 43736–43743.

Chen, S., Pavlic, D., Roux, J., Slippers, B., Xie, Y., Wingfield, M. J., & Zhou, X. D. (2011). Characterization of Botryosphaeriaceae from plantation-grown *Eucalyptus* species in South China. *Plant Pathology*, 60(4), 739–751.

Choi, Y. W., Hodgkiss, I. J., & Hyde, K. D. (2005). Enzyme production by endophytes of *Brucea javanica. Journal of Agricultural Technology*, 1, 55–66.

Cobos, R., Barreiro, C., Mateos, R. M., & Coque, J.-J. R. (2010). Cytoplasmic- and extracellular-proteome analysis of *Diplodia seriata*: a phytopathogenic fungus involved in grapevine decline. *Proteome Science*, 8, 46.

Coetzee, B., Schols, H. A., & Wolfaardt, F. (2011). Determination of pectin content of *eucalyptus* wood. *Holzforschung*, 65(3), 327–331.

Creze, C., Castang, S., Derivery, E., Haser, R., Hugouvieux-Cotte-Pattat, N., Shevchik, V. E., & Gouet, P. (2008). The crystal structure of pectate lyase peli from soft rot pathogen *Erwinia chrysanthemi* in complex with its substrate. *Journal of Biological Chemistry*, 283(26), 18260–18268.

Czemmel, S., Galarneau, E. R., Travadon, R., McElrone, A. J., Cramer, G. R., & Baumgartner, K. (2015). Genes expressed in grapevine leaves reveal latent wood infection by the fungal pathogen *Neofusicoccum parvum*. *PLoS One***,** 10(3), e0121828.

Deus, E., Silva, J. S., Castro-Díez, P., Lomba, A., Ortiz, M. L., & Vicente, J. (2018). Current and future conflicts between eucalypt plantations and high biodiversity areas in the Iberian Peninsula. *Journal for Nature Conservation*, 45, 107–117.

Do Vale, L. H. F., Gómez-Mendoza, D. P., Kim, M., Pandey, A., Ricart, C. A. O., Edivaldo, X. F. F., & Sousa, M. V. (2012). Secretome analysis of the fungus *Trichoderma harzianum* grown on cellulose. *Proteomics*, 12(17), 2716–2728.

Elkins, T., Zinn, K., McAllister, L., HoffMann, F. M., & Goodman, C. S. (1990). Genetic analysis of a Drosophila neural cell adhesion molecule: interaction of fasciclin I and Abelson tyrosine kinase mutations. *Cell*, 60(4), 565–575.

Endo, Y., & Tsurugi, K. (1987). RNA N-glycosidase activity of ricin A-chain. Mechanism of action of the toxic lectin ricin on eukaryotic ribosomes. *Journal of Biological Chemistry*, 262(17), 8128–8130.

Eshel, D., Miyara, I., Ailing, T., Dinoor, A., & Prusky, D. (2002). pH regulates endoglucanase expression and virulence of *Alternaria alternata* in persimmon fruit. *Molecular Plant-Microbe Interactions*, 15(8), 774–779.

Deus, E., Silva, J. S., Castro-Díez, P., Lomba, A., Ortiz, M. L., & Vicente, J. (2018). Current and future conflicts between eucalypt plantations and high biodiversity areas in the Iberian Peninsula. *Journal for Nature Conservation*, 45, 107–117.

Felix, C., Duarte, A. S., Vitorino, R., Guerreiro, A. C. L., Domingues, P., Correia, A. C. M., Esteves, A. C. (2016). Temperature modulates the secretome of the phytopathogenic fungus *Lasiodiplodia theobromae*. *Frontiers in Plant Science*, 7, 1096.

Felix, C., Meneses, R., Gonçalves, M. F. M., Tilleman, L., Duarte, A. S., Jorrín-Novo, J. V., Van de Peer, Y., Deforce, D., Van Nieuwerburgh, F., Esteves, A.C., Alves, A. (2019). A multi-omics analysis of the

grapevine pathogen *Lasiodiplodia theobromae* reveals that temperature affects the expression of virulence- and pathogenicity-related genes. *Scientific Reports*, 9(1), 13144.

Fernandes, I., Alves, A., Correia, A., Devreese, B., & Esteves, A. C. (2014). Secretome analysis identifies potential virulence factors of *Diplodia corticola*, a fungal pathogen involved in cork oak (*Quercus suber*) decline. *Fungal Biology*, 118(5–6), 516–523.

Fernandes, I. (2015). Infection mechanism of *Diplodia corticola*. PhD thesis. Aveiro University, Portugal.

Gaspar, Y., Johnson, K. L., McKenna, J. A., Bacic, A., & Schultz, C. J. (2001). The complex structures of arabinogalactan-proteins and the journey towards understanding function. *Plant Molecular Biology*, 47(1–2), 161–176.

Girard, V., Dieryckx, C., Job, C., & Job, D. (2013). Secretomes: the fungal strike force. *Proteomics*, 13(3–4), 597–608.

Gómez-Gómez, E., Ruız-Roldan, M. C., Di Pietro, A., Roncero, M. I. G., & Hera, C. (2002). Role in pathogenesis of two endo-β-1, 4-xylanase genes from the vascular wilt fungus *Fusarium oxysporum*. *Fungal Genetics and Biology*, 35(3), 213–222.

González-Fernández, R., Aloria, K., Valero-Galván, J., Redondo, I., Arizmendi, J. M., & Jorrín-Novo, J. V. (2014). Proteomic analysis of mycelium and secretome of different *Botrytis cinerea* wild-type strains. *Journal of Proteomics*, 97, 195–221.

González-Fernández, R., Valero-Galván, J., Gómez-Gálvez, F. J., & Jorrín-Novo, J. V. (2015). Unraveling the in vitro secretome of the phytopathogen *Botrytis cinerea* to understand the interaction with its hosts. *Frontiers in Plant Science*, 6, 839.

Gui, Y., Chen, J., Zhang, D., Li, N., Li, T., Zhang, W., & Guo, W. (2017). *Verticillium dahliae* manipulates plant immunity by glycoside hydrolase 12 proteins in conjunction with carbohydrate-binding module 1. *Environmental Microbiology*, 19(5), 1914–1932.

Herron, S. R., Benen, J. A. E., Scavetta, R. D., Visser, J., & Jurnak, F. (2000). Structure and function of pectic enzymes: virulence factors of plant pathogens. *Proceedings of the National Academy of Sciences*, 97(16), 8762–8769.

Hislop, E. C., Paver, J. L., & Keon, J. P. R. (1982). An acid protease produced by *Monilinia fructigena in vitro* and in infected apple fruits, and its possible role in pathogenesis. *Microbiology*, 128(4), 799–807.

Ismail, I. A., & Able, A. J. (2016). Secretome analysis of virulent *Pyrenophora teres f. teres* isolates. *Proteomics*, 16(20), 2625–2636.

Jami, M.-S., Barreiro, C., Garcia-Estrada, C., & Martin, J.-F. (2010). Proteome analysis of the penicillin producer *Penicillium chrysogenum*: characterization of protein changes during the industrial strain improvement. *Molecular & Cellular Proteomics: MCP*, 9(6), 1182–1198.

Jung, Y., Jeong, S., Kim, S. H., Singh, R., Lee, J., Cho, Y., & Jwa, N. (2012). Secretome analysis of *Magnaporthe oryzae* using in vitro systems. *Proteomics*, 12(6), 878–900.

Kang, Z., & Buchenauer, H. (2000). Ultrastructural and cytochemical studies on cellulose, xylan and pectin degradation in wheat spikes infected by *Fusarium culmorum*. *Journal of Phytopathology*, 148(5), 263–275.

Kars, I., & van Kan, J. A. L. (2007). Extracellular enzymes and metabolites Involved in pathogenesis of *Botrytis*. *Botrytis*: Biology, Pathology and Control. Springer, Dordrecht.

Kawamoto, T., Noshiro, M., Shen, M., Nakamasu, K., Hashimoto, K., Kawashima-Ohya, Y., & Kato, Y. (1998). Structural and phylogenetic analyses of RGD-CAP/βig-h3, a fasciclin-like adhesion protein expressed in chick chondrocytes. *Biochimica et Biophysica Acta (BBA)-Gene Structure and Expression*, 1395(3), 288–292.

Kouzai, Y., Mochizuki, S., Saito, A., Ando, A., Minami, E., & Nishizawa, Y. (2012). Expression of a bacterial chitosanase in rice plants improves disease resistance to the rice blast fungus *Magnaporthe oryzae*. *Plant Cell Reports*, 31(4), 629–636.

Kubicek, C. P., Starr, T. L., & Glass, N. L. (2014). Plant cell wall–degrading enzymes and their secretion in plant-pathogenic fungi. *Annual Review of Phytopathology*, 52, 427–451.

Kuroki, M., Okauchi, K., Yoshida, S., Ohno, Y., Murata, S., Nakajima, Y., & Taguchi, H. (2017). Chitin-deacetylase activity induces appressorium differentiation in the rice blast fungus *Magnaporthe oryzae*. *Scientific Reports*, 7(1), 9697.

Laemmli, U. K. (1970). Cleavage of structural proteins during the assembly of the head of bacteriophage T4. *Nature*, 227(5259), 680–685.

Lai, M.-W., & Liou, R.-F. (2018). Two genes encoding GH10 xylanases are essential for the virulence of the oomycete plant pathogen *Phytophthora parasitica*. *Current Genetics*, 64(4), 931–943.

Lakshman, D. K., Roberts, D. P., Garrett, W. M., Natarajan, S. S., Darwish, O., Alkharouf, N., & Mitra, A. (2016). Proteomic investigation of *Rhizoctonia solani* AG 4 identifies secretome and mycelial proteins with roles in plant cell wall degradation and virulence. *Journal of Agricultural and Food Chemistry*, 64(15), 3101–3110.

Leferink, N. G. H., Heuts, D. P. H. M., Fraaije, M. W., & Van Berkel, W. J. H. (2008). The growing VAO flavoprotein family. *Archives of Biochemistry and Biophysics*, 474(2), 292–301.

Li, G., Arnold, R. J., Liu, F., Li, J., & Chen, S. (2015). Identification and pathogenicity of *Lasiodiplodia* species from *Eucalyptus urophylla*× *grandis*, *Polyscias balfouriana* and *Bougainvillea spectabilis* in Southern China. *Journal of Phytopathology*, 163(11–12), 956–967.

Liu, T., Chen, G., Min, H., & Lin, F. (2009). MoFLP1, encoding a novel fungal fasciclin-like protein, is involved in conidiation and pathogenicity in *Magnaporthe oryzae*. *Journal of Zhejiang University Science B*, 10(6), 434–444.

Luhtala, N., & Parker, R. (2010). T2 Family ribonucleases: ancient enzymes with diverse roles. *Trends in Biochemical Sciences*, 35(5), 253–259.

Lyu, X., Shen, C., Fu, Y., Xie, J., Jiang, D., Li, G., & Cheng, J. (2015). Comparative genomic and transcriptional analyses of the carbohydrate-active enzymes and secretomes of phytopathogenic fungi reveal their significant roles during infection and development. *Scientific Reports*, 5, 15565.

Ma, Z., Song, T., Zhu, L., Ye, W., Wang, Y., Shao, Y., & Zheng, X. (2015). A *Phytophthora sojae* glycoside hydrolase 12 protein is a major virulence factor during soybean infection and is recognized as a PAMP. *The Plant Cell*, 27(7), 2057–2072.

MacIntosh, G. C. (2011). RNase T2 family: enzymatic properties, functional diversity, and evolution of ancient ribonucleases. In ribonucleases (pp. 89–114). Springer.

Mandelc, S., & Javornik, B. (2015). The secretome of vascular wilt pathogen *Verticillium albo-atrum* in simulated xylem fluid. *Proteomics*, 15(4), 787–797.

Martinez, M. J., Alconada, M. T., Guillén, F., Vázquez, C., & Reyes, F. (1991). Pectic activities from *Fusarium oxysporum* f. sp. *melonis*: purification and characterization of an exopolygalacturonase. *FEMS Microbiology Letters*, 81(2), 145–149.

Massonnet, M, Figueroa-Balderas, R, Galarneau, E. R. A., Miki, S., Lawrence, D. P., Sun, Q., Wallis, C. M., Baumgartner, K., & Cantu, D. (2017). *Neofusicoccum parvum* colonization of the grapevine woody stem triggers asynchronous host responses at the site of infection and in the leaves. *Frontiers in Plant Science*, 8, 1117.

Massonnet, M., Morales-Cruz, A., Figueroa-Balderas, R., Lawrence, D. P., Baumgartner, K., & Cantu, D. (2018). Condition-dependent co-regulation of genomic clusters of virulence factors in the grapevine trunk pathogen *Neofusicoccum parvum*. *Molcular Plant Pathology*, 19(1), 21–34.

Meerupati, T., Andersson, K.-M., Friman, E., Kumar, D., Tunlid, A., & Ahren, D. (2013). Genomic mechanisms accounting for the adaptation to parasitism in nematode-trapping fungi. *PLoS Genetics*, 9(11), e1003909.

Mohali, S., Slippers, B., & Wingfield, M. J. (2007). Identification of Botryosphaeriaceae from *Eucalyptus*, *Acacia* and *Pinus* in Venezuela. *Fungal Diversity*, 25(25), 103–125.

Movahedi, S., & Heale, J. B. (1990). Purification and characterization of an aspartic proteinase secreted by *Botrytis cinerea* Pers ex. Pers in culture and in infected carrots. *Physiological and Molecular Plant Pathology*, 36(4), 289–302.

Nguyen, Q. B., Itoh, K., Van Vu, B., Tosa, Y., & Nakayashiki, H. (2011). Simultaneous silencing of endo-β-1, 4 xylanase genes reveals their roles in the virulence of *Magnaporthe oryzae*. *Molecular Microbiology*, 81(4), 1008–1019.

Niture, S. K., Kumar, A. R., & Pant, A. (2006). Role of glucose in production and repression of polygalacturonase and pectate lyase from phytopathogenic fungus *Fusarium moniliforme* NCIM 1276. *World Journal of Microbiology and Biotechnology*, 22(9), 893–899.

Olombrada, M., Martínez-del-Pozo, Á., Medina, P., Budia, F., Gavilanes, J. G., & García-Ortega, L. (2014). Fungal ribotoxins: natural protein-based weapons against insects. *Toxicon*, 83, 69–74.

Panda, T., Nair, S. R., & Kumar, M. P. (2004). Regulation of synthesis of the pectolytic enzymes of *Aspergillus niger*. *Enzyme and Microbial Technology*, 34(5), 466–473.

Pavlic, D., Slippers, B., Coutinho, T. A., & Wingfield, M. J. (2007). Botryosphaeriaceae occurring on native *Syzygium cordatum* in South Africa and their potential threat to *Eucalyptus*. *Plant Pathology*, 56(4), 624–636.

Pérez, C. A., Wingfield, M. J., Slippers, B., Altier, N. A., & Blanchette, R. A. (2010). Endophytic and canker-associated Botryosphaeriaceae occurring on non-native *Eucalyptus* and native *Myrtaceae* trees in Uruguay. *Fungal Diversity*, 41(1), 53–69.

Petersen, T. N., Brunak, S., Von Heijne, G., & Nielsen, H. (2011). SignalP 4.0: discriminating signal peptides from transmembrane regions. *Nature Methods*, 8(10), 785.

Phillips, A. J. L., Alves, A., Abdollahzadeh, J., Slippers, B., Wingfield, M. J., Groenewald, J. Z., & Crous, P. W. (2013). The Botryosphaeriaceae: genera and species known from culture. *Studies in Mycology*, 76(1), 51–167.

Pierleoni, A., Martelli, P. L., Fariselli, P., & Casadio, R. (2006). BaCelLo: a balanced subcellular localization predictor. *Bioinformatics*, 22(14), e408–e416.

Poussereau, N., Creton, S., Billon-Grand, G., Rascle, C., & Fevre, M. (2001). Regulation of acp1, encoding a non-aspartyl acid protease expressed during pathogenesis of *Sclerotinia sclerotiorum*. *Microbiology*, 147(3), 717–726.

Poussereau, N., Gente, S., Rascle, C., Billon-Grand, G., & Fèvre, M. (2001). aspS encoding an unusual aspartyl protease from *Sclerotinia sclerotiorum* is expressed during phytopathogenesis. *FEMS Microbiology Letters*, 194(1), 27–32.

Raffaele, S., Win, J., Cano, L. M., & Kamoun, S. (2010). Analyses of genome architecture and gene expression reveal novel candidate virulence factors in the secretome of *Phytophthora infestans*. *BMC Genomics*, 11(1), 637.

Ride, J. P., & Barber, M. S. (1990). Purification and characterization of multiple forms of endochitinase from wheat leaves. *Plant Science*, 71(2), 185–197.

Rovenich, H., Zuccaro, A., & Thomma, B. P. H. J. (2016). Convergent evolution of filamentous microbes towards evasion of glycan-triggered immunity. *New Phytologist*, 212(4), 896–901.

Seidl, M. F., Van den Ackerveken, G., Govers, F., & Snel, B. (2011). A domain-centric analysis of oomycete plant pathogen genomes reveals unique protein organization. *Plant Physiology*, 155(2), 628–644.

Sexton, A. C., Paulsen, M., Woestemeyer, J., & Howlett, B. J. (2000). Cloning, characterization and chromosomal location of three genes encoding host-cell-wall-degrading enzymes in *Leptosphaeria maculans*, a fungal pathogen of Brassica spp. *Gene*, 248(1–2), 89–97.

Shah, P., Atwood III, J. A., Orlando, R., El Mubarek, H., Podila, G. K., & Davis, M. R. (2009). Comparative proteomic analysis of *Botrytis cinerea* secretome. *Journal of Proteome Research*, 8(3), 1123–1130.

Sharp, R. (2013). A review of the applications of chitin and its derivatives in agriculture to modify plant-microbial interactions and improve crop yields. *Agronomy*, 3(4), 757–793.

Sibbald, M., Ziebandt, A. K., Engelmann, S., Hecker, M., De Jong, A., Harmsen, H. J. M., & Dubois, J. Y. F. (2006). Mapping the pathways to staphylococcal pathogenesis by comparative secretomics. *Microbiol. Mol. Biol. Rev*., 70(3), 755–788.

Slippers, B, Burgess, T., Pavlic, D., Ahumada, R., Maleme, H., Mohali, S., & Wingfield, M. J. (2009). A diverse assemblage of Botryosphaeriaceae infect *Eucalyptus* in native and non-native environments. *Southern Forests*: *A Journal of Forest Science*, 71(2), 101–110.

Slippers, Bernard, Fourie, G., Crous, P. W., Coutinho, T. A., Wingfield, B. D., Carnegie, A. J., & Wingfield, M. J. (2004). Speciation and distribution of Botryosphaeria spp. on native and introduced *Eucalyptus* trees in Australia and South Africa. *Studies in Mycology*, 50(2), 343–358.

Slippers, Bernard, Roux, J., Wingfield, M. J., Van der Walt, F. J. J., Jami, F., Mehl, J. W. M., & Marais, G. J. (2014). Confronting the constraints of morphological taxonomy in the Botryosphaeriales. *Persoonia: Molecular Phylogeny and Evolution of Fungi*, 33, 155.

Slippers, Bernard, & Wingfield, M. J. (2007). Botryosphaeriaceae as endophytes and latent pathogens of woody plants: diversity, ecology and impact. *Fungal Biology Reviews*, 21(2), 90–106.

Smith, H., Wingfield, M. J., & Petrini, O. (1996). *Botryosphaeria dothidea* endophytic in *Eucalyptus grandis* and *Eucalyptus nitens* in South Africa. *Forest Ecology and Management*, 89(1–3), 189–195.

Stempien, E., Goddard, M.-L., Wilhelm, K., Tarnus, C., Bertsch, C., & Chong, J. (2017). Grapevine Botryosphaeria dieback fungi have specific aggressiveness factor repertory involved in wood decay and stilbene metabolization. *PloS One*, 12(12), e0188766.

Tomassini, A., Sella, L., Raiola, A., D'Ovidio, R., & Favaron, F. (2009). Characterization and expression of *Fusarium graminearum* endo-polygalacturonases *in vitro* and during wheat infection. *Plant Pathology*, 58(3), 556–564.

Uranga, C. C., Ghassemian, M., & Hernández-Martínez, R. (2017). Novel proteins from proteomic analysis of the trunk disease fungus *Lasiodiplodia theobromae* (Botryosphaeriaceae). *Biochimie Open*, 4, 88–98.

Urbanek, H., & Yirdaw, G. (1984). Hydrolytic ability of acid protease of *Fusarium culmorum* and its possible role in phytopathogenesis. *Acta Microbiologica Polonica*, 33(2), 131–136.

Van Vu, B., Itoh, K., Nguyen, Q. B., Tosa, Y., & Nakayashiki, H. (2012). Cellulases belonging to glycoside hydrolase families 6 and 7 contribute to the virulence of *Magnaporthe oryzae*. *Molecular Plant-Microbe Interactions*, 25(9), 1135–1141.

Wessel, D. M., & Flügge, U. I. (1984). A method for the quantitative recovery of protein in dilute solution in the presence of detergents and lipids. *Analytical Biochemistry*, 138(1), 141–143.

Yan, J. Y., Zhao, W. S., Chen, Z., Xing, Q. K., Zhang, W., Chethana, K. W. T., Xue, M. F., Xu, j. p., Phillips, A. J. L., Wang, Y., Liu, J. H., M., Liu, M., Zhou, Y., Jayawardena, R. S., Manawasinghe, I. S., Huang, J. B., Qiao, G. H., Fu, C. Y., Guo, F. F., Dissanayake, A. J., Peng, Y. L., Hyde, K. D., & Li, X. H. (2017). Comparative genome and transcriptome analyses reveal adaptations to opportunistic infections in woody plant degrading pathogens of Botryosphaeriaceae. *DNA Research*, 25(1), 87–102.

Zabel, R.A., & Morrell, J.J. (1992). Wood Microbiology, Decay and its Prevention. *Academic Press*, Orlando, 476 pp.

Zhang, L., & van Kan, J. A. L. (2013). 14 Pectin as a Barrier and Nutrient Source for Fungal Plant Pathogens. In: Kempken F. (eds) Agricultural Applications. The Mycota (A Comprehensive Treatise on Fungi as Experimental Systems for Basic and Applied Research), vol 11. Springer, Berlin, Heidelberg

Zhao, Y., Park, R.-D., & Muzzarelli, R. A. A. (2010). Chitin deacetylases: properties and applications. Marine Drugs, 8(1), 24–46.

SUPPLEMENTARY MATERIAL

The following tables (S3.1 and S3.2) are deposited in an excel file named "Supplementary Material Chapter 3":

Table S3.1| Differentially expressed proteins identified in the control and infection-like secretome of *N. parvum*.

Table S3.2| Common proteins identified in the control and infection-like secretome of *N. parvum*.

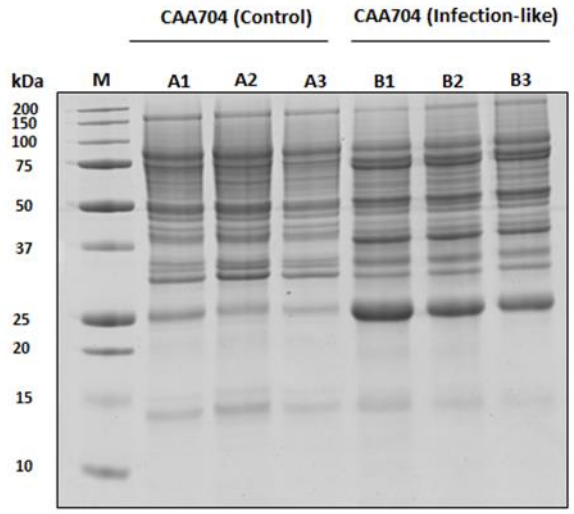

Figure S3.1 | SDS-PAGE of *N. parvum* secreted proteins (3 µg); A1-3 – Three biological replicates of control, B1-3 - Three biological replicates of infection-like, M - Precision Plus Protein Unstained Standard (Bio-Rad, USA). Gels were stained with CBB-G250.

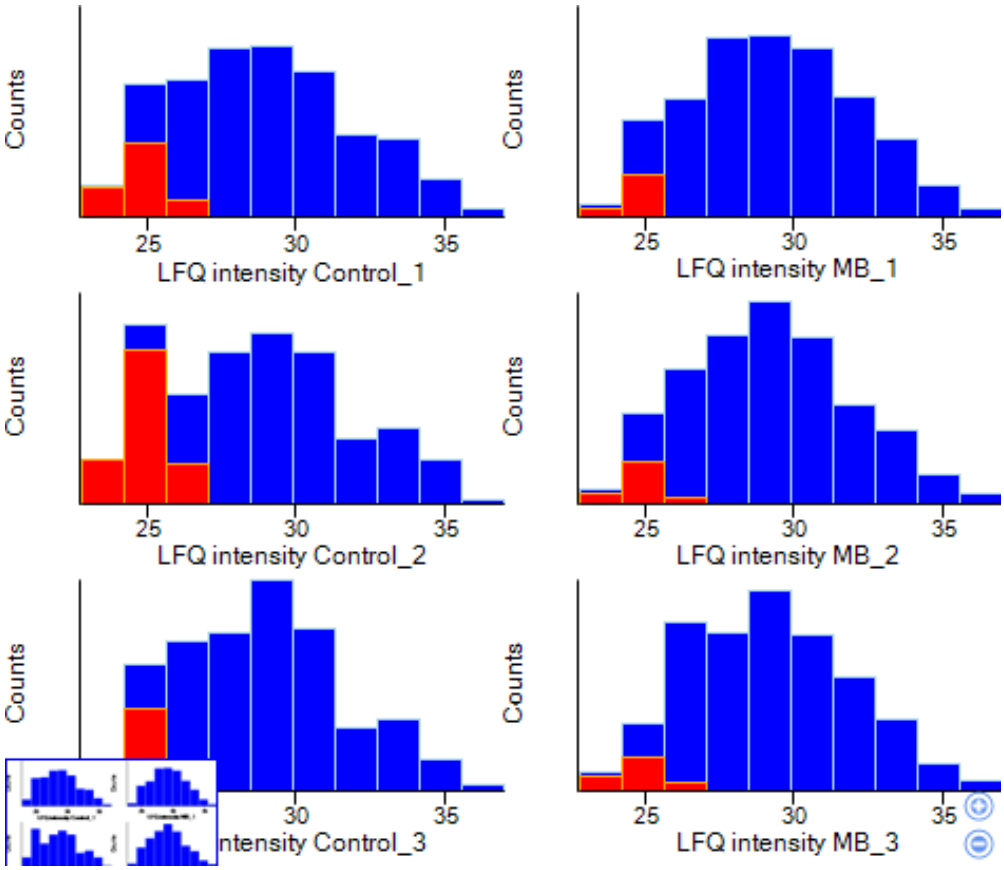

Figure S3.2 | Histograms of the LFQ intensity values of the nine samples under analysis. This representation is required after logarithmization of the data to verify a successful transformation to a normal distribution. The blue bars represent the intensity values of proteins in sample, while the red bars represent the missing values from normal distribution. Output image from Perseus software.

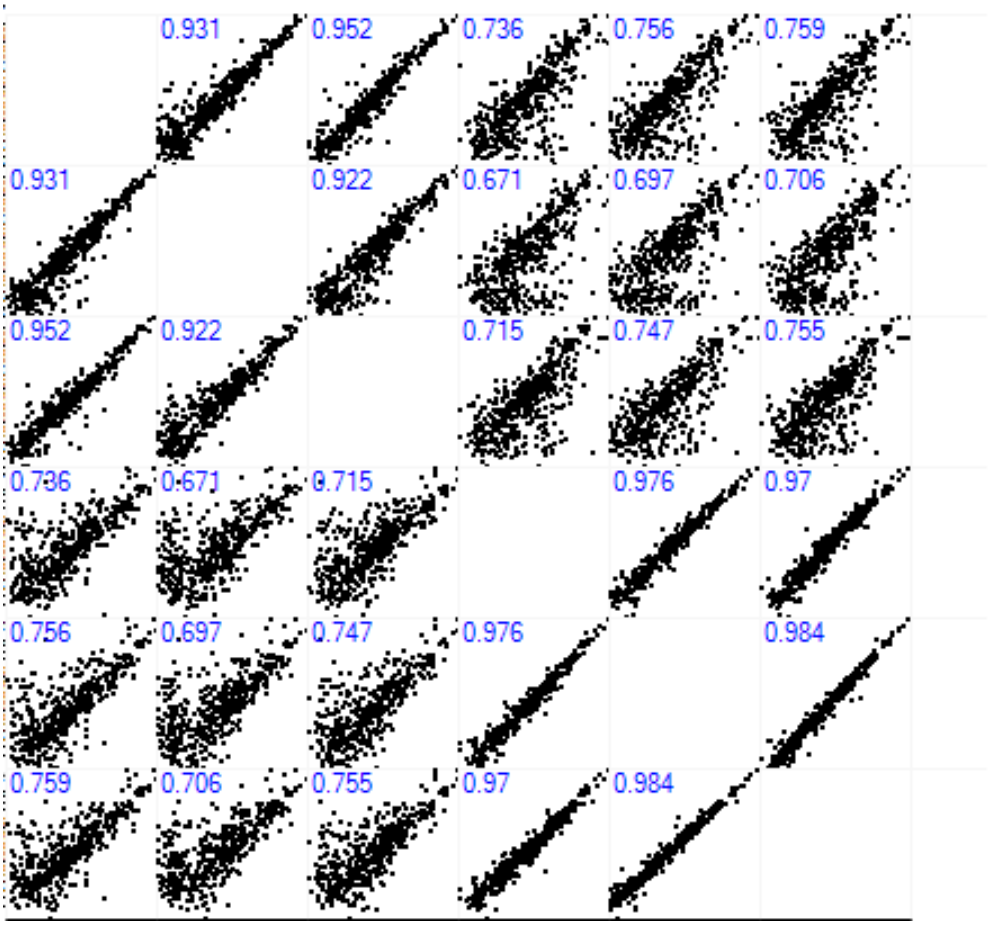

Figure S3.3 | Multi-scatter plot with Pearson correlation values of the nine samples against each other. This test is performed to analyze the correlation between samples and reassure the success or failure of the experiment. The r2 values between 0.67 and 0.98 show a high correlation between samples and imply that the data can be trusted. Output image from Perseus software.

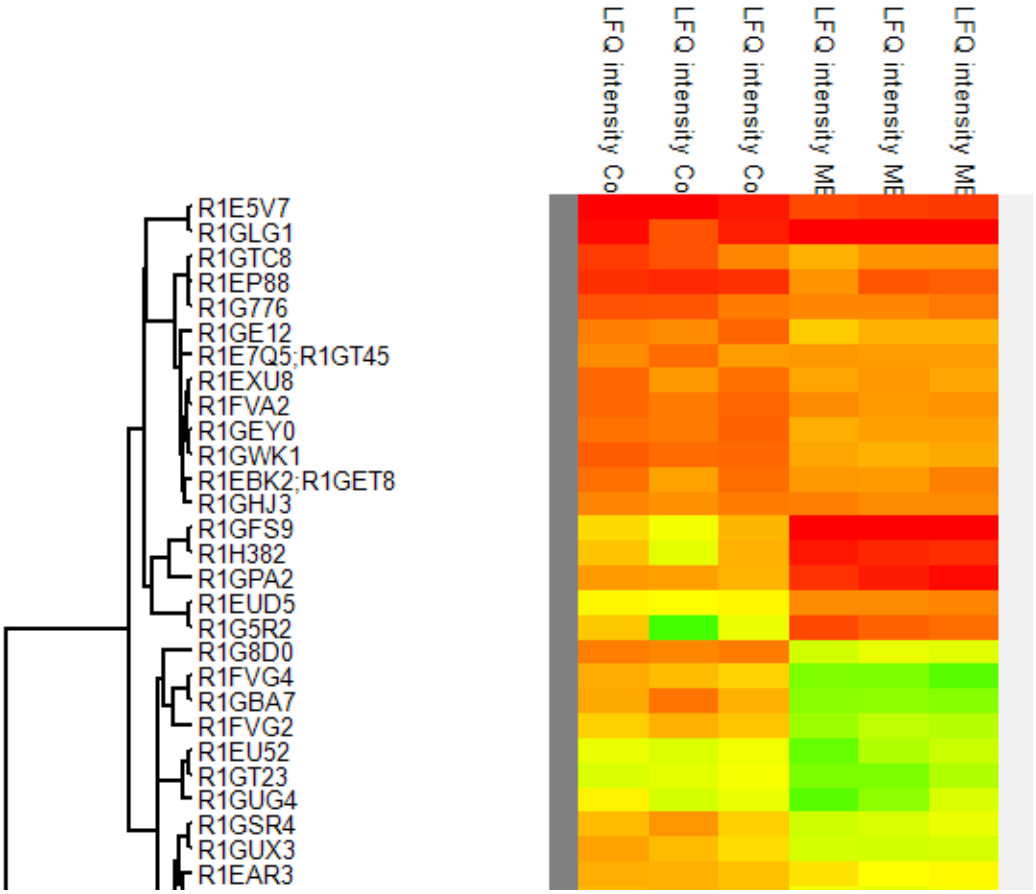

Figure S3.4 | Hierarchical clustering of the nine samples under analysis, displaying a cluster tree of identified proteins and a heatmap of their intensity in the samples. Samples look similar overall but at the top of the map it is possible to verify that some proteins show distinct behaviour between groups, and this feature ensures the success of the experiment. Contaminants can also be spotted on the grey bar on the side. Output image from Perseus software.

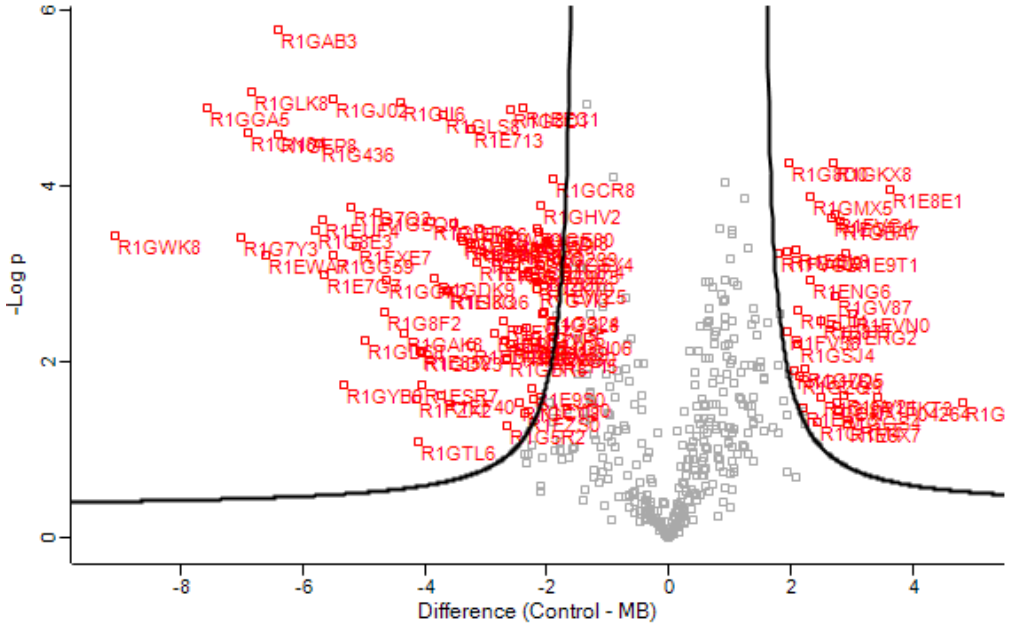

Figure S3.5 | First volcano scatterplot of the nine samples under analysis. The graph shows p-value versus fold-change, identifying the most meaningful changes between two groups of conditions: Control and infection-like. Combines a measure of statistical significance from T-test with the magnitude of the change. The black lines drawn represent the limit of statistically significant values, separating them from the non-significant. Output image from Perseus software.

CHAPTER 4

Toxicity of recombinant necrosis and ethylene-inducing proteins (NLPs) from *Neofusicoccum parvum*

ABSTRACT

Neofusicoccum parvum is a fungal pathogen associated with a wide range of plant hosts. Despite being widely studied, the molecular mechanism of infection of *N. parvum* is still far from being understood. Analysis of *N. parvum* genome led to the identification of six putative genes encoding necrosis and ethylene-inducing proteins (NLPs). The sequence of NLPs genes (*NprvNep* 1-6) was analyzed and four of the six NLP genes were successfully cloned, expressed in *E. coli* and purified by affinity chromatography. Pure recombinant proteins were characterized according to their phytotoxic and cytotoxic effects to tomato leaves and to mammalian Vero cells, respectively. These assays revealed that all NprvNeps tested are cytotoxic to Vero cells and induce cell death in tomato leaves. NprvNep2 was the most toxic to Vero cells, followed by NprvNep1 and 3. NprvNep4 induced weaker, but, nevertheless, still significant toxic effects to Vero cells. A similar trend of toxicity was observed in tomato leaves: the most toxic was NprvNep 2 and the least toxic NprvNep 4. This study describes for the first time an overview of the NLP gene family of *N. parvum* and provides additional insights into its pathogenicity mechanism.

KEYWORDS: Botryosphaeriaceae, Botryosphaeria dieback, necrosis and ethylene-inducing proteins (NLPs), phytotoxicity, cytotoxicity

INTRODUCTION

Neofusicoccum parvum is known as a pluriverse fungal pathogen infecting a wide range of plant hosts (Urbez-Torres & Gubler, 2009). This fungus can colonize woody tissue through pruning wounds and sites of mechanical or natural injuries (Castillo-Pando et al., 2001; Phillips, 2002; Urbez-Torres & Gubler, 2009), causing internal cankers in the host. The infection also causes characteristic foliar symptoms, although *N. parvum* has not been isolated from the leaves of infected plants (Larignon & Dubos, 1997; Mugnai et al., 1999; Urbez-Torres, 2011). Several studies have shown that *N. parvum* pathogenicity is multi factorial and involves the production of phytotoxins and extracellular proteins with phytotoxic properties leading to the expression of symptoms in distal tissues (Andolfi et al., 2011; Abou-Mansour et al., 2015; Bénard-Gellon et al., 2015). However, full understanding of the pathogenicity mechanism is still far from being accomplished. Most studies concerning *N. parvum* pathogenicity were conducted on grapevines (Abou-Mansour et al., 2015; Andolfi et al., 2011; Bénard-Gellon et al., 2015; Larignon & Dubos, 1997; Mugnai et al., 1999; Urbez-Torres, 2011) , but similar symptoms are found in many other species (Li et al., 2018; Serrato-Diaz et al., 2019; Valencia et al., 2019).

Secretome analysis of *Diplodia seriata*, another member of the family *Botryosphaeriaceae*, expresses necrosis and ethylene-inducing proteins (Cobos et al., 2010), whose involvement in the infection mechanism was suggested. These proteins are necrotic elicitors connected to a transduction cascade that causes cell death at the site of infection, thereby limiting the spread of the pathogen (Nimchuk et al., 2003). Nep1 (necrosis and ethylene-inducing peptide 1) was first isolated from *Fusarium oxysporum* culture filtrates as a 24-kDa protein (Bae et al., 2006; Bailey, 1995). Over the last decade, several Nep1-like proteins (NLPs) have been found in a diversity of plant-associated microorganisms, such as bacteria, fungi, and oomycetes (Gijzen & Nurnberger 2006; Pemberton and Salmond, 2004). NLPs cause necrosis and ethylene production only in dicotyledonous plants (Bailey et al., 2005; Fellbrich et al., 2002; Jennings et al., 2001; Keates et al., 2003; Veit et al., 2001; Verica et al., 2004). All monocotyledonous plants tested so far are insensitive to NLPs (Bailey, 1995; Qutob et al., 2006; Schouten et al., 2008; Staats et al., 2007; Teh et al., 2019), suggesting that NLP cytotoxicity requires a dicot-specific target protein or membrane architecture. Recently, glycosylinositol phosphorylceramide (GIPC) sphingolipids were identified as NLP toxin receptors in tobacco (Lenarčič et al., 2017). Most monocot GIPCs have three hexose units whereas dicot GIPCs have only two hexose units, thus the difference in the length of GIPC head group may be the cause of insensitivity of monocot plants to NLPs (Lenarčič et al., 2017). Likewise, the sensitivity of other organisms like animals, fungi and bacteria to NLPs has not been thoroughly investigated. It is known that the NLP homologue from *Vibrio pommerensis* CH-291 possesses some haemolytic activity against human and animal erythrocytes (Jores et al., 2003). On the other hand, Qutob et al. (2006) suggested that different cell and tissue types from mammalian and lower plant cell lines, and *Pichia pastoris* spheroplasts are not affected by NLPs.

NLPs are classified into two groups, named type 1 and type 2, according to the presence of either two or four conserved cysteine residues (Gijzen & Nurnberger, 2006). An additional third type of NLPs – that possess six conserved cysteine residues - has been characterized in Ascomycete fungi (Oome & Van den Ackerveken, 2014). Several studies have identified the key residues of NLPs for their cell-death-inducing activity (Fellbrich et al., 2002; Ottmann et al., 2009). A conserved 24-aa peptide in type 1 NLPs was identified as being potentially involved in triggering plant immunity responses (Böhm et al., 2014; Oome et al., 2014) and it includes the conserved regions I and II. Most of the identified NLPs contain a signal peptide, indicating that they are secreted. The expression of NLPs lacking the secretion signal peptide did not induce plant cell death (Qutob et al., 2002; Qutob et al., 2006), consistent with their extracellular activity.

Nonetheless, the exact mechanism by which NLPs cause necrosis is not clear. Induction of necrosis in plants exposed to NLPs can be accompanied by production of ethylene, superoxide anions,

overexpression of transcripts coding pathogenesis-related proteins and induction of programmed cell death (Bailey et al., 1997; Fellbrich et al., 2002; Jennings et al., 2000; Keates et al., 2003; Pemberton et al., 2005). However, in some plants for example, necrosis induction did not occur by ethylene production (Bailey, 1995; Bailey et al., 1997), indicating that other mechanisms may be involved.

Several studies suggested the contribution of NLPs to the virulence of plant pathogens. For example, MpNEP1 and MpNEP2, from *Moniliophthora perniciosa*, were able to induce necrosis and ethylene emission in tobacco and cacao leaves (Garcia et al., 2007). Furthermore, a drastic increase in virulence of the fungus *Colletotrichum coccodes* towards *Abutilon theophrasti* was observed after overexpression of Nep1 from *Fusarium* sp. (Amsellem et al., 2002). Similarly, individual deletion of two NLP genes in the fungus *Verticillium dahliae* decreased virulence on different host plants (Santhanam et al., 2013). In contrast, the complete deletion of NLPs in the fungal pathogens *Magnaporthe oryzae*, *Mycosphaerella graminicola*, and *Botrytis elliptica* did not reduce their virulence, suggesting that NLP genes of those fungi are dispensable for the fungal pathogen to cause disease (Fang et al., 2017; Motteram et al., 2009; Staats et al., 2007). There is a wide functional diversity of NLPs among plant pathogens that need further exploration.

Several species of the family *Botryosphaeriaceae* have been classified as human opportunists, suggesting that they possess the molecular machinery that allows infecting both plants and humans (Félix et al., 2016, Félix et al., 2019). Nonetheless, there are no reports describing the contribution of NLPs from those human pathogens by testing on mammalian cells.

We aimed to, for the first time, identify and characterize NLPs genes from *N. parvum* (*NprvNeps*), in order to infer their role in *N. parvum* pathogenicity.

MATERIALS AND METHODS

Fungal strain and plant material

The strain used in this study, *Neofusicoccum parvum* CAA704, was isolated from symptomatic branch of *Eucalyptus globulus* in Portugal by Barradas and co-workers (Barradas et al., 2016). Fungus was grown on cellophane over Czapek-Dox agar plate at 25 °C for 5 days prior to the inoculations. For liquid growth, a plug (5 mm diameter) was inoculated into a 250 mL flask containing 50 mL Czapeck-Dox broth and incubated at 25 °C for 3 days in an orbital shaker at 150 rpm. Mycelia were harvested by filtration (filter paper), washed with sterile water and immediately frozen with N_2 (l) prior to DNA and RNA extraction.

The tomato seeds (*Solanum lycopersicum var. cerasiforme*) were cultivated in plastic trays filled with vermiculite: peat [2:1 (w/w)] mixture and kept at 25-28 °C (16 h light period) in a growth chamber. All seedlings were equally well watered and fertilized weekly (5 ml/L Nutriquisa 5-8-10®) and grown for 90 days under the conditions described.

DNA and RNA extraction and cDNA synthesis

Extraction of genomic DNA from mycelium (120 mg) was performed as described by Alves et al. (2004). Genomic DNA was used for the amplification of *NprvNep* genes by PCR using the primers (Table S4.2) designed from *N. parvum* (UCRNP2) genomic sequence in the NCBI database. RNA was extracted from 50 mg of frozen mycelia with Spectrum™ Plant Total RNA Kit (Sigma-Aldrich, St. Louis, MO, USA) following the manufacturer's instructions. The quality and quantity of both DNA and RNA were checked by gel electrophoresis (1% agarose gel) and spectrophotometrical assays. A total of 1 µg RNA was treated with DNase l, RNase-free (Thermo scientific, Lisbon, Portugal) and cDNA was synthesized using an NZY First-Strand cDNA Synthesis Kit (NZYTech, Lisbon, Portugal) according to the manufacturer's instructions.

Cloning, expression and purification of recombinant NprvNeps

The synthesized cDNA was used as a template for amplification of *NprvNep1-5* genes using primers (designed from *N. parvum*-UCRNP2 genomic sequence in the NCBI database) described in Table S2, supplementary file. PCR reactions were prepared with 2×Platinum SuperFi PCR Master Mix (Invitrogen, Carlsbad, CA, USA), 10 µM of each primer, and 20 ng of template DNA. The program consisted of an initial step of 30 s at 98 °C, followed by 34 cycles of denaturation at 98 °C for 10 s, annealing at 65 °C for 10 s, and elongation at 72 °C for 30 s. A final extension was performed at 72 °C for 5 min. For each amplification, PCR products were excised and purified from gel using Zymoclean™ Gel DNA Recovery Kit (Zymo Research, Irvine, CA, USA). Purified sequence-verified PCR products were cloned into pET SUMO vector using Champion™ pET SUMO protein expression system (Invitrogen, CA, USA) according to the manufacturer's instructions. The One Shot® Mach1™-T1R Chemically Competent *E. coli* (Invitrogen, CA, USA) was transformed with the recombinant plasmid constructions. Transformants were analyzed by restriction analysis to confirm the presence and correct orientation of the insert. Recombinant plasmids were extracted from positive transformants and confirmed by sequencing and propagated in BL21 (DE3) One Shot® Chemically Competent *E. coli* (Invitrogen, CA, USA) cultured in LB broth supplemented with 50 µg/mL kanamycin. Protein expression was induced with 1 mM isopropyl-1-thio-b-D-galactopyranoside (IPTG), producing proteins with his-tags. Cells were harvested by centrifugation, resuspended in a lysis buffer (20 mM sodium phosphate; 500 mM NaCl; 10 mM imidazole; 2 % SDS, pH 7.4) and sonicated. Cell debris was removed by centrifugation (10,000 g for 10 min at 4 °C) and the supernatant filtered (0.20 µm pore size filter, Orange Scientific) and loaded onto a His-Trap FF Ni affinity column (GE Healthcare). The recombinant His6-tagged proteins were eluted in the elution buffer (20 mM sodium phosphate; 500 mM NaCl; 500 mM imidazole, pH 7.4) using an ÄKTA FPLC system (GE Healthcare, USA). Fractions containing His6-tagged recombinant

NprvNeps were pooled and dialysed overnight against ultrapure water at 4 °C in dialysis cellulose membranes (Sigma-Aldrich). The desalted recombinant fusion protein solutions were then lyophilized and solubilized in ultrapure water. To remove the 6xHis tag and SUMO protein and generate native recombinant proteins, the purified recombinant fusion proteins were treated with SUMO Protease (Invitrogen) according to the manufacturer's instructions. Subsequently, recombinant proteins were purified by Ni affinity chromatography (His-Trap FF, GE-Healthcare). Salts were removed by dialysis against ultrapure water, lyophilized and stored until further analysis. The protein purity was assessed by SDS–PAGE (Laemmli et al., 1970) at the various stages of the purification process.

Protein concentration

Protein concentration was determined using the Pierce™ 660 nm Protein Assay kit (Thermo Scientific) according to the manufacturer's instructions. Bovine Serum Albumin was used as standard. The procedure was performed in triplicate.

Phytotoxic activity

Recombinant NprvNeps were inoculated into detached leaves of 3-month old tomato plants, which is an important model plant system as well (Ji & Scott, 2006), to assess their ability to cause necrosis. Each detached leaf was punctured on 3 spots with a sterile needle and the stem placed in sterile water in a closed Petri dish to avoid dehydration. Twenty µl drops (3 drops per leaf) of four concentrations of the recombinant NprvNep proteins (1, 5, 10, and 20 µM) were placed on the top of the leaves at the punctured spots (three leaves per treatment). Sterile ultrapure water was used as a control. Inoculated leaves were kept at room temperature (22-25 °C). Symptom development was monitored for 8 days after inoculations. The same procedure was used for *Eucalyptus* leaves without success. *Eucalyptus* leaves presented considerable water repellence with the droplets tending to avoid the leaf surface. Results did not have the quality for publication.

Chlorophyll fluorescence imaging

In vivo chlorophyll fluorescence images of tomato leaves were measured by using a FluorCAM 800MF imaging fluorometer (Photon System Instruments, Brno, Czech Republic), comprising a computer operated control unit (SN-FC800-082; Photon System Instruments) and a CCD camera (CCD381; PSI) with a f1.2 (2.8-6 mm) objective (Eneo, Rödermark, Germany), as describe by Serôdio et al. (2013). Images of chlorophyll fluorescence parameters F_o and F_m (dark-level and maximum fluorescence level, respectively), were captured on tomato leaves dark-adapted for 20 min by applying modulated measuring light and saturation pulses (<0.1 and >7,500 µmol photons m^{-2} s^{-1}, respectively), provided by red LED panels (612 nm emission peak, 40-nm bandwidth). Images (512×512 pixels) were processed

by defining areas of interest (AOIs) matching the whole area of each leaf, by excluding the non-fluorescent background signal (outside the leave) and the necrosis areas (see below), using the FluorCam7 software (Photon System Instruments). Areas of necrosis were quantified by counting the number of pixels of the leave that drawn manually, using the FluorCAM7 software. The values of F_o and F_m were calculated by averaging all pixel values in each AOI (Serôdio et al., 2017). The maximum quantum yield of PSII was calculated as $F_v/F_m = (F_m-F_o)/F_m$ (Schreiber et al., 1986). For the production of the images shown in Figure 4.4B and Figures S4.2,3,4, and 6B, the scale of false colour of F_v/F_m values was normalized between 0.0 and 0.8 to ensure consistency between the different treatments.

Cytotoxicity Assay

In vitro cytotoxic effects of recombinant NprvNeps was assessed as described previously (Cruz et al., 2013; Duarte et al., 2015) with slight modifications. A Vero cell line (ECACC 88020401, African Green Monkey kidney) was grown and maintained according to Ammerman et al. (2008). Microtiter plates were incubated at 37 °C in 5 % CO_2 for 24 h. Recombinant NprvNeps in PBS were filtered through a sterile 0.2 µm pore size syringe membrane filter and prepared at 1 µM, 5 µM, and 10 µM concentrations. All NprvNep dilutions then were added to Vero cells [1:1 (v/v) in DMEM - Dulbecco's Modified Eagle Medium] and incubated for 20 h. After cell treatment, the medium was removed by aspiration and 50 µL of DMEM with 10 % resazurin (0.1 $mg.mL^{-1}$ in PBS) was directly added to each well. The microtiter plates were incubated at 37 °C in 5 % CO_2 for 3 h. The absorbance was read at 570 and 600 nm in a microtiter plate spectrophotometer (Biotek Synergy). Phosphate-buffered saline buffer (PBS) was used as control.

Bioinformatics Analysis

Gene database from NCBI was used to detect putative *NprvNep* genes in the genome of *N. parvum* isolate UCR-NP2. The SignalP 4.1 Server (Petersen et al., 2011) was used to identify the signal peptide sequences. Molecular weight (MW) predictions for the deduced protein were carried out using the Compute pI/Mw tool (Lausanne, Switzerland, www.expasy.org/tools/protparam.html).

Statistical analysis

Two-way analysis of variance (ANOVA) followed by a Tukey multiple comparison test was used to determine the statistical significance of cytotoxicity of each recombinant NprvNeps within the same concentration against the control (*p<0.05, **p<0.01, ***p<0.001, ****p<0.0001). Differences between F_v/F_m among the different experiences were tested using a two-way ANOVA, followed by the Dunnett's multiple comparison test and Tukey multiple comparison to determine the statistical significance of phytotoxicity of each protein within the same concentration against the control (*p<0.05, **p<0.01, ***p<0.001, ****p<0.0001). All the analyses were performed with GraphPad

Prism v.7 (GraphPad Software, Inc., La Jolla, CA, USA). Data are shown as the average of three independent replicates of each condition.

RESULTS

Effect of culture filtrate of *N. parvum* on detached tomato leaves

In a preliminary test, we observed that inoculation of 10-day-old *N. parvum* CAA704 culture filtrate into tomato leaves induced necrosis on the treated leaf (Figure 4.1). The first symptoms were observed approximately at 2 days post inoculation (dpi) with yellowing around inoculated sites. As time passed, these lesions gradually became irregular, dark brown, surrounded by a yellow halo, at 6 dpi. In contrast, no symptoms were observed in the control leaves.

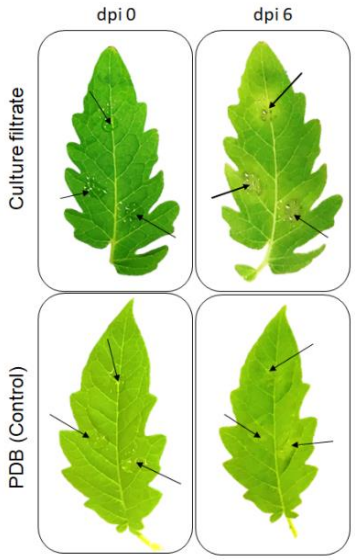

Figure 4.1 |. Effect of culture filtrate of *N. parvum* CAA704 on detached tomato leaves after 6 dpi. Potato dextrose broth (PDB) was used as a control. Photographs are representative of three independent experiments, and similar results were obtained in each experiment.

NprvNep proteins' sequence analysis

Six NLP genes containing a necrosis-inducing phytophthora protein domain (NPP1) were identified in the genome of *N. parvum* UCRNP2 (Blanco-Ulate et al., 2013) and named *NprvNep 1-6* (Table S4.1). Of these NLPs, the size of the predicted protein NprvNep6 (163 aa) was dramatically short due to a truncation detected at the N-terminus of the protein. In addition, one of two conserved cysteine crucial for the stability of the protein is absent, leading to a non-functional product. Therefore, NprvNep6 was not further analyzed. Five genes (*NprvNep1*, *NprvNep2*, *NprvNep3*, *NprvNep4*, and *NprvNep5*) were selected for functional analysis.

The conservation of these key residues among *N. parvum* NLPs was assessed (Figure 4.2). The presence of two conserved cysteines in all NprvNep predicted sequences, confirms that the five NprvNep proteins belong to type 1. Conservation of the 24-aa peptide was detected in all NprvNeps, with some variations. The first four residues (AIMY) of the conserved region I are conserved in NprvNep1, 4, and 5, but variable in NprvNep2 and 3. The conserved region II, GHRHDWE, was also present in NprvNep 1-5. A mutation on heptapeptide sequence was noticed only on NprvNep2, from GHRH**D**WE to GHRH**E**WE (Figure 4.2). All NprvNep proteins have a signal peptide consisting of 18 to 28 amino acid residues, targeting them for secretion.

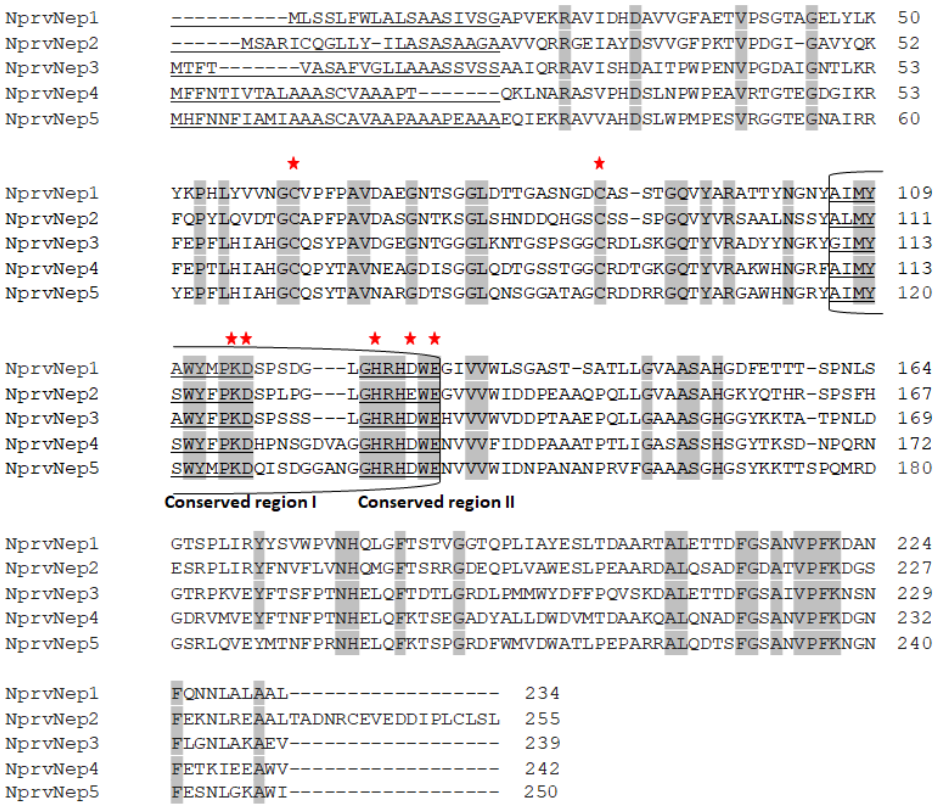

Figure 4.2| Alignment of the predicted amino acid sequences of the *N. parvum* NLPs proteins. Conserved amino acid residues are shaded grey. Asterisks indicate residues crucial for NLP activity (Fellbrich et al., 2002; Ottmann et al., 2009). The nlp24 peptide consisting of conserved region I (11-aa) and conserved region II (the heptapeptide GHRHDWE motif) (Böhm et al., 2014; Oome et al., 2014) is denoted by a box. Signal peptide, conserved regions I and II are underlined.

Cloning, expression and purification of NprvNep proteins

The *NprvNep* genes were successfully amplified from *N. parvum* genomic DNA. Amplicon sequencing indicated that all *NprvNep* genes contain one intron, except for *NprvNep5* which has 2 introns (Figure

S4.1). The cDNAs of *NprvNeps 1-5*, without the signal peptide, were successfully cloned in a pET SUMO vector. This vector allows expression of a recombinant protein with an N-terminal peptide containing the hexahistidine tag (H6-SUMO tag) fused to a SUMO protein.

Recombinant his-tagged NprvNep1-4 proteins were successfully overexpressed in *E. coli* BL21 (DE3) and the optimum induction conditions for them were obtained with 1 mM IPTG at 30 °C for 24 h (Figure 4.3, lane 1). The overexpression of NprvNep5 was not possible in this expression system, probably due to very high associated toxicity.

Each fusion protein was purified from the soluble fraction of a cell lysate by affinity binding of the H6 tag to nickel beads, under nondenaturing conditions (Figure 4.3, lane 2). The N-terminal H6-SUMO tag was removed by SUMO protease (Figure 4.3, lane 3). Cleavage products were successfully purified as pure NprvNep proteins (Figure 4.3, lane 4) while H6-SUMO tag remained bound to the column and eluted later at higher concentration of imidazole (Figure 4.3, lane 5). SDS-PAGE analysis of pure proteins clearly shows a single band for purified protein with the expected molecular weight of the NprvNep proteins.

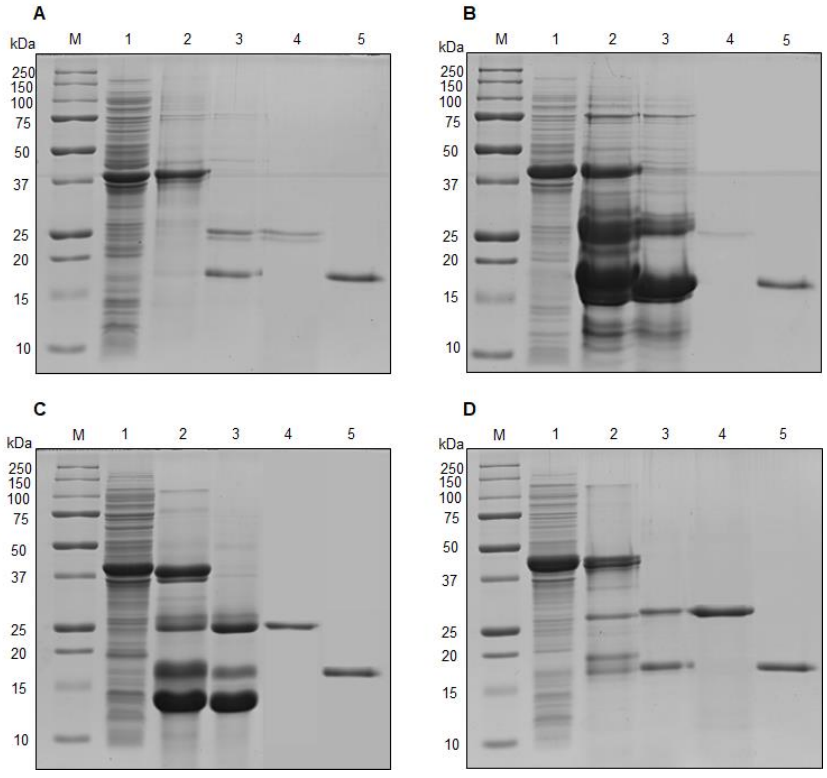

Figure 4.3 | Protein expression and purification of recombinant NprvNeps. SDS-PAGE analysis of (**A**) NprvNep1 protein; (**B**) NprvNep2 protein; (**C**) NprvNep3 protein; and (**D**) NprvNep4 protein. Lanes correspond to: (**M**) Molecular weight marker; (**1**) Crude extract of lysed cells 24 hours after IPTG induction; (**2**) H6-SUMO fusion protein after HisTrap purification; (**3**) SUMO protease-treated fusion protein (**4**) purified recombinant NprvNep protein (after removal of H6-SUMO tag by HisTrap column); (**5**) purified 6×His-SUMO by HisTrap column.

Activity of NprvNep proteins – toxicity to tomato leaves

The necrosis-inducing activity of the recombinant NprvNep proteins to tomato leaves was tested. Leaves from young tomato plants were excised and inoculated with each protein (1 to 20 µM). Symptoms were measured for up to 8 days for presence and extent of local necrosis lesions.

No symptoms were observed in controls during the time of the experiment (Figure 4.4A). None of the recombinant NprvNeps induced visible effects on detached tomato leaves at 1 µM after 8 dpi (Figure S4.2A). At 5 µM, NprvNep3 induced a distinct white necrosis (at 2 dpi, Figure S4.3A) that gradually expanded and turned brown. At the same concentration (5 µM), NprvNep2 induced very small white areas. NprvNep1 induced a small discoloration around the punctured area in the inoculated site at 4 dpi, and necrosis was detected at 5 dpi (Figure S4.3A). NprvNep4 induced no visible symptoms until 5 dpi, when very small necrotic lesions were detected (Figure S4.3A).

At 10 µM, necrosis symptoms were visible at 1 dpi for NprvNep1, 2, and 3. These lesions expanded over time, especially in the case of NprvNep2-induced lesions. NprvNep4 induced chlorotic areas at 3 dpi that did not evolve until the end of the experiment (Figure S4.4A).

Tomato leaves treated with 20 µM of recombinant NprvNeps (Figure 4.4A) developed necrosis at 1 dpi for NprvNeps 1, 2, and 3, and at 2 dpi for NprvNep4. The leaves inoculated with NprvNep2 were severely damaged: the necrotic area expanded through the leaves that died at 3 dpi. Similar symptoms were observed for NprvNep1 and 2, but with milder severity. NprvNep4 induced visually detectable necrosis symptoms only at this concentration (20 µM).

Activity of NprvNep proteins – Effect of NprvNep proteins on chlorophyll fluorescence

The visual symptoms caused by inoculation of recombinant NprvNeps into tomato leaves were analyzed by chlorophyll fluorescence imaging (Figures 4.4B, C). The average F_v/F_m values for control leaves were consistently above 0.79 throughout the experiment time course (Figures S4.2-4C and Figure 4.4C). As expected, F_v/F_m values for leaves inoculated with 1 µM NprvNep proteins showed no significant differences in relation to the control leaves (Figure S4.2). F_v/F_m of leaves exposed to 5 µM of recombinant NprvNep 4 (at 8 dpi) revealed no significant difference to healthy plants (Figure S4.3C). For recombinant NprvNeps 1 and 2 a slight, but significant, decline in F_v/F_m values from 0.81 ± 0.003 and 0.82 ± 0.005 to 0.72 ± 0.04 ($p < 0.0001$) and 0.75 ± 0.04 ($p < 0.001$), respectively, were measured at 8 dpi (Figure S4.3C). However, under 5 µM, NprvNep3 induced a slight decrease in F_v/F_m (0.70 ± 0.03, $p < 0.0001$) at 2 dpi that steadily decreased until the end of the experiment: 0.63 ± 0.04 ($p < 0.0001$) at 3 dpi, and 0.60 ± 0.03 at 8 dpi ($p < 0.0001$) (Figure S4.3C). These F_v/F_m values results are consistent with the symptoms development.

At 10 µM (1 dpi), recombinant NprvNeps 1-3 induced a significant decrease of F_v/F_m: from 0.82 ± 0.005, 0.81 ± 0.003 and 0.81 ± 0.005 to 0.73 ± 0.03 ($p < 0.001$), 0.55 ± 0.04 ($p < 0.0001$) and 0.63 ± 0.03 ($p < 0.0001$) respectively. In contrast, NprvNep4 induced no significant changes (Figure S4.4C). After 8 dpi, all leaves exhibited significant changes in the values of F_v/F_m (Figure S4.4C): F_v/F_m of 0.23 ± 0.05, 0.43 ± 0.05, 0.51 ± 0.05 and 0.73 ± 0.04 for leaves challenged with NprvNep 2 ($p < 0.0001$), NprvNep 1 ($p < 0.0001$), NprvNep 3 ($p < 0.0001$), and NprvNep4 ($p < 0.001$), respectively (Figure S4.4C).

A rapid decrease in F_v/F_m associated with the inoculation of a higher concentration of recombinant NprvNep proteins (20 µM) was observed (Figure 4.4C). The F_v/F_m values for leaves inoculated with NprvNeps 1, 2 and 3 proteins dramatically decreased within 1 dpi from 0.82 ± 0.005, 0.81 ± 0.005 and 0.81 ± 0.0 to 0.49 ± 0.09 ($p < 0.0001$), 0.38 ± 0.03 ($p < 0.0001$) and 0.56 ± 0.04 ($p < 0.0001$), respectively (Figure 4.4C). These values were consistent with the visible severe necrosis symptoms observed after the inoculation of NprvNep proteins on tomato leaves at 1dpi (Figure 4.4A). At the end of the experiment (8 dpi), leaves were severely damaged by recombinant NprvNeps leading to F_v/F_m values of 0.16 ± 0.05, 0.23 ± 0.06, 0.32 ± 0.1 and 0.62 ± 0.06 (NprvNeps 2, 1, 3 and 4, respectively, Figure 4.4C).

Necrosis area induced by recombinant NprvNep proteins (10 and 20 µM) was determined (Figure S4.4D and Figure 4.4D). All tomato leaves treated with NprvNep1, 2, and 3 at 20 µM showed large necrosis areas (68.3 ± 3.06, 102.3 ± 1.87 mm^2 and 54.3 ± 2.28, respectively) at 8 dpi (Figure 4.4D). In contrast, inoculation with NprvNep4 resulted in the smallest lesions (18.6 ± 2.26 mm^2) (Figure 4.4D). Interestingly, our data indicate that necrosis area correlates well with a decrease in the F_v/F_m values (Figure S4.5), mainly for NprvNep 1, 2 and 3 (high necrosis area/ low F_v/F_m values). For very low necrosis areas (initial symptom development), F_v/F_m seems to be a more sensitive parameter.

A summary of the comparison between F_v/F_m values for leaves treated with water and different concentration of NprvNep1-4 proteins at 0 dpi and 8 dpi is represented in Figure 4.4E, discussed in detail previously. We also compared their symptom development at 0 dpi and 8 dpi by F_v/F_m images, which is shown in Figure S4.6B.

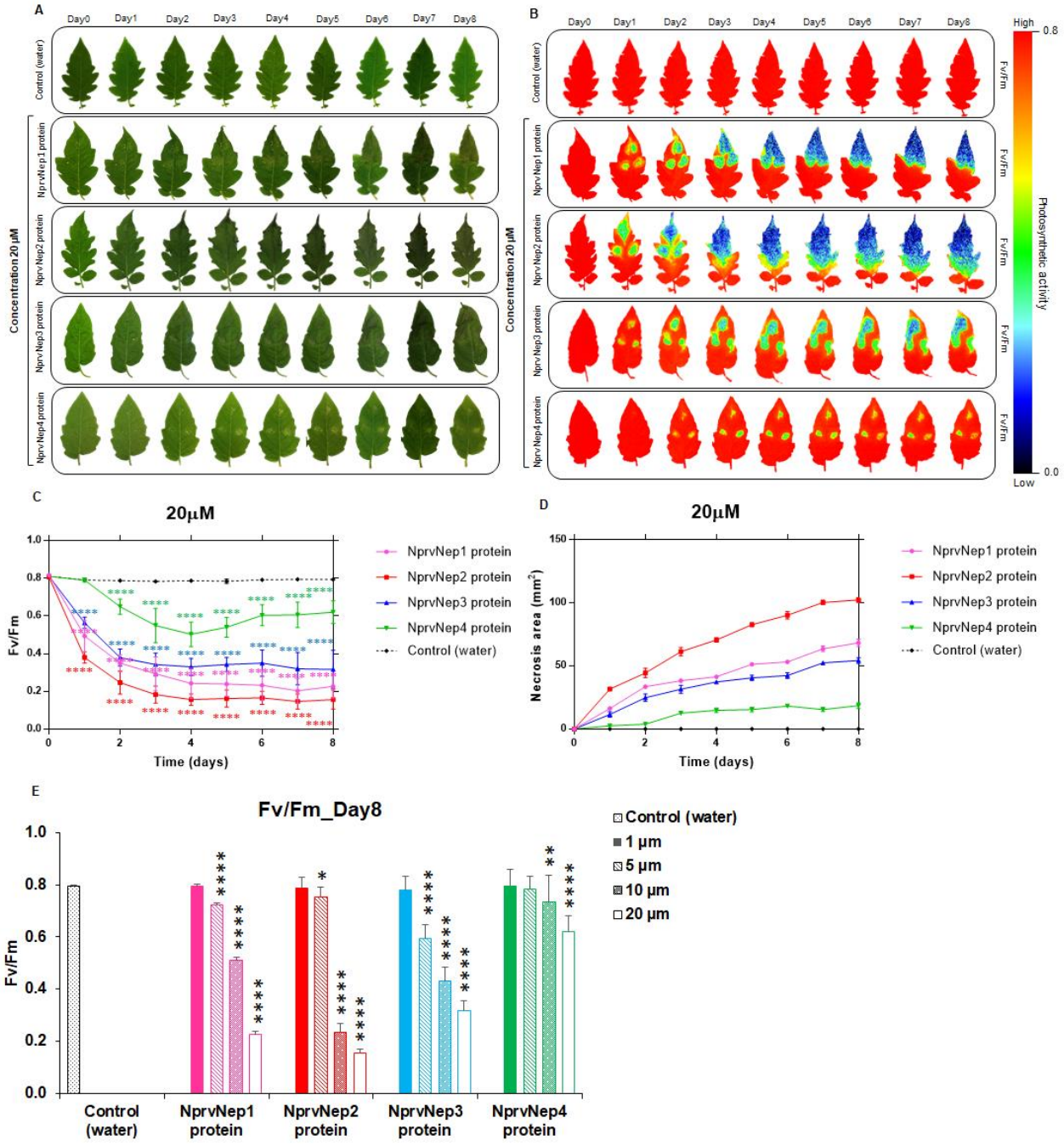

Figure 4.4 | Effect of recombinant NprvNeps on detached tomato leaves. Photographs of tomato leaves inoculated with 20 µM recombinant NprvNeps (**A**), chlorophyll fluorescence (**B**), evolution of F_v/F_m (**C**), evolution of the necrosis area (**D**) and comparison of F_v/F_m at 0 and 8 dpi (**E**). Ultra-pure water was used as a control. The colour scale bar indicates the F_v/F_m intensity of the leaf pixels given in false colours from high (red) to low (black) values. All measurements were performed in biological triplicates and error bars show the standard deviation. Two-way ANOVA, followed by a Dunnett's multiple comparison test (**C**) and a Tukey multiple comparison test (**E**) was used to determine the statistical significance of phytotoxicity of each protein within the same concentration against the control (**C**) (**p*<0.05, ***p*<0.01, ****p*<0.001, *****p*<0.0001).

Activity of NprvNep proteins – toxicity to Vero cells

We investigated the cytotoxic effect of recombinant NprvNeps to mammalian Vero cell line (Figure 4.5). All pure recombinant proteins significantly decreased Vero cells' viability at all concentrations tested, except for NprvNep1, NprvNep3, and NprvNep4 at 1 µM (Figure 4.5).

Cell mortality increased with increasing protein concentration, leading to the loss of more than 98 % of cell viability for NprvNeps1, 2 and 3 at 10 µM. NprvNep2 was the most toxic, being able to cause 55 % mortality at 1 µM. NprvNep4 induced weaker, but, nevertheless, still significant toxic effects for mammalian cells.

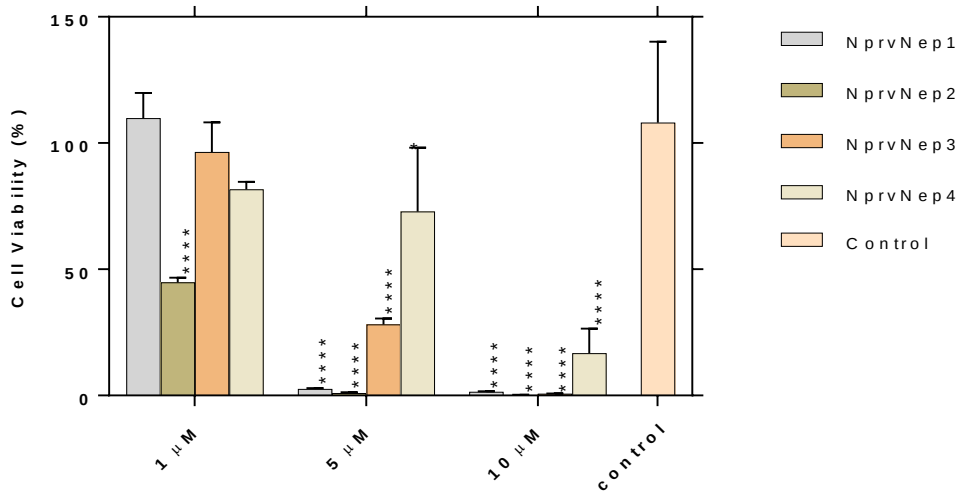

Figure 4.5 | Cytotoxicity of pure recombinant NprvNep proteins to Vero cells. Pure recombinant NprvNep1, 2, 3, and 4 were tested on Vero cells at three different concentrations (1, 5, and 10 µM). Two-way ANOVA, followed by a Tukey multiple comparison test was used to determine the statistical significance of cytotoxicity of each protein within the same concentration against the control (**p*<0.05, ***p*<0.01, ****p*<0.001, *****p*<0.0001). Data is presented as average ± standard error.

DISCUSSION

Aiming to understand the potential influence of NLP proteins from *N. parvum* in its virulence, we cloned and expressed four genes. In addition, knowing that the family Botryosphaeriaceae comprises several opportunistic human pathogens, we hypothesized that NprvNep proteins could be toxic not only for plants, but also for mammalian cells. In recent decades, various studies have shown that *N. parvum* virulence is associated with the production of a varity of compounds in its hosts as well as in artificial media, such as secreted proteins and phytotoxins (Abou-Mansour et al., 2015; Andolfi et al., 2011; Bénard-Gellon et al., 2015; Pour et al., 2020). However, very little is known about the effector proteins that contribute to *N. parvum,* as well as other *Botryosphaeriaceae,* virulence. Cobos et. al (2010) reported the presence of three necrosis and ethylene inducing proteins in the secretome of *D. seriata*. Later, the same authors have cloned the NLP genes and expressed in *E. coli* BL21 (DE3) and

subsequently purified. The pure recombinant proteins showed to be phytotoxic to *Vitis* cell culture (Cobos et al., 2019). We hypothesized that homologous proteins are expressed by *N. parvum* and analyzed *N. parvum* genome for NLP genes. In fact, the analysis of the genome of *N. parvum* revealed the presence of 6 NLP genes that were named *NprvNep 1-6* (Table S4.2). The presence of a signal peptide is crucial for NLP-induced necrosis since NLPs' activity is extracellular (Qutob et al., 2006). Therefore, proteins (González-García et al., 2019) lacking signal peptide should not be functional *in vivo*. Furthermore, the formation of at least one disulphide bridge is required for NLPs' activity (Gijzen & Nurnberger, 2006). Selected *NprvNep* genes (1-5) contained both requisites: a signal peptide and two conserved cysteine residues, belonging to the type 1 NLPs (Gijzen & Nurnberger, 2006). *NprvNep6* lacked the signal peptide, one conserved cysteine and the upstream sequence, making this protein unqualified for further analysis. A similar truncated version of NLPs was described for *Verticillium dahliae*, in which a lack of the N-terminal, including the two conserved cysteines, was suggested as being responsible for the absence of necrotic and elicitor activities of VdNLP6 (Zhou et al., 2012).

The 24-aa (nlp24) sequence is a highly central conserved region in NLPs and can trigger plant immune responses (Böhm et al., 2014; Oome et al., 2014). Substitutions in the nlp24 region of the fungal VdNLP2 protein lead to, in most cases, loss of cytotoxicity (Zhou et al., 2012). All NprvNep proteins contain the nlp24 peptide with a bit variable degeneracy (Figure 4.2). This peptide has two regions that are strongly conserved in type 1 NLPs: conserved regions I and II (Figure 4.2). Conserved region I (11 aa) contains relevant residues for the phytotoxic activity of NLP such as D and K (Figure 4.2) (Ottmann et al., 2009). Conserved region II is a seven–amino-acid motif, GHRHDWE, strongly conserved among NLP of different species. Ottman and co-workers (Ottmann et al., 2009) also investigated three amino acid residues in this motif (G**H**RH**D**W**E**) showing that these residues are required for cytotoxicity (Ottman et al., 2009). These residues are involved in the formation of a cation-binding pocket (Ottman et al., 2009). The acidic pocket was proposed to interact with polar head groups of membrane lipids, thereby damaging or interacting with the plant cell membrane (Küfner et al., 2009). Our results show that the heptapeptide motif of NprvNep proteins is strongly conserved. The exception is NprvNep 2 heptapeptide, which has a mutation: aspartic acid (D_{138}) to glutamic acid (E) (Figure 4.2). Our data suggest that this is a conservative mutation, since NprvNep2 protein exhibits high phytotoxic activity compared to the rest of NprvNep, and that this substitution did not affect the cytotoxicity.

We noted that key residues are mostly conserved among NprvNep proteins (Figure 4.2). However, NprvNep2 exhibiting the D_{138}→E substitution, induced stronger symptoms to the detached tomato leaves. Similarly, two NLP of *Phytophthora capsica* (Pc109174 and Pc118548) with the variable residues at the key sites of the heptapeptide motif showed to be phytotoxic (Chen et al., 2018).

Furthermore, PsNLP54 lacking a conserved Cys residue can cause necrosis (Dong et al., 2012). In contrast, six PsNLPs are not able to trigger necrosis even though they contain all the key residues (Dong et al., 2012). These findings indicate that it is not straightforward to predict the phytotoxicity of NLPs from sequence analysis only (Dong et al., 2012).

Several studies have been performed to test phytotoxic ability of NLP by infiltration of recombinant pure proteins in detached leaves. In 1995, Bailey (Bailey, 1995), who was the first to purify NLP proteins from culture filtrate of the phytopathogen *Fusarium oxysporum*, showed that the application of only 50 ng of the protein could induce ethylene and necrosis on cacao leaves (Bailey, 1995). Similarly, infiltration of 2.5 µM of *Phytophthora parasitica* NPP1 into parsley and *Arabidopsis* leaves and 2 µM in tobacco leaves resulted in necrotic lesion formation. However, infiltration of similar and higher concentrations (10 µM) of NLP protein failed to induce necrosis in monocot plants (Fellbrich et al., 2002). Purified BcNEP1 (0.04 to 4 µM) and BcNEP2 (0.4 to 40 µM) from the necrotrophic fungus *Botrytis cinerea* caused necrosis in all dicotyledonous plant species tested, but not in monocotyledons (Schouten et al., 2008). In *Moniliophthora perniciosa,* causal agent of witches' broom in *Theobroma cacao*, MpNEP1 and 2 also showed necrosis and ethylene emission after infiltration into tobacco and cacao leaves at 1 µM (Garcia et al., 2007). However, infiltration of NLPs into detached leaves of plants does not always cause cell death and necrosis symptoms. Purified HaNLP1, 2, and 3 (2-20 µM) from downy mildew pathogen *Hyaloperonospora arabidopsidis*, failed to induce necrosis into leaves of *Arabidopsis thaliana* Col-0 and *Nicotiana tabacum* (Cabral et al., 2012). Similarly, the sole *NLP* gene in fungal wheat leaf pathogen *Mycosphaerella graminicola* induced necrotic cell death and defense-related genes after infiltration into *Arabidopsis* leaves at 2 µM, but not in the same concentration in leaves of a susceptible wheat genotype (Motteram et al., 2009).

NLPs are best known to cause necrosis, cell death and wilting symptoms on plants (Fellbrich et al., 2002; Wang et al., 2004). To analyse whether the NLPs from *N. parvum* can cause necrosis, we evaluated the effect of heterologously-expressed NprvNep1-4 proteins, *in vitro*, on detached tomato leaves and on a mammalian cell line. The lack of overexpression of the NprvNep5 is likely associated with the high toxicity of NprvNep5 for *E. coli* cells. Even after several attempts (including transformation of NprvNep5 in a more resistant strain of *E. coli*- BL21 (DE3) pLysS competent cells; the addition of glucose to culture medium; among others), NprvNep expression was not attained (data not shown).

We were able to confirm that *NprvNep* genes encode biologically active proteins able to cause necrosis in tomato leaves, in a dose-dependent manner. The fact that the same gene family of NLP could have distinct phytotoxic activities was also observed in the case of BcNEPs from *B. cinerea.* Both BcNEP1 and BcNEP2 induced necrosis in all tested leaves of dicot plants, but BcNEP2-induced symptoms were

consistently less severe than those induced by BcNEP1 (Arenas et al., 2010). Similarly, phytotoxic activity of NLPs from a tomato-pathogenic *V. dahliae* strain were distinct whereas only two of the seven NLP displayed cytotoxic activity in plants (Santhanam et al., 2013).

Besides the classic visual observation of symptoms, we assessed the photosystem II (PSII) activity of tomato leaves upon inoculation of the recombinant NprvNeps. Photodamage resulting from biotic or abiotic stress factors was indicated by a reduction in F_v/F_m values, from the typical 0.80 of unstressed leaves. Extensive studies have used F_v/F_m images to follow fungal infections such as *Colletotrichum lindemuthianum* in *P. vulgaris* (Meyer et al., 2001), *B. cinerea* in *S. lycopersicum* (Berger et al., 2004), *Puccina polysora* in *Zea mays* (Duraes et al., 2001) and *Colletotrichum orbiculare* in *Nicotiana benthamiana* (Tung et al., 2013). Our results showed that F_v/F_m values of recombinant NprvNep treated leaves exhibited a time and concentration-dependent decrease, representative of the photosynthetic damage induced by NprvNeps.

It is well established that NLPs toxicity is restricted to dicot plants (Gijzen & Nürnberger, 2006; Pemberton & Salmond, 2004, Qutob et al., 2002; Schouten et al., 2008). Nonetheless, bacterial virulence and haemolysis activity of *Vibrio navarrensis* against animal erythrocytes has been related to a genomic region that contained a gene encoding an NLP (Jores et al., 2003). Furthermore, type 2 NLPs in animal-related microorganisms such as the coral pathogen *Vibrio coralliilyticus* (O de Santos et al., 2011) and the bivalve endosymbiont *Teredinibacter turnerae* (Yang et al., 2009) have been reported, but additional studies are needed to clarify whether their NLPs are functional and have cytotoxic effects on mammalian cells or not. As far as we are aware, only one report described the activity of NLPs towards other cells like animal, moss, yeast, and lower plants' cells (Qutob et al., 2006). The viability of each of these cell types was not significantly reduced by incubation with up to 1 µM NLP. In contrast, at 1 µM NprvNep 2 induced cell mortality. At higher concentrations, all NprvNeps induced cell mortality in a dose dependent manner. A similar trend of toxicity to the one observed in tomato leaves was observed in Vero cells (the most toxic NprvNep 2 and the least toxic NprvNep 4) suggesting that similar pathways may be used in plants and mammals. In addition, the susceptibility of Vero cells to pure recombinant NprvNeps suggests implications in the ability of *N. parvum* to infect animal/human hosts. This is the first report of animal cell toxicity induced by NLPs proteins, but to rule out a general effect of NLPs on any cell type more tests need to be done with a larger range of cell lines.

CONCLUSIONS

We characterized for the first time the characterization of NLPs from the plant pathogen, *N. parvum*. Our results showed that four NLP genes in *N. parvum* are functional genes encoding proteins toxic

both to plant and mammalian cells, most probably involved in virulence or cell death during infection by *N. parvum*. We also show that chlorophyll fluorescence imaging can be used to accurately quantify the effect of toxic proteins on plant leaves. In fact, we provided the first monitoring of NLPs effect on detached leaves using the commonly used chlorophyll fluorescence index F_v/F_m.

ACKNOWLEDGMENTS

Thanks are due to FCT/MCTES for the financial support to CESAM (UID/AMB/50017/2019), through national funds. This study was partially supported by FEDER funding through COMPETE program (POCI-01-0145-FEDER-016788) and Programa Operacional Regional de Lisboa - POR Lisboa (LISBOA-01-0145-FEDER-016788) and by national funding through FCT within the research project ALIEN (PTDC/AGR-PRO/2183/2014). The authors acknowledge the FCT financial support to F Nazar Pour (BD/98971/2013) and also COST Action FA1303: Sustainable control of grapevine trunk diseases. COST Action is supported by the EU RTD Framework program and ESF provides the COST Office through an EC contract.

REFERENCES

Abou-Mansour, E., Débieux, J.-L., Ramírez-Suero, M., Bénard-Gellon, M., Magnin-Robert, M., Spagnolo, A., & L'Haridon, F. (2015). Phytotoxic metabolites from *Neofusicoccum parvum*, a pathogen of Botryosphaeria dieback of grapevine. *Phytochemistry*, 115, 207–215.

Alves, A., Correia, A., Luque, J., & Phillips, A. (2004). *Botryosphaeria corticola*, sp. nov. on *Quercus* species, with notes and description of *Botryosphaeria stevensii* and its anamorph, *Diplodia mutila*. *Mycologia*, 96(3), 598–613.

Ammerman, N. C., Beier-Sexton, M., & Azad, A. F. (2008). Growth and maintenance of Vero cell lines. *Current Protocols in Microbiology*, Appendix 4, Appendix 4E.

Amsellem, Z., Cohen, B. A., & Gressel, J. (2002). Engineering hypervirulence in a mycoherbicidal fungus for efficient weed control. *Nature Biotechnology*, 20(10), 1035–1039.

Andolfi, A., Mugnai, L., Luque, J., Surico, G., Cimmino, A., & Evidente, A. (2011). Phytotoxins produced by fungi associated with grapevine trunk diseases. *Toxins*, 3(12), 1569–1605.

Arenas, Y. C., Kalkman, E. R. I. C., Schouten, A., Dieho, M., Vredenbregt, P., Uwumukiza, B., & van Kan, J. A. L. (2010). Functional analysis and mode of action of phytotoxic Nep1-like proteins of *Botrytis cinerea*. *Physiological and Molecular Plant Pathology*, 74(5–6), 376–386.

Bae, H., Kim, M. S., Sicher, R. C., Bae, H.-J., & Bailey, B. A. (2006). Necrosis- and ethylene-inducing peptide from *Fusarium oxysporum* induces a complex cascade of transcripts associated with signal transduction and cell death in Arabidopsis. *Plant Physiology*, 141(3), 1056–1067.

Bailey, B. A. (1995). Purification of a protein from culture filtrates of *Fusarium oxysporum* that induces ethylene and necrosis in leaves of *Erythroxylum coca. Phytopathology*, 85(10), 1250–1255.

Bailey, B. A., Bae, H., Strem, M. D., Antunez de Mayolo, G., Guiltinan, M. J., Verica, J. A., & Bowers, J. H. (2005). Developmental expression of stress response genes in *Theobroma cacao* leaves and their response to Nep1 treatment and a compatible infection by *Phytophthora megakarya*. *Plant Physiology and Biochemistry: PPB*, 43(6), 611–622.

Bailey, B. A., Jennings, J. C., & Anderson, J. D. (1997). Sensitivity of Coca (*Erythroxylum coca var. coca*) to Ethylene and Fungal Proteins. *Weed Science*, 45(5), 716–721.

Bénard-Gellon, M., Farine, S., Goddard, M. L., Schmitt, M., Stempien, E., Pensec, F., & Larignon, P. (2015). Toxicity of extracellular proteins from *Diplodia seriata* and *Neofusicoccum parvum* involved in grapevine Botryosphaeria dieback. *Protoplasma*, 252(2), 679–687.

Berger, S., Papadopoulos, M., Schreiber, U., Kaiser, W., & Roitsch, T. (2004). Complex regulation of gene expression, photosynthesis and sugar levels by pathogen infection in tomato. *Physiologia Plantarum*, 122(4), 419–428.

Blanco-Ulate, B., Rolshausen, P., & Cantu, D. (2013). Draft genome sequence of *Neofusicoccum parvum* isolate UCR-NP2, a fungal vascular pathogen associated with grapevine cankers. *Genome Announcements*, 1(3), e00339-13.

Böhm, H., Albert, I., Oome, S., Raaymakers, T. M., Van den Ackerveken, G., & Nürnberger, T. (2014). A Conserved Peptide Pattern from a Widespread Microbial Virulence Factor Triggers Pattern-Induced Immunity in *Arabidopsis*. *PLOS Pathogens*, 10(11), e1004491.

Cabral, A., Oome, S., Sander, N., Küfner, I., Nürnberger, T., & Van den Ackerveken, G. (2012). Nontoxic Nep1-like proteins of the downy mildew pathogen *Hyaloperonospora arabidopsidis*: repression of necrosis-inducing activity by a surface-exposed region. *Molecular Plant-Microbe Interactions*, 25(5), 697–708.

Castillo-Pando, M., Somers, A., Green, C. D., Priest, M., & Sriskanthades, M. (2001). Fungi associated with dieback of Semillon grapevines in the Hunter Valley of New South Wales. *Australasian Plant Pathology*, 30(1), 59–63.

Chen, X.-R., Huang, S. X., Zhang, Y., Sheng, G.-L., Li, Y. P., & Zhu, F. (2018). Identification and functional analysis of the NLP-encoding genes from the phytopathogenic oomycete *Phytophthora capsici*. *Molecular Genetics and Genomics:* MGG, 293(4), 931–943.

Cobos, R., Barreiro, C., Mateos, R. M., & Coque, J. J. R. (2010). Cytoplasmic- and extracellular-proteome analysis of *Diplodia seriata*: a phytopathogenic fungus involved in grapevine decline. *Proteome Science*, 8, 46.

Cobos, R., Calvo-Peña, C., Álvarez-Pérez, J. M., Ibáñez, A., Diez-Galán, A., González-García, S., Acebes, J. L., & Coque, J. J. R. (2019). Necrotic and Cytolytic Activity on Grapevine Leaves Produced by Nep1-Like Proteins of *Diplodia seriata*. *Frontiers in Plant Science*, 10, 1282.

Cruz, A., Areias, D., Duarte, A., Correia, A., Suzuki, S., & Mendo, S. (2013). *Aeromonas molluscorum* Av27 is a potential tributyltin (TBT) bioremediator: phenotypic and genotypic characterization indicates its safe application. *Antonie van Leeuwenhoek*, 104(3), 385–396.

Dong, S., Kong, G., Qutob, D., Yu, X., Tang, J., Kang, J., & Wang, Y. (2012). The NLP toxin family in *Phytophthora sojae* includes rapidly evolving groups that lack necrosis-inducing activity. *Molecular Plant-Microbe Interactions:* MPMI, 25(7), 896–909.

Duarte, A. S., Cavaleiro, E., Pereira, C., Merino, S., Esteves, A. C., Duarte, E. P., &Correia, A. C. (2015). *Aeromonas piscicola* AH-3 expresses an extracellular collagenase with cytotoxic properties. *Letters in Applied Microbiology*, 60(3), 288–297.

Duraes, F. O. M., Casela, C. R., Friesen A.F.E., D. K. |Palme., Gama, E. E. G., Junior, A. L., Magalhaes, P. C., & Shanahan, J. F. (2001). The usefulness of chlorophyll fluorescence in screening for disease resistance, water stress tolerance, aluminium toxicity tolerance, and N use efficiency in maize (C. I. de M. de M. y T. (CIMMYT) Kenya & 7. Proceedings of the Eastern and Southern Africa Regional Maize Conference, eds.). Nairobi (Kenya): KARI|CIMMYT.

Fang, Y.-L., Peng, Y.-L., & Fan, J. (2017). The Nep1-like protein family of *Magnaporthe oryzae* is dispensable for the infection of rice plants. *Scientific Reports*, 7(1), 4372.

Félix, C., Duarte, A. S., Vitorino, R., Guerreiro, A. C. L., Domingues, P., Correia, A. C. M., & Esteves, A. C. (2016). Temperature modulates the secretome of the phytopathogenic fungus *Lasiodiplodia theobromae*. *Frontiers in Plant Science*, 7, 1096.

Félix, C., Meneses, R., Gonçalves, M.F.M., Tilleman, L., Duarte, A.S., Jorrin-Novo, J.V., Van de Peer, Y., Deforce, D., Van Nieuwerburgh, F., Esteves, A.C., & Alves, A. (2019) A multi-omics analysis of the grapevine pathogen Lasiodiplodia theobromae reveals that temperature affects the expression of virulence- and pathogenicity-related genes. *Scientific Rreports*, 9.

Fellbrich, G., Romanski, A., Varet, A., Blume, B., Brunner, F., Engelhardt, S., & Nurnberger, T. (2002). NPP1, a *Phytophthora*-associated trigger of plant defense in parsley and *Arabidopsis*. *The Plant Journal: For Cell and Molecular Biology*, 32(3), 375–390.

Garcia, O., Macedo, J. A. N., Tiburcio, R., Zaparoli, G., Rincones, J., Bittencourt, L. M. C., & Cascardo, J. C. M. (2007). Characterization of necrosis and ethylene-inducing proteins (NEP) in the basidiomycete *Moniliophthora perniciosa*, the causal agent of witches' broom in *Theobroma cacao*. *Mycological Research*, 111(Pt 4), 443–455.

Gijzen, M., & Nurnberger, T. (2006). Nep1-like proteins from plant pathogens: recruitment and diversification of the NPP1 domain across taxa. *Phytochemistry*, 67(16), 1800–1807.

Jennings, J. C., Apel-Birkhold, P. C., Bailey, B. A., & Anderson, J. D. (2000). Induction of ethylene biosynthesis and necrosis in weed leaves by a *Fusarium oxysporum* protein. *Weed Science*, 48(1), 7–14.

Jennings, J. C., Apel-Birkhold, P. C., Mock, N. M., Baker, C. J., Anderson, J. D., & Bailey, B. A. (2001). Induction of defense responses in tobacco by the protein Nep1 from *Fusarium oxysporum*. *Plant Science*, 161(5), 891–899.

Ji, Y., & Scott, J.W. (2006), "Tomato", in: Singh, R.J. (ed.), Genetic Resources, Chromosome Engineering, and Crop Improvement Series IV: Vegetable Crops, CRC Press, Boca Raton, Florida, pp. 59-113.

Jores, J., Appel, B., & Lewin, A. (2003). Cloning and molecular characterization of a unique hemolysin gene of *Vibrio pommerensis* sp. nov.: development of a DNA probe for the detection of the hemolysin gene and its use in identification of related Vibrio spp. from the Baltic Sea. *FEMS Microbiology Letters*, 229(2), 223–229.

Keates, S. E., Kostman, T. A., Anderson, J. D., & Bailey, B. A. (2003). Altered gene expression in three plant species in response to treatment with Nep1, a fungal protein that causes necrosis. *Plant Physiology*, 132(3), 1610–1622.

Küfner, I., Ottmann, C., Oecking, C., & Nürnberger, T. (2009). Cytolytic toxins as triggers of plant immune response. *Plant Signaling & Behavior*, 4(10), 977–979.

Laemmli, U. K. (1970). Cleavage of structural proteins during the assembly of the head of bacteriophage T4. *Nature*, 227(5259), 680–685.

Larignon, P., & Dubos, B. (1997). Fungi associated with esca disease in grapevine. *European Journal of Plant Pathology*, 103(2), 147–157.

Lenarčič, T., Albert, I., Bohm, H., Hodnik, V., Pirc, K., Zavec, A. B., & Nurnberger, T. (2017). Eudicot plant-specific sphingolipids determine host selectivity of microbial NLP cytolysins. *Science (New York, N.Y.)*, 358(6369), 1431–1434.

Li, G. Q., Liu, F. F., Li, J. Q., Liu, Q. L., & Chen, S. F. (2018). Botryosphaeriaceae from *Eucalyptus* plantations and adjacent plants in China. *Persoonia: Molecular Phylogeny and Evolution of Fungi*, 40, 63–95.

Meyer, S., Saccardy-Adji, K., Rizza, F., & Genty, B. (2001). Inhibition of photosynthesis by *Colletotrichum lindemuthianum* in bean leaves determined by chlorophyll fluorescence imaging. *Plant, Cell & Environment*, 24(9), 947–956.

Motteram, J., Kufner, I., Deller, S., Brunner, F., Hammond-Kosack, K. E., Nurnberger, T., & Rudd, J. J. (2009). Molecular characterization and functional analysis of MgNLP, the sole NPP1 domain-containing protein, from the fungal wheat leaf pathogen *Mycosphaerella graminicola*. *Molecular Plant-Microbe Interactions: MPMI*, 22(7), 790–799.

Mugnai, L., Graniti, A., & Surico, G. (1999). Esca (black measles) and brown wood-streaking: two old and elusive diseases of grapevines. *Plant Disease*, 83(5), 404–418.

Pour, F. N., Ferreira, V., Félix, C., Serôdio, J., Alves, A., Duarte, A. S., and Esteves, A. C. (2020). Effect of temperature on the phytotoxicity and cytotoxicity of Botryosphaeriaceae fungi. *Fungal biology*. doi: 10.1016 / j.funbio.2020.02.012

Nimchuk, Z., Eulgem, T., Holt, B. F. 3rd, & Dangl, J. L. (2003). Recognition and response in the plant immune system. *Annual Review of Genetics*, 37, 579–609.

Oome, S., Raaymakers, T. M., Cabral, A., Samwel, S., Böhm, H., Albert, I., & Van den Ackerveken, G. (2014). Nep1-like proteins from three kingdoms of life act as a microbe-associated molecular pattern in *Arabidopsis*. *Proceedings of the National Academy of Sciences*, 111(47), 16955–16960.

Oome, S., & Van den Ackerveken, G. (2014). Comparative and functional analysis of the widely occurring family of Nep1-like proteins. *Molecular Plant-Microbe Interactions: MPMI*, 27(10), 1081–1094.

Ottmann, C., Luberacki, B., Küfner, I., Koch, W., Brunner, F., Weyand, M., & Oecking, C. (2009). A common toxin fold mediates microbial attack and plant defense. *Proceedings of the National Academy of Sciences*, 106(25), 10359 LP – 10364.

Pemberton, C L, Whitehead, N. A., Sebaihia, M., Bell, K. S., Hyman, L. J., Harris, S. J., & Salmond, G. P. C. (2005). Novel quorum-sensing-controlled genes in *Erwinia carotovora* subsp. *carotovora*: identification of a fungal elicitor homologue in a soft-rotting bacterium. *Molecular Plant-Microbe Interactions: MPMI*, 18(4), 343–353.

Pemberton, Clare L, & Salmond, G. P. C. (2004). The Nep1-like proteins-a growing family of microbial elicitors of plant necrosis. *Molecular Plant Pathology*, 5(4), 353–359.

Petersen, T. N., Brunak, S., Von Heijne, G., & Nielsen, H. (2011). SignalP 4.0: discriminating signal peptides from transmembrane regions. *Nature Methods*, 8(10), 785.

Phillips, A. J. L. (2002). *Botryosphaeria* species associated with diseases of grapevines in Portugal. *Phytopathologia Mediterranea*, 41(1), 3–18.

Qutob, D., Kamoun, S., & Gijzen, M. (2002). Expression of a *Phytophthora sojae* necrosis-inducing protein occurs during transition from biotrophy to necrotrophy. *The Plant Journal: For Cell and Molecular Biology*, 32(3), 361–373.

Qutob, D., Kemmerling, B., Brunner, F., Kufner, I., Engelhardt, S., Gust, A. A., & Nurnberger, T. (2006). Phytotoxicity and innate immune responses induced by Nep1-like proteins. *The Plant Cell*, 18(12), 3721–3744.

Santhanam, P., van Esse, H. P., Albert, I., Faino, L., Nurnberger, T., & Thomma, B. P. H. J. (2013). Evidence for functional diversification within a fungal NEP1-like protein family. *Molecular Plant-Microbe Interactions: MPMI*, 26(3), 278–286.

Santos, E. de O., Alves, N. J., Dias, G. M., Mazotto, A. M., Vermelho, A., Vora, G. J., & Thompson, F. L. (2011). Genomic and proteomic analyses of the coral pathogen *Vibrio coralliilyticus* reveal a diverse virulence repertoire. *The ISME Journal*, 5(9), 1471–1483.

Schouten, A., van Baarlen, P., & van Kan, J. A. L. (2008). Phytotoxic Nep1-like proteins from the necrotrophic fungus *Botrytis cinerea* associate with membranes and the nucleus of plant cells. *The New Phytologist*, 177(2), 493–505.

Schreiber, U., Schliwa, U., & Bilger, W. (1986). Continuous recording of photochemical and non-photochemical chlorophyll fluorescence quenching with a new type of modulation fluorometer. *Photosynthesis Research* 10 (1-2), 51–62.

Serrato-Diaz, L. M., Aviles-Noriega, A., Soto-Bauzó, A., Rivera-Vargas, L. I., Goenaga, R., & Bayman, P. (2019). Botryosphaeriaceae Fungi as Causal Agents of Dieback and Corky Bark in Rambutan and Longan. *Plant Disease*, 104(1), 105–115.

Serôdio, J., Ezequiel, J., Frommlet, J., Laviale, M., & Lavaud, J. (2013). A method for the rapid generation of nonsequential light-response curves of chlorophyll fluorescence. *Plant Physiology*, 163(3), 1089–1102.

Serôdio, J., Schmidt, W., & Frankenbach, S. (2017). A chlorophyll fluorescence-based method for the integrated characterization of the photophysiological response to light stress. *Journal of Experimental Botany* 68(5), 1123–1135.

Staats, M., VAN Baarlen, P., Schouten, A., & VAN Kan, J. A. L. (2007). Functional analysis of NLP genes from *Botrytis elliptica*. *Molecular Plant Pathology*, 8(2), 209–214.

Teh, C.-Y., Pang, C.-L., Tor, X.-Y., Ho, P.-Y., Lim, Y.-Y., Namasivayam, P., & Ho, C.-L. (2019). Molecular cloning and functional analysis of a necrosis and ethylene inducing protein (NEP) from *Ganoderma boninense*. *Physiological and Molecular Plant Pathology*, *106*, 42–48.

Tung, J., Goodwin, P. H., & Hsiang, T. (2013). Chlorophyll fluorescence for quantification of fungal foliar infection and assessment of the effectiveness of an induced systemic resistance activator. *European Journal of Plant Pathology*, 136(2), 301–315.

Urbez-Torres, J R, & Gubler, W. D. (2009). Pathogenicity of *Botryosphaeriaceae* Species Isolated from Grapevine Cankers in California. *Plant Disease*, 93(6), 584–592.

Urbez-Torres, & Jose Ramon. (2011). The status of Botryosphaeriaceae species infecting grapevines. *Phytopathologia Mediterranea*, 50(4), 5–45.

Valencia, A. L., Gil, P. M., Latorre, B. A., & Rosales, I. M. (2019). Characterization and Pathogenicity of Botryosphaeriaceae Species Obtained from Avocado Trees with Branch Canker and Dieback and from Avocado Fruit with Stem End Rot in Chile. *Plant Disease*, 103(5), 996–1005.

Veit, S., Wörle, J. M., Nürnberger, T., Koch, W., & Seitz, H. U. (2001). A novel protein elicitor (PaNie) from *Pythium aphanidermatum* induces multiple defense responses in carrot, Arabidopsis, and tobacco. *Plant Physiology*, 127(3), 832–841.

Verica, J. A., Maximova, S. N., Strem, M. D., Carlson, J. E., Bailey, B. A., & Guiltinan, M. J. (2004). Isolation of ESTs from cacao (*Theobroma cacao L.*) leaves treated with inducers of the defense response. *Plant Cell Reports*, 23(6), 404–413.

Wang, J.-Y., Cai, Y., Gou, J.-Y., Mao, Y.-B., Xu, Y.-H., Jiang, W.-H., Chen, X.-Y. (2004) VdNEP, an elicitor from *Verticillium dahliae*, induces cotton plant wilting. *Applied and Environmental Microbiology*, 70, 4989–4995.

Yang, J. C., Madupu, R., Durkin, A. S., Ekborg, N. A., Pedamallu, C. S., Hostetler, J. B., & Coutinho, P. M. (2009). The complete genome of *Teredinibacter turnerae* T7901: an intracellular endosymbiont of marine wood-boring bivalves (shipworms). *PloS One*, 4(7), e6085.

Zhou, B.-J., Jia, P.-S., Gao, F., & Guo, H.-S. (2012). Molecular characterization and functional analysis of a necrosis- and ethylene-inducing, protein-encoding gene family from *Verticillium dahliae*. *Molecular Plant-Microbe Interactions: MPMI*, 25(7), 964–975.

SUPPLEMENTARY MATERIAL

A

```
DNANprvNep1     ATGCTGTCTTCCCTCTTCTGGCTTGCGCTCTCCGCTGCGAGCATTGTTTCAGGCGCCCCG 60
cDNANEP1        ATGCTGTCTTCCCTCTTCTGGCTTGCGCTCTCCGCTGCGAGCATTGTTTCAGGCGCCCCG 60

 DNANprvNep1    GTCGAGAAGCGCGCCGTCATTGATCATGATGCCGTTGTGGGCTTTGCCGAGACGGTCCCC 120
cDNANprvNep1    GTCGAGAAGCGCGCCGTCATTGATCATGATGCCGTTGTGGGCTTTGCCGAGACGGTCCCC 120

 DNANprvNep1    AGCGGCACGGCCGGCGAGCTGTACCTGAAGTACAAGCCGCACTTGTATGTCGTGAACGGC 180
cDNANprvNep1    AGCGGCACGGCCGGCGAGCTGTACCTGAAGTACAAGCCGCACTTGTATGTCGTGAACGGC 180

 DNANprvNep1    TGCGTGCCGTTCCCAGCAGTGGATGCCGAGGGCAACACGAGCTTAGTCTTCCCTCTTATT 240
cDNANprvNep1    TGCGTGCCGTTCCCAGCAGTGGATGCCGAGGGCAACACGAGCG----------------- 223

 DNANprvNep1    TCTGCCGACGACCATCTCGCTCACTCCCTTCCCAGCGGCGGCCTCGACACCACCGGAGCC 300
cDNANprvNep1    ------------------------------------GCGGCCTCGACACCACCGGAGCC 246

 DNANprvNep1    TCCAACGGCGACTGCGCCAGCAGCACCGGCCAGGTCTACGCGCGCGCCACCACCTACAAC 360
cDNANprvNep1    TCCAACGGCGACTGCGCCAGCAGCACCGGCCAGGTCTACGCGCGCGCCACCACCTACAAC 306

 DNANprvNep1    GGCAACTACGCCATCATGTACGCGTGGTACATGCCCAAGGACTCGCCGTCGGACGGGCTG 420
cDNANprvNep1    GGCAACTACGCCATCATGTACGCGTGGTACATGCCCAAGGACTCGCCGTCGGACGGGCTG 366

 DNANprvNep1    GGCCACCGCCACGACTGGGAGGGCATCGTCGTCTGGCTGTCGGGCGCCTCCACCTCCGCC 480
cDNANprvNep1    GGCCACCGCCACGACTGGGAGGGCATCGTCGTCTGGCTGTCGGGCGCCTCCACCTCCGCC 426

 DNANprvNep1    ACCCTGCTCGGCGTCGCCGCCTCCGCCCACGGCGACTTCGAAACCACCACCAGCCCCAAC 540
cDNANprvNep1    ACCCTGCTCGGCGTCGCCGCCTCCGCCCACGGCGACTTCGAAACCACCACCAGCCCCAAC 486

 DNANprvNep1    CTTAGCGGCACCAGCCCTCTCATCCGCTACTACAGCGTCTGGCCCGTCAACCACCAGCTC 600
cDNANprvNep1    CTTAGCGGCACCAGCCCTCTCATCCGCTACTACAGCGTCTGGCCCGTCAACCACCAGCTC 546

 DNANprvNep1    GGCTTCACCAGCACGGTCGGCGGCACGCAGCCGCTCATTGCGTACGAGAGCTTGACGGAT 660
cDNANprvNep1    GGCTTCACCAGCACGGTCGGCGGCACGCAGCCGCTCATTGCGTACGAGAGCTTGACGGAT 606

 DNANprvNep1    GCGGCGAGGACGGCGTTGGAGACTACGGATTTCGGCAGCGCGAATGTGCCGTTCAAGGAT 720
cDNANprvNep1    GCGGCGAGGACGGCGTTGGAGACTACGGATTTCGGCAGCGCGAATGTGCCGTTCAAGGAT 666

 DNANprvNep1    GCGAACTTCCAAAACAACCTAGCGTTAGCGGCGTTGTAG   759
cDNANprvNep1    GCGAACTTCCAAAACAACCTAGCGTTAGCGGCGTTGTAG   705
```

B

```
DNANprvNep2     ATGTCGGCCCGTATCTGCCAAGGACTCCTTTACATTCTTGCCAGTGCCAGCGCAGCCGGT 60
cDNANprvNep2    ATGTCGGCCCGTATCTGCCAAGGACTCCTTTACATTCTTGCCAGTGCCAGCGCAGCCGGT 60

DNANprvNep2     GCTGCGGTTGTTCAACGCCGCGGCGAGATTGCCTATGATTCCGTTGTTGGCTTCCCCAAA 120
cDNANprvNep2    GCTGCGGTTGTTCAACGCCGCGGCGAGATTGCCTATGATTCCGTTGTTGGCTTCCCCAAA 120

DNANprvNep2     ACAGTTCCAGATGGGATTGGTGCCGTCTACCAGAAGTTCCAGCCCTACCTGCAGGTGGAC 180
cDNANprvNep2    ACAGTTCCAGATGGGATTGGTGCCGTCTACCAGAAGTTCCAGCCCTACCTGCAGGTGGAC 180

DNANprvNep2     ACGGGCTGTGCTCCTTTCCCGGCTGTGGATGCCTCAGGAAACACGAACTGAGTGCCACTG 240
cDNANprvNep2    ACGGGCTGTGCTCCTTTCCCGGCTGTGGATGCCTCAGGAAACACGAACTC---------- 230

DNANprvNep2     AAACCAAACTCCGCCGACACCAATAACAACCCATATCTCCGCAGCTCCGGCCTCAGCCAC 300
cDNANprvNep2    ----------------------------------------------CGGCCTCAGCCAC 243

DNANprvNep2     AACGACGACCAGCACGGCAGTTGCTCCAGCAGCCCCGGCCAAGTCTACGTCCGCTCCGCC 360
cDNANprvNep2    AACGACGACCAGCACGGCAGTTGCTCCAGCAGCCCCGGCCAAGTCTACGTCCGCTCCGCC 303

DNANprvNep2     GCCCTCAACTCCAGCTACGCGCTGATGTACTCGTGGTACTTTCCCAAGGACTCGCCGCTC 420
cDNANprvNep2    GCCCTCAACTCCAGCTACGCGCTGATGTACTCGTGGTACTTTCCCAAGGACTCGCCGCTC 363

DNANprvNep2     CCCGGCCTCGGGCACCGGCACGAGTGGGAGGGCGTCGTCGTCTGGATCGACGACCCCGAG 480
cDNANprvNep2    CCCGGCCTCGGGCACCGGCACGAGTGGGAGGGCGTCGTCGTCTGGATCGACGACCCCGAG 423

DNANprvNep2     GCCGCCCAGCCGCAGCTGCTCGGCGTGGCGGCGTCCGCCCATGGCAAGTACCAGACCCAC 540
cDNANprvNep2    GCCGCCCAGCCGCAGCTGCTCGGCGTGGCGGCGTCCGCCCATGGCAAGTACCAGACCCAC 483

DNANprvNep2     AGGAGCCCGAGCTTTCACGAGTCCAGACCGCTGATCAGGTACTTCAACGTTTTCTTGGTC 600
cDNANprvNep2    AGGAGCCCGAGCTTTCACGAGTCCAGACCGCTGATCAGGTACTTCAACGTTTTCTTGGTC 543

DNANprvNep2     AACCATCAGATGGGCTTCACGAGCAGGCGGGGCGACGAGCAGCCGTTGGTGGCGTGGGAG 660
cDNANprvNep2    AACCATCAGATGGGCTTCACGAGCAGGCGGGGCGACGAGCAGCCGTTGGTGGCGTGGGAG 603

DNANprvNep2     AGCCTGCCGGAGGCGGCGAGGGATGCGCTGCAGAGCGCGGACTTTGGGGATGCGACTGTG 720
cDNANprvNep2    AGCCTGCCGGAGGCGGCGAGGGATGCGCTGCAGAGCGCGGACTTTGGGGATGCGACTGTG 663

DNANprvNep2     CCGTTTAAGGACGGGAGTTTCGAGAAGAATCTGCGCGAGGCTGCGTTGACGGCGGACAAC 780
cDNANprvNep2    CCGTTTAAGGACGGGAGTTTCGAGAAGAATCTGCGCGAGGCTGCGTTGACGGCGGACAAC 723

DNANprvNep2     AGATGTGAGGTGGAGGACGACATACCCCTGTGCCTGTCGTTGTGA 825
cDNANprvNep2    AGATGTGAGGTGGAGGACGACATACCCCTGTGCCTGTCGTTGTGA 768
```

C

```
DNANprvNep3     ATGACTTTCACTGTTGCCTCTGCTTTCGTTGGCCTCCTGGCCGCAGCCAGCTCCGTCAGC 60
CDNANprvNep3    ATGACTTTCACTGTTGCCTCTGCTTTCGTTGGCCTCCTGGCCGCAGCCAGCTCCGTCAGC 60

DNANprvNep3     AGTGCTGCCATCCAACGCCGCGCAGTCATTTCCCACGACGCCATCACCCCCTGGCCCGAG 120
CDNANprvNep3    AGTGCTGCCATCCAACGCCGCGCAGTCATTTCCCACGACGCCATCACCCCCTGGCCCGAG 120

DNANprvNep3     AACGTCCCCGGCGATGCCATTGGCAACACGTTGAAGAGATTCGAGCCGTTCCTGCACATC 180
CDNANprvNep3    AACGTCCCCGGCGATGCCATTGGCAACACGTTGAAGAGATTCGAGCCGTTCCTGCACATC 180

DNANprvNep3     GCCCACGGCTGCCAATCCTACCCTGCCGTCGACGGCGAGGGCAACACCGGCTGAGCCGCA 240
CDNANprvNep3    GCCCACGGCTGCCAATCCTACCCTGCCGTCGACGGCGAGGGCAACACCGGC--------- 231

DNANprvNep3     AGCCAACTCCAGCCGCAGCCGGCCACGACACTGACGCGGCCATCTCGCAGCGGCGGCCTG 300
CDNANprvNep3    ----------------------------------------------------GGCGGCCTG 240

DNANprvNep3     AAGAACACAGGCAGCCCGTCGGGCGGGTGCCGCGACCTCTCCAAGGGCCAGACGTACGTG 360
CDNANprvNep3    AAGAACACAGGCAGCCCGTCGGGCGGGTGCCGCGACCTCTCCAAGGGCCAGACGTACGTG 300

DNANprvNep3     CGGGCCGACTACTACAACGGCAAGTACGGCATCATGTACGCGTGGTACTTCCCCAAGGAC 420
CDNANprvNep3    CGGGCCGACTACTACAACGGCAAGTACGGCATCATGTACGCGTGGTACTTCCCCAAGGAC 360

DNANprvNep3     TCGCCGTCGTCGTCGCTGGGCCACCGGCACGACTGGGAGCACGTCGTCGTCTGGGTCGAC 480
CDNANprvNep3    TCGCCGTCGTCGTCGCTGGGCCACCGGCACGACTGGGAGCACGTCGTCGTCTGGGTCGAC 420

DNANprvNep3     GACCCCACCGCCGCCGAGCCACAGCTGCTGGGCGCCGCCGCCTCCGGCCACGGCGGCTAC 540
CDNANprvNep3    GACCCCACCGCCGCCGAGCCACAGCTGCTGGGCGCCGCCGCCTCCGGCCACGGCGGCTAC 480

DNANprvNep3     AAGAAGACGGCCACCCCGAACCTGGACGGCACGCGCCCGAAGGTCGAGTACTTCACCAGC 600
CDNANprvNep3    AAGAAGACGGCCACCCCGAACCTGGACGGCACGCGCCCGAAGGTCGAGTACTTCACCAGC 540

DNANprvNep3     TTCCCCACCAACCACGAGCTGCAGTTCACCGACACCCTCGGCCGCGACCTGCCCATGATG 660
CDNANprvNep3    TTCCCCACCAACCACGAGCTGCAGTTCACCGACACCCTCGGCCGCGACCTGCCCATGATG 600

DNANprvNep3     TGGTACGACTTCTTCCCGCAGGTGAGCAAGGACGCGCTGGAGACCACGGATTTCGGCAGC 720
CDNANprvNep3    TGGTACGACTTCTTCCCGCAGGTGAGCAAGGACGCGCTGGAGACCACGGATTTCGGCAGC 660

DNANprvNep3     GCAATCGTGCCGTTTAAGAACTCGAACTTCTTGGGCAACCTCGCCAAGGCTGAGGTCTGA 780
CDNANprvNep3    GCAATCGTGCCGTTTAAGAACTCGAACTTCTTGGGCAACCTCGCCAAGGCTGAGGTCTGA 720
```

D

```
DNANprvNep4     ATGTTCTTCAACACTATTGTTACCGCTCTCGCTGCTGCTTCCTGCGTTGCAGCTGCTCCC 60
CDNANprvNep4    ATGTTCTTCAACACTATTGTTACCGCTCTCGCTGCTGCTTCCTGCGTTGCAGCTGCTCCC 60

DNANprvNep4     ACGCAGAAGCTGAACGCTCGTGCAAGCGTCCCCCACGACTCGCTCAACCCGTGGCCTGAA 120
CDNANprvNep4    ACGCAGAAGCTGAACGCTCGTGCAAGCGTCCCCCACGACTCGCTCAACCCGTGGCCTGAA 120

DNANprvNep4     GCTGTCAGGACCGGCACTGAGGGTGACGGCATCAAGAGGTTTGAGCCGACTCTCCACATT 180
CDNANprvNep4    GCTGTCAGGACCGGCACTGAGGGTGACGGCATCAAGAGGTTTGAGCCGACTCTCCACATT 180

DNANprvNep4     GCCCATGGCTGCCAGCCGTACACTGCCGTCAACGAAGCCGGCGACATCAGGTTAGTGCCC 240
CDNANprvNep4    GCCCATGGCTGCCAGCCGTACACTGCCGTCAACGAAGCCGGCGACATCAG---------- 230

DNANprvNep4     ATGCTCTCGATCTCCCCTTAGCCCACTAACACACAACACAGCGGCGGCCTCCAAGACACC 300
CDNANprvNep4    ----------------------------------------CGGCGGCCTCCAAGACACC 249

DNANprvNep4     GGCAGCTCCACCGGCGGCTGCAGGGACACCGGCAAGGGCCAGACCTACGTCCGGGCCAAG 360
CDNANprvNep4    GGCAGCTCCACCGGCGGCTGCAGGGACACCGGCAAGGGCCAGACCTACGTCCGGGCCAAG 309

DNANprvNep4     TGGCACAACGGCCGCTTCGCCATCATGTACTCGTGGTACTTCCCGAAGGACCACCCCAAC 420
CDNANprvNep4    TGGCACAACGGCCGCTTCGCCATCATGTACTCGTGGTACTTCCCGAAGGACCACCCCAAC 369

DNANprvNep4     AGCGGCGACGTGGCCGGCGGCCACCGCCACGACTGGGAGAACGTCGTCGTCTTCATCGAC 480
CDNANprvNep4    AGCGGCGACGTGGCCGGCGGCCACCGCCACGACTGGGAGAACGTCGTCGTCTTCATCGAC 429

DNANprvNep4     GACCCGGCCGCCGCCACCCCGACGCTGATCGGCGCCTCGGCATCCAGCCACAGCGGCTAC 540
CDNANprvNep4    GACCCGGCCGCCGCCACCCCGACGCTGATCGGCGCCTCGGCATCCAGCCACAGCGGCTAC 489

DNANprvNep4     ACCAAGAGCGACAACCCCCAGCGCAACGGCGACCGCGTCATGGTCGAGTACTTCACCAAC 600
CDNANprvNep4    ACCAAGAGCGACAACCCCCAGCGCAACGGCGACCGCGTCATGGTCGAGTACTTCACCAAC 549

DNANprvNep4     TTCCCCACCAACCACGAGCTGCAGTTCAAGACCAGCGAGGGCGCCGACTACGCCCTGCTC 660
CDNANprvNep4    TTCCCCACCAACCACGAGCTGCAGTTCAAGACCAGCGAGGGCGCCGACTACGCCCTGCTC 609

DNANprvNep4     GACTGGGACGTTATGACCGACGCTGCCAAGCAGGCCCTCCAGAATGCCGACTTTGGCAGT 720
CDNANprvNep4    GACTGGGACGTTATGACCGACGCTGCCAAGCAGGCCCTCCAGAATGCCGACTTTGGCAGT 669

DNANprvNep4     GCCAACGTTCCCTTCAAGGACGGCAACTTTGAGACCAAGATTGAGGAGGCTTGGGTCTAA 780
CDNANprvNep4    GCCAACGTTCCCTTCAAGGACGGCAACTTTGAGACCAAGATTGAGGAGGCTTGGGTCTAA 729
```

E

```
DNANprvNep5     ATGCATTTCAACAACTTCATCGCCATGATCGCCGCCGCTTCCTGCGCTGTGGCTGCTCCT 60
CDNANprvNep5    ATGCATTTCAACAACTTCATCGCCATGATCGCCGCCGCTTCCTGCGCTGTGGCTGCTCCT 60

DNANprvNep5     GCTGCTGCCCCCGAGGCTGCCGCCGAGCAGATCGAGAAGCGCGCTGTTGTCGCTCACGAC 120
CDNANprvNep5    GCTGCTGCCCCCGAGGCTGCCGCCGAGCAGATCGAGAAGCGCGCTGTTGTCGCTCACGAC 120

DNANprvNep5     TCTCTCTGGCCCATGCCGGAGAGCGTCCGTGGCGGCACTGAAGGAAACGCCATTCGCCGC 180
CDNANprvNep5    TCTCTCTGGCCCATGCCGGAGAGCGTCCGTGGCGGCACTGAAGGAAACGCCATTCGCCGC 180

DNANprvNep5     TACGAGCCGTTCCTCCACATTGCTCACGGCTGCCAGTCGTACACCGCCGTCAACGCCCGC 240
CDNANprvNep5    TACGAGCCGTTCCTCCACATTGCTCACGGCTGCCAGTCGTACACCGCCGTCAACGCCCGC 240

DNANprvNep5     GGTGACACCAGGTGAGAACTCTCCTCCGCCCCCTTCGCAATTGCGCATCAACTGACATTC 300
CDNANprvNep5    GGTGACAC---------------------------------------------------- 248

DNANprvNep5     AACACAGCGGTGGTCTTCAGAACTCCGGCGGTGCCACTGCCGGCTGCCGTGATGACCGCA 360
CDNANprvNep5    ----CAGCGGTGGTCTTCAGAACTCCGGCGGTGCCACTGCCGGCTGCCGTGATGACCGCA 304

DNANprvNep5     GGGGCCAGACCTACGCCAGAGGTGCTTGGCACAATGGCCGCTACGCCATCATGTACTCCT 420
CDNANprvNep5    GGGGCCAGACCTACGCCAGAGGTGCTTGGCACAATGGCCGCTACGCCATCATGTACTCCT 364

DNANprvNep5     GGTACATGCCCAAGGACCAGATCTCCGACGGTGGTGCCAACGGTGGACACCGTCACGACT 480
CDNANprvNep5    GGTACATGCCCAAGGACCAGATCTCCGACGGTGGTGCCAACGGTGGACACCGTCACGACT 424

DNANprvNep5     GGGAGAACGTTGTTGTCTGGATTGATAACCCTCAGTCACCTCCTCTCCTCTACTTTAATA 540
CDNANprvNep5    GGGAGAACGTTGTTGTCTGGATTGATAACCC---------------------------- 455

DNANprvNep5     CCCCAAACTGGACAATAGCTGACTTCCCACACAGCGGCCAACGCGAACCCTCGTGTCTTC 600
CDNANprvNep5    ---------------------------------GGCCAACGCGAACCCTCGTGTCTTC 480

DNANprvNep5     GGTGCTGCTGCTTCTGGCCACGGCAGCTACAAGAAGACGACCAGCCCGCAGATGCGCGAC 660
CDNANprvNep5    GGTGCTGCTGCTTCTGGCCACGGCAGCTACAAGAAGACGACCAGCCCGCAGATGCGCGAC 540

DNANprvNep5     GGCAGCCGCCTCCAGGTCGAATACATGACCAACTTCCCCAGGAACCACGAGCTTCAGTTC 720
CDNANprvNep5    GGCAGCCGCCTCCAGGTCGAATACATGACCAACTTCCCCAGGAACCACGAGCTTCAGTTC 600

DNANprvNep5     AAGACCAGCCCTGGCCGCGACTTCTGGATGGTCGACTGGGCTACCCTGCCCGAGCCCGCC 780
CDNANprvNep5    AAGACCAGCCCTGGCCGCGACTTCTGGATGGTCGACTGGGCTACCCTGCCCGAGCCCGCC 660

DNANprvNep5     AGGAGGGCTCTCCAGGACACGTCTTTCGGCAGCGCGAACGTGCCCTTCAAGAACGGCAAC 840
CDNANprvNep5    AGGAGGGCTCTCCAGGACACGTCTTTCGGCAGCGCGAACGTGCCCTTCAAGAACGGCAAC 720

DNANprvNep5     TTCGAGAGCAACCTCGGCAAGGCCTGGATCTAA   873
CDNANprvNep5    TTCGAGAGCAACCTCGGCAAGGCCTGGATCTAA   753
```

Figure S4.1 | Alignment of the DNA and cDNA sequence of *N. parvum* NLPs; A: NprvNep1, B: NprvNep2, C: NprvNep3, D: NprvNep4, and E: NprvNep5. Red boxes indicate the absence and presence of the introns in cDNA and DNA, respectively.

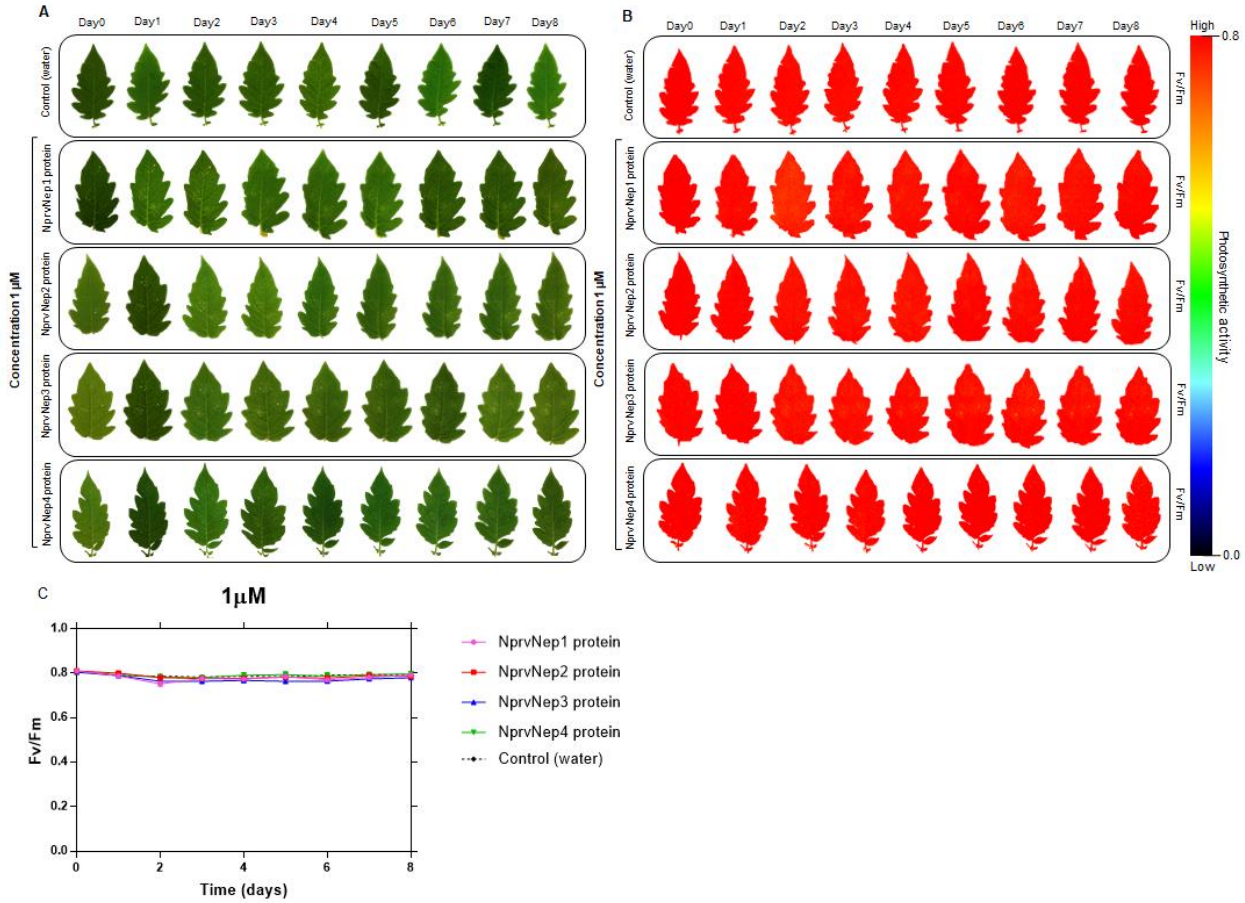

Figure S4.2 | Effect of recombinant NprvNeps on detached tomato leaves. Effect of 1 µM recombinant NprvNeps on symptoms development (A), chlorophyll fluorescence (B), and F_v/F_m (C). Ultra-pure water was used as a control. The colour scale bar indicates the F_v/F_m intensity of the leaf pixels given in false colours from high (red) to low (black) values. All measurements were performed in biological triplicates and error bars show the standard deviation. Two-way ANOVA, followed by a Dunnett's multiple comparison test was used to determine the statistical significance of phytotoxicity of each protein within the same concentration against the control (c) (*p<0.05, **p<0.01, ***p<0.001, ****p<0.0001).

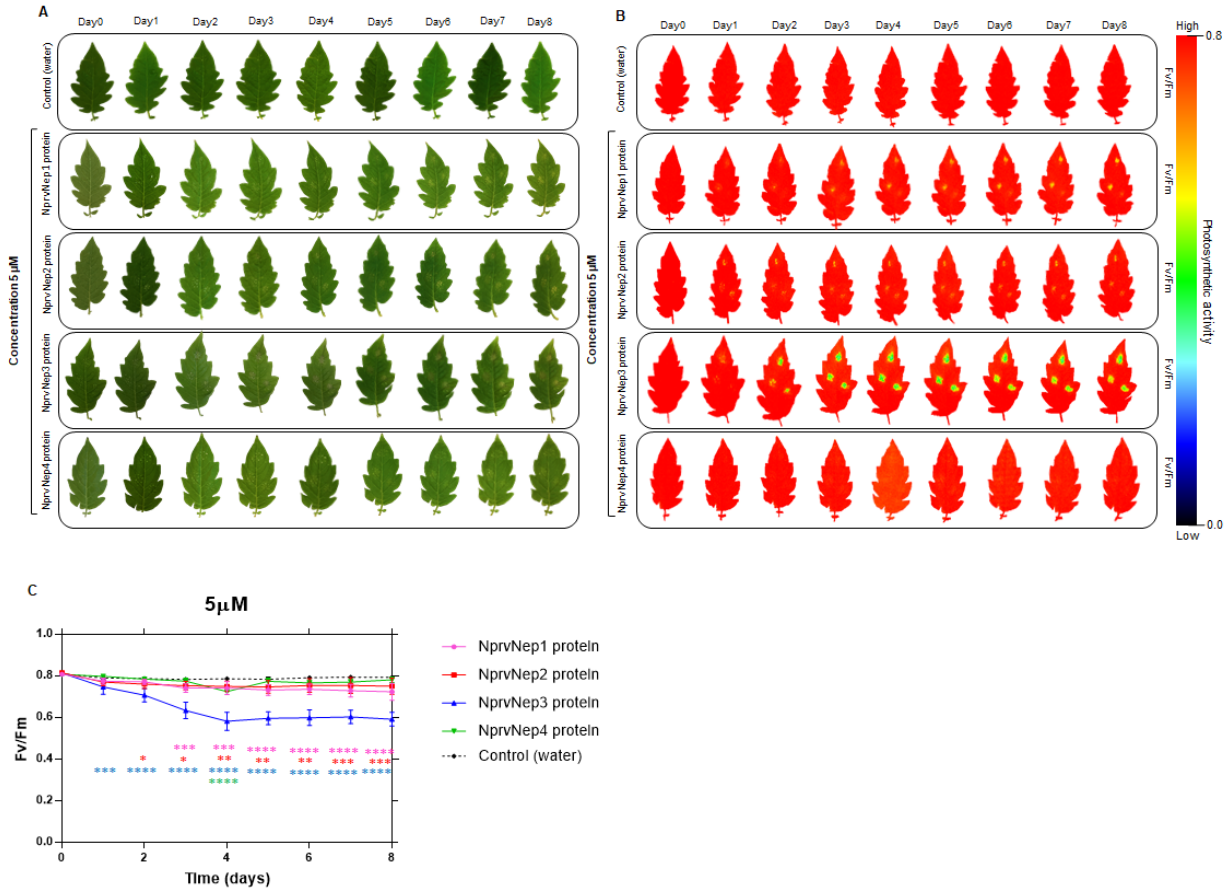

Figure S4.3 | Effect of recombinant NprvNeps on detached tomato leaves. Effect of 5 µM recombinant NprvNeps on symptoms development (A), chlorophyll fluorescence (B), and F_v/F_m (C). Ultra-pure water was used as a control. The colour scale bar indicates the F_v/F_m intensity of the leaf pixels given in false colours from high (red) to low (black) values. All measurements were performed in biological triplicates and error bars show the standard deviation. Two-way ANOVA, followed by a Dunnett's multiple comparison test was used to determine the statistical significance of phytotoxicity of each protein within the same concentration against the control (C) (*p<0.05, **p<0.01, ***p<0.001, ****p<0.0001).

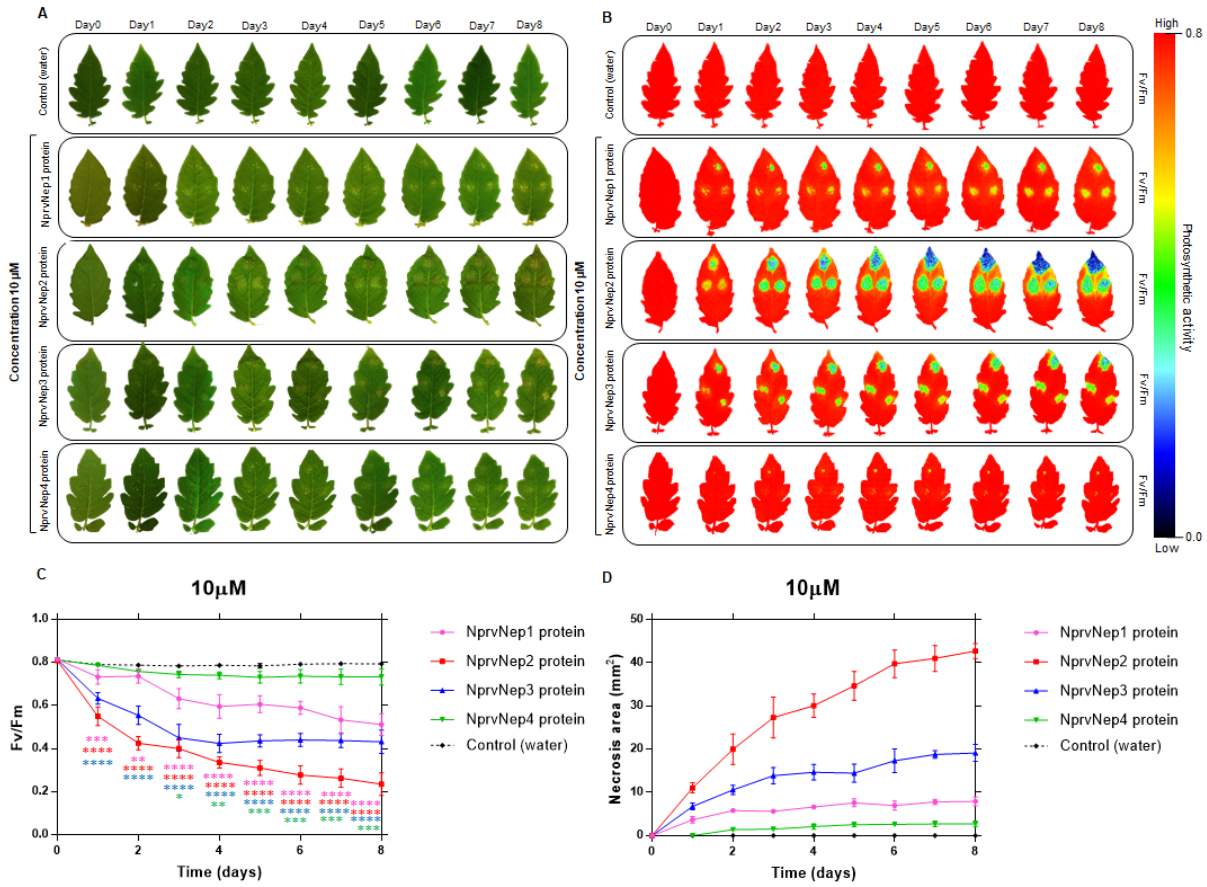

Figure S4.4 | Effect of recombinant NprvNeps on detached tomato leaves. Effect of 10 µM recombinant NprvNeps on symptoms development (A), chlorophyll fluorescence (B), and F_v/F_m (C) and necrosis area (D). Ultra-pure water was used as a control. The colour scale bar indicates the F_v/F_m intensity of the leaf pixels given in false colours from high (red) to low (black) values. All measurements were performed in biological triplicates and error bars show the standard deviation. Two-way ANOVA, followed by a Dunnett's multiple comparison test was used to determine the statistical significance of phytotoxicity of each protein within the same concentration against the control (C) (*p<0.05, **p<0.01, ***p<0.001, ****p<0.0001).

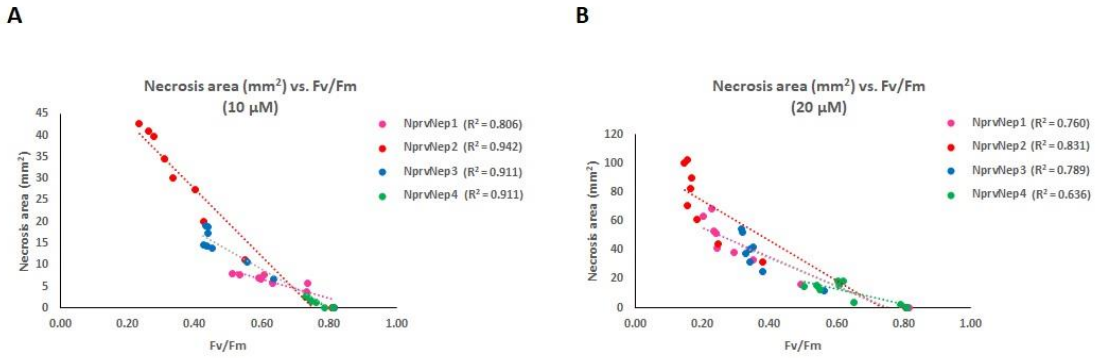

Figure S4.5 | Scatter plot of necrosis area vs. F_v/F_m values for 8 days. The correlation between necrosis area and Fv/Fm values of detached tomato leaves treated with 10 µM (A) and 20 µM (B) recombinant NprvNeps (1-4) for 8 days is shown. Each point is the mean of biological triplicates.

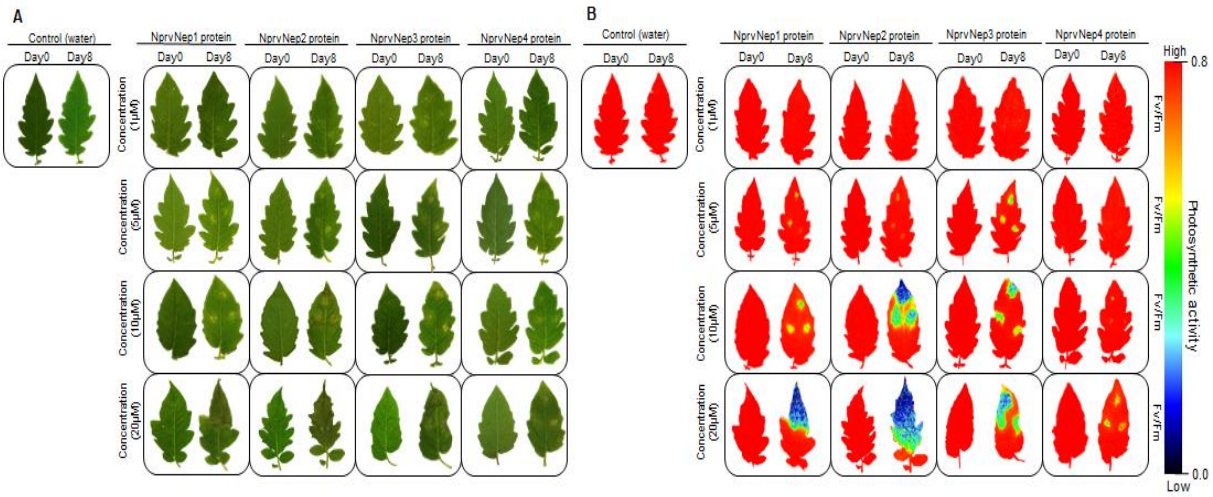

Figure S4.6 | Toxicity of recombinant NprvNeps to detached tomato leaves evaluated by chlorophyll fluorescence. Effect of 1, 5, 10, and 20 µM recombinant NprvNeps on symptoms development (A), and chlorophyll fluorescence (B) at 0 and 8 dpi. Ultra-pure water was used as a control. The colour scale bar indicates the F_v/F_m intensity of the leaf pixels given in false colours from high (red) to low (black) values. All experiments were performed in biological triplicates.

Table S4.1 | Primers used for cloning and amplification

Gene Name	Sequences (5' to 3')
NparvNep1	F: GCCCCGGTCGAGAAGCGC
	R: CTACAACGCCGCTAACGCTAGGTTG
NparvNep2	F: GCGGTTGTTCAACGCCGCGG
	R: TCACAACGACAGGCACAGGGG
NparvNep3	F: GCTGCCATCCAACGCCGC
	R: TCAGACCTCAGCCTTGGCGAGG
NparvNep4	F: GCTCCCACGCAGAAGCTGAACG
	R: TTAGACCCAAGCCTCCTCAATCTTGG
NparvNep5	F: GAGCAGATCGAGAAGCGCGCTG
	R: TTAGATCCAGGCCTTGCCGAGGTTG

Table S4.2 | The data of 6 *NprNep* genes

Genes	GenBank No	Extracellular protein /signal peptide	Signal peptide length	Protein molecular weight (kDa)
NprvNep1*	gi|615425645	Y	18	26.5
NprvNep2*	gi|485922125	Y	21	27.6
NprvNep3*	gi|485923842	Y	21	25.8
NprvNep4*	gi|485928552	Y	18	26.2
NprvNep5*	gi|485917230	Y	28	27.3
NprvNep6	gi|615411409	N	0	17.9

A signal peptide of the NprvNep was predicted with the tool SignalP4.0. The SignalP Network predicted cleavage sites between 17 and 29 amino acid residues.

*The *NprvNep* genes were selected for functional analysis. 'Y' has a signal peptide. 'N' has no a signal peptide.

CHAPTER 5

General discussion

GENERAL DISCUSSION

Botryosphaeriaceae species are a serious threat to the productivity and sustainability of a wide range of forests worldwide (Wingfield et al., 2015). Some Botryosphaeriaceae species are latent pathogens of mostly woody hosts, becoming pathogens under stress conditions such as extreme temperature fluctuation (Slippers & Wingfield, 2007). Thus, climate change raises concerns on how the interaction between these pathogens and their hosts will be affected (Jami et al., 2012; Jami et al., 2017). Nevertheless, little effort has been directed to the identification of the impact that increased temperature will have on microorganism-host interactions. Accordingly, we proposed to investigate the impact of temperature on phyto- and cytotoxicity of culture filtrates produced by these fungi. We concluded that temperature modulates both phytotoxicity and cytotoxicity of the Botryosphaeriaceae fungi investigated. All culture filtrates (grown at 25 and 37 °C) from species of Botryosphaeriaceae used in the study presented evidences of phyto- and cytotoxicity but with different aggressiveness levels. In general, phyto- and cytotoxicity are higher when fungi are grown at 25 °C, which agrees with the fact that their optimum growth temperature is 25 °C. Nonetheless, *B. dothidea, D. corticola* and *N. parvum* CAA704 induced high cell mortality when grown at 37 °C.

Despite the relevance of these fungi, the infection mechanisms are still uncertain (Cruywagen et al., 2015; Cruywagen et al., 2017). A comprehensive understanding of how these pathogens interact with their host is essential for developing effective strategies for disease control. *Neofusicoccum parvum* CAA704, was recovered from *E. globulus* displaying symptoms of dieback and decline in Portugal (Barradas et al., 2016). This strain also showed to be pathogenic to *E. globulus* in artificial inoculation trials (Barradas et al., 2016). However, very little is known about the strategies that *N. parvum* employs to infect its hosts, or about the molecules it expresses during infection. Accordingly, we proposed to characterize for the first time the set of proteins expressed by *N. parvum* in an infection-like environment to assess the molecular alterations induced by host mimicry (*Eucalyptus* stem). The host mimicry strategy, already used before by Fernandes et al. (2014), provided important insights into the mechanism of infection. In our study, identified proteins were mostly induced under host mimicry and were especially involved in plant cell wall degradation (targeting pectin and hemicellulose). In general, the extracellular proteins profile of *N. parvum* suggests that the fungus has adjusted its secretome to the host cell wall chemical properties, which might facilitate growth on a plant host during infection. Likewise, the existence of a several of pectin-degrading enzymes even in the absence of host material, indicates that this fungus is more adapted to degrade intact or living plants than decaying biomass, which implies that the fungus is likely to be a latent pathogen. In addition to, our results indicate that *N. parvum* aggressiveness could explain by synergistic activity of extracellular PCWDE, particularly GH and PL, in order to fully colonize the host. It has been demonstrated that *N. parvum* is able to produce

cell wall-degrading enzymes and phytotoxic metabolites whose synergistic action plays a role in the development of foliar symptoms (Andolfi et al*.,* 2011).

We identified some proteins that might be directly involved in the pathogenicity of *N. parvum*. We noticed an up-regulation of Putative GH 12 protein (R1GQP5) in response to *Eucalyptus* stem. Prior studies confirmed that GH12 protein is responsible for inducing cell death and triggering PAMP-triggered immunity (PTI) in dicot plants (Gui et al., 2017; Ma et al., 2015). Likewise, a glucanase (R1GZN3, GH7) and two endoxylanase enzymes [Beta-xylanase GH10 (R1FWZ0) and an endo-1,4-beta-xylanase GH11 (R1GCT8)], were induced in the presence of *Eucalyptus* stem. Cellulases belonging to GH6 and GH7 families have been described as being related to fungal virulence in the phytopathogenic fungi *Magnaporthe oryzae* (Van vu et al., 2012) and *Diplodia corticola* (Fernandes et al., 2014), as well as hemicellulases (GH10 and GH11) in the rice pathogen *M. oryzae* (Nguyen et al., 2011), in the oomycete plant pathogen *Phytophthora parasitica* (Lai & Liou, 2018) and in the fungal pathogen *B. cinerea* (Brito et al., 2006). Oxidoreductases, such as the putative berberine-like protein (R1GD68), were previously disclosed as important virulence factors induced during plant infection (Raffaele et al., 2010; Seidl et al., 2011). We showed, for the first time in this work, that the berberine-like protein is more abundant in the presence of *eucalyptus* than in control conditions. Metalloproteases such as deuterolysin have been suggested to not only to target proteins in the plant cell wall (Lakshman et al., 2016), but also be induced in a virulent strain of *Diplodia corticola* upon challenge by the host (*Quercus suber*) (Fernandes et al., 2015). *Neofusicoccum parvum* deuterolysin is over-represented in the secretome supplemented with *Eucalyptus* stem. A putative ricin B lectin protein (R1GAK8), involved in carbohydrate binding, was also induced in response to host mimicry. This protein contains a pectin_lyase_fold/virulence domain considered a virulence factor in several species (González-Fernandez et al., 2014; Ismail & Able, 2016; Kubicek et al., 2014). Ricin b lectins inhibit protein synthesis (Endo & Tsurugi, 1987) and is highly expressed during infection (Andersson et al., 2014; Meerupati et al., 2013). In addition, several proteins containing ribonuclease/ribotoxin domains, potentially related to pathogenicity, are more abundant in the secretome of *N. parvum* supplemented with *Eucalyptus* stem (Luhtala & Parker, 2010; Olombrada et al., 2014). A putative chitin binding protein (R1EW80) containing a chitin deacetylase domain and a putative chitin deacetylase (CE4, R1E7G7), was highly upregulated in the presence of host material. The chitin deacetylase can modify chitin, either loosening the chitin polymer bonds or converting the chitin to chitosan. Like the rust fungus *Uromyces viciae-faba* (Deising & Siegrist, 1995) and *Moniliophthora roreri* (Meinhardt et al., 2014)*, N. parvum* may use chitin deacetylase and other enzymes to modify its own cell wall to avoid degradation by host lytic enzymes, and conversion of the cell wall chitin to chitosan is likely be one infection strategy employed by these pathogens.

In this study, it was shown that *N. parvum* secretome is modulated by the presence of woody substrate, *in vitro*. Focusing on the secreted proteins, proteins putatively involved in plant cell wall degradation were identified. At the same time, *N. parvum* appears to be masking or modifying the fungal cell surface to avoid plant defenses, allowing the fungus to colonize the host plant, while actively releasing enzymes and toxins such as proteins containing ribonuclease/ribotoxin domains, putative ricin b lectins, putative epl1 protein containing cerato-platanin domain and necrosis inducing protein, suggesting that this species may have a hemibiotrophic lifestyle.

NLP-like proteins are effector proteins, not only as toxins to induce plant cell death, but also enable pathogens to rapid activation of plant defense. However, very little is known about the effector proteins that contribute to *N. parvum* as well as other *Botryosphaeriaceae* virulence. Cobos et al. (2010) reported the presence of three necrosis and ethylene inducing proteins (NLPs) in the secretome of *Diplodia seriata* another member of Botryosphaeriaceae family (Cobos et al., 2010). We described for the first time the characterization of NLPs (4 out of 6 genes) from *N. parvum*. Our results showed that 4 NLP genes in *N. parvum* are toxic both to plant (detached tomato leaves) and mammalian cells (Vero cells) in a dose-dependent manner. NprvNep2 was the most toxic to Vero cells, followed by NprvNep1 and 3. NprvNep4 induced weaker, but, nevertheless, still significant toxic effects to Vero cells. A similar trend of toxicity was observed in tomato leaves: the most toxic was NprvNep 2 and the least toxic NprvNep 4. Thus, NLP genes in *N. parvum* are functional genes encoding proteins toxic both to plant and mammalian cells, most probably involved in virulence or cell death during infection by *N. parvum*. Interestingly, we also identified in *N. parvum* secretome NprvNep1 (R1FXG6) (Chapter 3). However, no significant differences between the control and infection-like profiles (Table S3.2) were observed, suggesting that this phytotoxin is constitutively expressed by *N. parvum*.

We also show that for the first time the well-known chlorophyll fluorescence index F_v/F_m can be used to accurately quantify the damages on plant leaves during pathogenicity assays (Chapter 2 and 4).

In short, this work contributed largely to the pathogenicity characterization of *N. parvum* and subsequently for the Botryosphaeriaceae family. Further, we could infer about the molecular biology of the fungus, highlighting concomitantly some proteins that might play a crucial role during infection. Lastly, in this work we studied an important effector from *N. parvum* (NLPs proteins) that could provide with further new leads to an increased understanding of *N. parvum* and Botryosphaeriaceae virulence mechanisms. Such information will be particularly valuable for the development of subsequent studies.

FUTURE PERSPECTIVES

The present work has contributed to the knowledge of *N. parvum* and Botryosphaeriaceae family, especially regarding their molecular pathogenesis mechanism.

Our results show that Botryosphaeriaceae culture filtrates contain extracellular compounds able to cause necrosis in detached tomato leaves and cell mortality in mammalian cells. In this regard, further work such as proteomics (for those species that their secretome have not been analysed yet) and metabolomics should be conducted in order to identify the exact composition of the extracellular compounds produced by these fungi. The modulation by temperature of the phytotoxic and cytotoxic potential of these species was also revealed. Nonetheless, a study using more test temperatures would be valuable to fully understand the effect of temperature on Botryosphaeriaceae pathogenicity. Several species of Botryosphaeriaceae showed the ability to cause mammalian cell mortality at 37 °C, suggesting their potential to infect humans. Although testing different type of mammalian and human cells would be important to guarantee the robustness of the study to strongly suggest that the species used in this study have human infection potential. In general, a deeper understanding of the human/animal pathogenic potential of these fungi is still necessary.

As described, 4 NLPs genes in *N. parvum* were found to be functional genes and recombinant pure proteins caused necrosis in detached tomato leaves and mammalian cells. Additional studies such as developing protocols to knockout *NprvNep* genes, analysing gene expression, testing ethylene emission on detached tomato leaves inoculated with NprvNeps proteins, studying the induction of cell death mechanism and testing varieties of mammalian cell lines may be needed to clarify the role of NLPs in virulence or cell death during infection by *N. parvum.*

This works has mainly focused in the proteins involved in *Eucalyptus-N. parvum* interaction. However, in order to fully comprehend all the diverse and complicated cellular activities that are involved in interaction, it is important to perform multi-omics approaches. Sequencing and annotation of a pathogen's genome give us the possibility to identify gene, and gene products, that are involved in pathogen-host interaction. Fortunately, the genome sequence of *N. parvum* is known and was released in 2013 (Blanco-Ulate et al., 2013). However, the number of studies using a multi-omics integrated approach for a more detailed, comprehensive characterisation of the Botryosphaeriaceae is rather low (Felix et al., 2019). For this, we could integrate RNA-seq with proteomics data to study the molecular basis of *N. parvum* pathogenicity during interaction with *Eucalyptus*. Another useful approach is interactomics which can be also applied to understand the different protein - protein interaction (PPI) networks. Investigating PPI can enhance our understanding of the cellular process and biological interactions within an organism. This will enhance our knowledge of the biology,

pathogenicity, and protein interactions of *N. parvum* and ultimately contribute to the development of novel disease control.

REFERENCES

Andersson, K. M., Kumar, D., Bentzer, J., Friman, E., Ahrén, D., & Tunlid, A. (2014). Interspecific and host-related gene expression patterns in nematode-trapping fungi. *BMC Genomics*, 15(1), 968.

Andolfi, A., Mugnai, L., Luque, J., Surico, G., Cimmino, A., & Evidente, A. (2011). Phytotoxins produced by fungi associated with grapevine trunk diseases. *Toxins*, 3(12), 1569–1605.

Barradas, C., Alan J. L., P., Correia, A., Eugénio, D., Bragança, H., & Alves, A. (2016). Diversity and potential impact of Botryosphaeriaceae species associated with *Eucalyptus globulus* plantations in Portugal. *European Journal of Plant Pathology*, 146(2), 245–257.

Blanco-Ulate, B., Rolshausen, P., & Cantu, D. (2013). Draft genome sequence of *Neofusicoccum parvum* isolate UCR-NP2, a fungal vascular pathogen associated with grapevine cankers. *Genome Announcements*, 1(3), e00339-13.

Brito, N., Espino, J. J., & González, C. (2006). The endo-β-1, 4-xylanase Xyn11A is required for virulence in *Botrytis cinerea*. *Molecular Plant-Microbe Interactions*, 19(1), 25–32.

Cobos, R., Barreiro, C., Mateos, R. M., & Coque, J. J. R. (2010). Cytoplasmic- and extracellular-proteome analysis of *Diplodia seriata*: a phytopathogenic fungus involved in grapevine decline. *Proteome Science*, 8, 46.

Cruywagen, E. M., Crous, P. W., Roux, J., Slippers, B., & Wingfield, M. J. (2015). Fungi associated with black mould on baobab trees in southern Africa. *Antonie van Leeuwenhoek*, 108(1), 85–95.

Cruywagen, E. M., Slippers, B., Roux, J., & Wingfield, M. J. (2017). Phylogenetic species recognition and hybridisation in *Lasiodiplodia*: A case study on species from baobabs. *Fungal Biology*, 121(4), 420–436.

Deising, H., & Siegrist, J. (1995). Chitin deacetylase activity of the rust *Uromyces viciae-fabae* is controlled by fungal morphogenesis. *FEMS Microbiology Letters*, 127(3), 207–211.

Endo, Y., & Tsurugi, K. (1987). RNA N-glycosidase activity of ricin A-chain. Mechanism of action of the toxic lectin ricin on eukaryotic ribosomes. *Journal of Biological Chemistry*, 262(17), 8128–8130.

Felix, C., Meneses, R., Gonçalves, M. F. M., Tilleman, L., Duarte, A. S., Jorrín-Novo, J. V., Van de Peer, Y., Deforce, D., Van Nieuwerburgh, F., Esteves, A.C., & Alves, A. (2019). A multi-omics analysis of the grapevine pathogen *Lasiodiplodia theobromae* reveals that temperature affects the expression of virulence- and pathogenicity-related genes. *Scientific Reports*, 9(1), 13144.

Fernandes, I., Alves, A., Correia, A., Devreese, B., & Esteves, A. C. (2014). Secretome analysis identifies potential virulence factors of *Diplodia corticola*, a fungal pathogen involved in cork oak (*Quercus suber*) decline. *Fungal Biology*, 118(5–6), 516–523.

González-Fernández, R., Aloria, K., Valero-Galván, J., Redondo, I., Arizmendi, J. M., & Jorrín-Novo, J. V. (2014). Proteomic analysis of mycelium and secretome of different *Botrytis cinerea* wild-type strains. *Journal of Proteomics*, 97, 195–221.

Gui, Y., Chen, J., Zhang, D., Li, N., Li, T., Zhang, W., Guo, W. (2017). *Verticillium dahliae* manipulates plant immunity by glycoside hydrolase 12 proteins in conjunction with carbohydrate-binding module 1. *Environmental Microbiology*, 19(5), 1914–1932.

Ismail, I. A., & Able, A. J. (2016). Secretome analysis of virulent *Pyrenophora teres f. teres* isolates. *Proteomics*, 16(20), 2625–2636.

Jami, F., Slippers, B., Wingfield, M. J., & Gryzenhout, M. (2012). Five New Species of the Botryosphaeriaceae from *Acacia karroo* in South Africa. *Cryptogamie, Mycologie*, 33(3), 245–266.

Jami, F., Wingfield, M. J., Gryzenhout, M., & Slippers, B. (2017). Diversity of tree-infecting Botryosphaeriales on native and non-native trees in South Africa and Namibia. *Australasian Plant Pathology*, 46(6), 529–545.

Kubicek, C. P., Starr, T. L., & Glass, N. L. (2014). Plant cell wall–degrading enzymes and their secretion in plant-pathogenic fungi. *Annual Review of Phytopathology*, 52, 427–451.

Lai, M. W., & Liou, R. F. (2018). Two genes encoding GH10 xylanases are essential for the virulence of the oomycete plant pathogen *Phytophthora parasitica*. *Current Genetics*, 64(4), 931–943.

Luhtala, N., & Parker, R. (2010). T2 Family ribonucleases: ancient enzymes with diverse roles. *Trends in Biochemical Sciences*, 35(5), 253–259.

Ma, Z., Song, T., Zhu, L., Ye, W., Wang, Y., Shao, Y., Zheng, X. (2015). A *Phytophthora sojae* glycoside hydrolase 12 protein is a major virulence factor during soybean infection and is recognized as a PAMP. *The Plant Cell*, 27(7), 2057–2072.

Meerupati, T., Andersson, K. M., Friman, E., Kumar, D., Tunlid, A., & Ahren, D. (2013). Genomic mechanisms accounting for the adaptation to parasitism in nematode-trapping fungi. *PLoS Genetics*, 9(11), e1003909.

Meinhardt, L. W., Costa, G. G. L., Thomazella, D. P. T., Teixeira, P. J. P. L., Carazzolle, M. F., Schuster, S. C., Carlson, J. E., Guiltinan, M. J., Mieczkowski, P., Farmer, A., Ramaraj, T., Crozier, J., Davis, R. E., Shao, J., Melnick, R. L., Pereira, G. A., Bailey, B. A. (2014). Genome and secretome analysis of the hemibiotrophic fungal pathogen, *Moniliophthora roreri*, which causes frosty pod rot disease of cacao: mechanisms of the biotrophic and necrotrophic phases. *BMC Genomics*, 15, 164.

Nguyen, Q. B., Itoh, K., Van Vu, B., Tosa, Y., & Nakayashiki, H. (2011). Simultaneous silencing of endo-β-1, 4 xylanase genes reveals their roles in the virulence of *Magnaporthe oryzae*. *Molecular Microbiology*, 81(4), 1008–1019.

Olombrada, M., Martínez-del-Pozo, Á., Medina, P., Budia, F., Gavilanes, J. G., & García-Ortega, L. (2014). Fungal ribotoxins: natural protein-based weapons against insects. *Toxicon*, 83, 69–74.

Raffaele, S., Win, J., Cano, L. M., & Kamoun, S. (2010). Analyses of genome architecture and gene expression reveal novel candidate virulence factors in the secretome of *Phytophthora infestans*. *BMC Genomics*, 11(1), 637.

Seidl, M. F., Van den Ackerveken, G., Govers, F., & Snel, B. (2011). A domain-centric analysis of oomycete plant pathogen genomes reveals unique protein organization. *Plant Physiology*, 155(2), 628–644.

Slippers, B., & Wingfield, M. J. (2007). Botryosphaeriaceae as endophytes and latent pathogens of woody plants: diversity, ecology and impact. *Fungal Biology Reviews*, 21(2), 90–106.

Van Vu, B., Itoh, K., Nguyen, Q. B., Tosa, Y., & Nakayashiki, H. (2012). Cellulases belonging to glycoside hydrolase families 6 and 7 contribute to the virulence of *Magnaporthe oryzae*. *Molecular Plant-Microbe Interactions*, 25(9), 1135–1141.

Wingfield, M. J., Brockerhoff, E. G., Wingfield, B. D., & Slippers, B. (2015). Planted forest health: the need for a global strategy. Science (New York, N.Y.), 349(6250), 832–836.